Alkane Elimination Reactions between Transition Metal Hydrides and Rare-Earth Alkyls

Dissertation

zur Erlangung des Doktorgrades der Naturwissenschaften
(Dr. rer. nat.)

Fakultät für Biologie, Chemie und Geowissenschaften
Universität Bayreuth

vorgelegt von

Dipl.-Chem. Adam Paul Sobaczynski

Bayreuth 2014

Alkane Elimination Reactions between Transition Metal Hydrides and Rare-Earth Alkyls

Dissertation

zur Erlangung des Doktorgrades der Naturwissenschaften
(Dr. rer. nat.)

Fakultät für Biologie, Chemie und Geowissenschaften
Universität Bayreuth

vorgelegt von

Dipl.-Chem. Adam Paul Sobaczynski

Bayreuth 2014

This work was carried out from July 2010 to April 2014 at the Lehrstuhl für Anorganische Chemie II of the Universität Bayreuth under the supervision of Prof. Dr. Rhett Kempe.

A special thank goes to my academic supervisor Prof. Dr. Rhett Kempe.

This is a full reprint of the dissertation submitted to obtain the academic degree of Doctor of Natural Sciences (Dr. rer. nat.) and approved by the Fakultät für Biologie, Chemie und Geowissenschaften of the Universität Bayreuth.

Thesis submitted:	23rd April 2014
Admission by the executive committee:	30th April 2014
Date of scientific colloquium:	2nd July 2014

Acting dean:

Prof. Dr. Rhett Kempe

Doctoral committee:

First referee:	Prof. Dr. Rhett Kempe
Second referee:	Prof. Dr. Rainer Schobert
Third referee:	Dr. Daria Andreeva-Bäumler
Chairman:	Prof. Dr. Andreas Greiner

"Anyone who has never made a mistake has never tried anything new."

Albert Einstein

To Julia.

Abbreviations

δ . . . . . chemical shift

Å . . . . . Ångström

J . . . . . coupling constant

i . . . . . *ipso*

m . . . . . *meta*

o . . . . . *ortho*

p . . . . . *para*

*t*Bu . . . . . *tert*-butyl

Ap*H . . . . . (2,6-diisopropylphenyl)[6-(2,4,6-triisopropylphenyl)pyridin-2-yl]amine

br . . . . . broad

COD 1,5-cyclooctadiene

Cp . . . . . cyclopentadienyl

Cp* . . . . . pentamethylcyclopentadienyl

d . . . . . day

d . . . . . doublet

dfmpf . . . . . 1,1'-bis(bis(trifluoromethyl)phosphino)ferrocene

DFT . . . . . density functional theory

dippf . . . . . 1,1'-bis(diisopropylphosphino)ferrocene

DMF . . . . . dimethylformamide

dmpe . . . . . 1,2-bis(dimethylphosphino)ethane

equiv . . . . . equivalents

Et . . . . . ethyl

eV . . . . . electronvolt

Fp . . . . . [$CpFe(CO)_2$]

g . . . . . .gram

h . . . . . .hour

HOMO . . . . .highest occupied molecular orbital

Hz . . . . . .Hertz

IR . . . . . .infrared

L . . . . . .liter

Ln . . . . . .lanthanoid

LUMO . . . . .lowest unoccupied molecular orbital

Me . . . . . .methyl

min . . . . . .minute

MO . . . . . .molecular orbital

NMR . . . . . .nuclear magnetic resonance

Ph . . . . . .phenyl

ppm . . . . . .parts per million

Pr . . . . . .propyl

q . . . . . .quartet

RE . . . . . .rare-earth metal

Rp . . . . . .[CpRu(CO)$_2$]

rt . . . . . .room temperature

s . . . . . .singlet

sept . . . . . .septet

t . . . . . .triplet

thf . . . . . .tetrahydrofuran

TM . . . . . .transition metal

V . . . . . .volt

°C . . . . . .degree Celsius

Contents

1

Summary

In the present work various transition metal hydrides were examined regarding their potential to form unsupported bonds towards rare-earth metals. Selected rare-earth alkyls were reacted with the metal hydrides in question. Motivated by previous results of the Kempe group in which the alkane elimination reaction of $[Cp^*RuH_2]_2$ with $[Cp_2Y(CH_2SiMe_3)(thf)]$ yielded $[H(Cp^*Ru)_2H_2YCp_2]$, it was assumed that the reaction of the formal dihydride $[Cp^*RuH_2]_2$ with two equivalents of a rare-earth bis(alkyl) should lead to products with unsupported metal-metal bonds. $[Cp^*RuH_2]_2$ was reacted with two equivalents of $[Ln(CH_2SiMe_3)_2(OC_6H_3tBu_2\text{-}2,6)(thf)_2]$ (Ln = Y, Lu). However the heteromultimetallic polyhydride complexes $[(Cp^*Ru)_3(\mu\text{-}H)_4Ln(OC_6H_3tBu_2\text{-}2,6)(\mu\text{-}H)_2RuCp^*]$ (Ln = Y, Lu) were obtained (Scheme 1). Regardless the stoichiometry (0.5-2.0 equiv $[Cp^*RuH_2]_2$) the cluster compounds were obtained selectively. Solid state structures of both compounds could be established by XRD analyses. The isostructural compounds feature four Ln-Ru intramolecular distances of which one is significantly shorter than the three others. Six bridging hydride ligands are located between the metal centers.

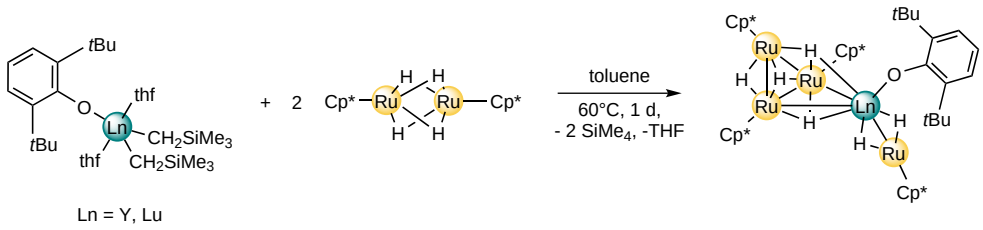

Scheme 1. Synthesis of $[(Cp^*Ru)_3(\mu\text{-}H)_4Ln(OC_6H_3tBu_2\text{-}2,6)(\mu\text{-}H)_2RuCp^*]$.

As the reaction of $[Cp^*RuH_2]_2$ towards rare-earth alkyls forms polyhydride complexes further studies focused on transition metal monohydrides. Inspired by the use of Rp and Fp fragments (Fp = $[CpFe(CO)_2]$, Rp = $[CpRu(CO)_2]$) in metal-metal bonding the reactivity of $[HW(CO)_3Cp]$ towards yttrium alkyls was examined. The relatively high acidity of the metal-hydrogen bond should allow alkane elimination reactions. Indeed, reactions of $[HW(CO)_3Cp]$ with yttrium alkyls proceeded rapidly with evolution of

tetramethylsilane. However, isocarbonyl bridged products were isolated. Several bonding modes in RE-TM carbonyl complexes are possible, namely unsupported metal-metal bonds, isocarbonyl linkages and solvate separated ion-pairs. Which bonding mode is preferred mainly depends on the nucleophilicity of the transition metal, the carbonyls' oxygen atoms and the used solvent. Reactions in several solvents were performed, always yielding isocarbonyl bridged compounds of type $[\{CpW(CO)_2(\mu\text{-}CO)\}_3Y(thf)_5]$ which was obtained by the reaction of $[Y(CH_2SiMe_3)_3(thf)_2]$ with three equivalents of $[HW(CO)_3Cp]$ in THF (Scheme 2). The nucleophilicity of the carbonyls' oxygen atoms appears to be higher than that of the tungsten atom. Thus, isocarbonyl linkages are preferred.

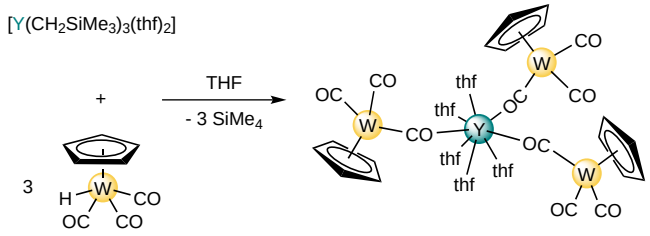

Scheme 2. Synthesis of $[\{CpW(CO)_2(\mu\text{-}CO)\}_3Y(thf)_5]$.

To avoid the observed isocarbonyl linkages the carbonyl ligands in $[HRu(CO)_2Cp]$ were replaced by a chelating phosphine ligand. Thus, identifying [HRu(dmpe)Cp] as a possible candidate for the formation of unsupported rare-earth metal–transition metal bonds by alkane elimination. Reaction of [HRu(dmpe)Cp] with the rare-earth monoalkyls $[Cp_2Ln(CH_2SiMe_3)(thf)]$ (Ln = Y, Lu) led to the formation of C-H bond activated products by deprotonation of the Cp ligands on Ru. Heterometallic hydride complexes of the type $[Cp_2Ln(\mu\text{-}H)(\mu\text{-}\eta^1\text{:}\eta^5\text{-}C_5H_4)Ru(dmpe)]$ (Ln = Y, Lu) were isolated (Scheme 3). The reaction of bis(alkyl) complexes $[Ln(CH_2SiMe_3)_2(OC_6H_3tBu_2\text{-}2,6)(thf)_2]$ (Ln = Y, Lu) with [HRu(dmpe)Cp] gave the products $[(OC_6H_3tBu_2\text{-}2,6)Ln(\mu\text{-}H)(\mu\text{-}\eta^1\text{:}\eta^5\text{-}C_5H_4)\{\kappa^3C,P,P'\text{-}CH_2(Me)P(CH_2)_2PMe_2\}Ru]_2$ (Ln = Y, Lu) by double C-H bond activation. In addition to deprotonation at the Cp ligand a methyl-group of the phosphine was deprotonated.

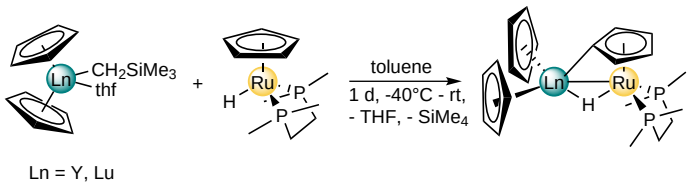

Scheme 3. Synthesis of $[Cp_2Ln(\mu\text{-}H)(\mu\text{-}\eta^1\text{:}\eta^5\text{-}C_5H_4)Ru(dmpe)]$.

As these results show, however, substitution of the carbonyls in $[HRu(CO)_2Cp]$ by an electron-rich phosphine changed the electronic properties of the resulting hydride complex. The hydride became unreactive towards rare-earth alkyls. Instead, the pro-

tons of the Cp ligand showed higher acidity. Thus, C-H bond activated products were obtained. To overcome this problem the carbonyls in [HRu(CO)$_2$Cp] were replaced by electron-poor phosphines to mimic the electronic properties of the parent compound. Fluorinated diphosphines serve as bidentate CO analogues. Primarily the readily available bidentate (perfluoroalkyl)phosphine dfmpf was chosen. The hydride complexes [HRu(dfmpf)Cp] (Scheme 4) and [HCo(dfmpf)(CO)$_2$] were prepared. Preliminary reactivity studies showed [HCo(dfmpf)(CO)$_2$] to be more reactive towards rare-earth alkyls than [HRu(dfmpf)Cp]. This is consistent with DFT calculations which predicted a weakend metal-hydrogen bond in [HCo(dfmpf)(CO)$_2$].

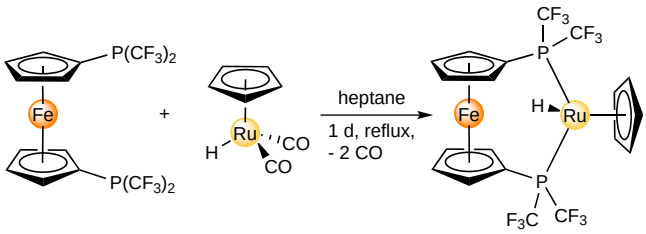

Scheme 4. Synthesis of [HRu(dfmpf)Cp].

Zusammenfassung

In der vorliegenden Arbeit wurden verschiedene Übergangs-Metall-Hydride hinsichtlich ihrer Eignung zur Ausbildung unverbrückter Bindungen zu Seltenerd-Metallen untersucht. Ausgewählte Seltenerd-Alkyle wurden mit den zu untersuchenden Metall-Hydriden umgesetzt. Motiviert durch vorhergehende Arbeiten von Kempe, in denen die Alkaneliminierungsreaktion von $[Cp^*RuH_2]_2$ mit $[Cp_2Y(CH_2SiMe_3)(thf)]$ die Verbindung $[H(Cp^*Ru)_2H_2YCp_2]$ ergab, wurde erwartet, dass die Reaktion des formalen Dihydrids $[Cp^*RuH_2]_2$ mit zwei Äquivalenten eines Seltenerd-Dialkyls zu Verbindungen mit unverbrückten Metall-Metall-Bindungen führen sollte. $[Cp^*RuH_2]_2$ wurde mit zwei Äquivalenten $[Ln(CH_2SiMe_3)_2(OC_6H_3tBu_2\text{-}2,6)(thf)_2]$ (Ln = Y, Lu) zur Reaktion gebracht. Es wurden jedoch heteromultimetallische Polyhydride des Typs $[(Cp^*Ru)_3(\mu\text{-}H)_4Ln(OC_6H_3tBu_2\text{-}2,6)(\mu\text{-}H)_2RuCp^*]$ (Ln = Y, Lu) erhalten (Schema 1). Unabhängig von der gewählten Stöchiometrie (0.5-2.0 Äquiv. $[Cp^*RuH_2]_2$) ergaben sich stets diese Clusterverbindungen. Festkörperstrukturen beider Verbindungen konnten mittes Einkristall-Röntgenstrukturanalyse bestimmt werden. Beide Verbindungen weisen jeweils vier intramolekulare Ln-Ru-Abstände auf, von denen jeweils einer deutlich kürzer als die drei übrigen ist. Sechs verbrückende Hydride befinden sich jeweils zwischen den Metallzentren.

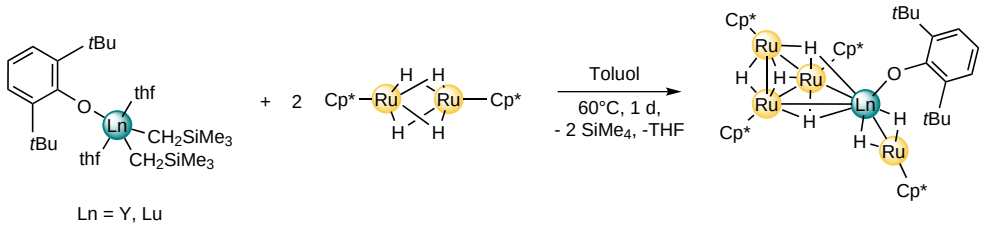

Schema 1. Synthese von $[(Cp^*Ru)_3(\mu\text{-}H)_4Ln(OC_6H_3tBu_2\text{-}2,6)(\mu\text{-}H)_2RuCp^*]$.

Da $[Cp^*RuH_2]_2$ mit Seltenerd-Alkylen bevorzugt zu Polyhydridverbindungen reagiert, wurden in weiteren Studien Übergangs-Metall-Monohydride untersucht. Angeregt durch den Einsatz der Fragmente Rp und Fp (Fp = $[CpFe(CO)_2]$, Rp = $[CpRu(CO)_2]$) in der Metall-Metall-Bindungschemie wurde die Reaktivität von $[HW(CO)_3Cp]$ gegenüber Seltenerd-Alkylen untersucht. Die relativ hohe Acidität der Metall-Wasserstoff-Bindung sollte Alkaneliminierungsreaktionen erlauben. In der Tat verlaufen Reaktionen von $[HW(CO)_3Cp]$ mit Yttriumalkylen schnell unter Freisetzung von Tetramethylsilan. Aller-

dings konnten nur isocarbonylverbrückte Verbindungen isoliert werden. Es sind verschiedene Bindungsmodi in Seltenerd-Übergangs-Metall-Verbindungen möglich: unverbrückte Metall-Metall-Bindungen, Isocarbonyl-Brücken sowie Lösungsmittel-separierte Ionenpaare. Welcher Bindungsmodus bevorzugt wird, hängt hauptsächlich von der Nucleophilie des Übergangs-Metalls, der Sauerstoffatome in den Carbonyl-Liganden sowie des eingesetzten Lösungsmittels ab. Es wurden Reaktionen in verschiedenen Lösungsmitteln untersucht. Hierbei wurden jedoch nur Verbindungen wie $[\{CpW(CO)_2(\mu\text{-}CO)\}_3Y(thf)_5]$, welches sich durch Reaktion von $[Y(CH_2SiMe_3)_3(thf)_2]$ mit drei Äquivalenten von $[HW(CO)_3Cp]$ in THF bildet, erhalten (Schema 2). Die Nucleophilie der Sauerstoffatome in den Carbonyl-Liganden ist offensichtlich größer, als die des Wolframatoms, womit Isocarbonyl-Brücken bevorzugt werden.

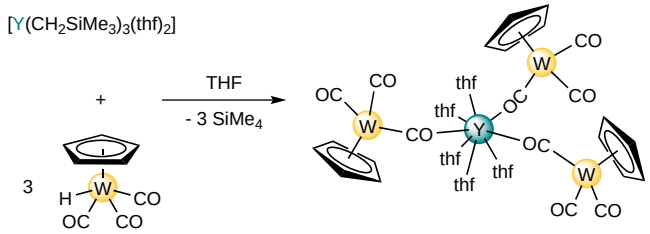

Schema 2. Synthese von $[\{CpW(CO)_2(\mu\text{-}CO)\}_3Y(thf)_5]$.

Um die beobachtete Ausbildung von Isocarbonyl-Brücken zu verhindern, wurden die beiden Carbonyl-Liganden in $[HRu(CO)_2Cp]$ durch ein chelatisierendes Phosphin ersetzt. Somit wurde [HRu(dmpe)Cp] als möglicher Kandidat für die Ausbildung unverbrückter Metall-Metall-Bindungen mittels Alkaneliminierung gewählt. Die Reaktion von [HRu(dmpe)Cp] mit Seltenerd-Alkylen des Typs $[Cp_2Ln(CH_2SiMe_3)(thf)]$ (Ln = Y, Lu) führte zur Ausbildung C-H-bindungsaktivierter Produkte durch Deprotonierung des Cp-Liganden am Ru. Es wurden Produkte des Typs $[Cp_2Ln(\mu\text{-}H)(\mu\text{-}\eta^1\text{:}\eta^5\text{-}C_5H_4)Ru(dmpe)]$ (Ln = Y, Lu) isoliert (Schema 3). Die Reaktion der Bis(alkyl)-Komplexe $[Ln(CH_2SiMe_3)_2(OC_6H_3tBu_2\text{-}2,6)(thf)_2]$ (Ln = Y, Lu) mit [HRu(dmpe)Cp] lieferte die Produkte $[(OC_6H_3tBu_2\text{-}2,6)Ln(\mu\text{-}H)(\mu\text{-}\eta^1\text{:}\eta^5\text{-}C_5H_4)\{\kappa^3C,P,P'\text{-}CH_2(Me)P(CH_2)_2PMe_2\}Ru]_2$ (Ln = Y, Lu) mittels zweifacher C-H-Bindungsaktivierung. Zusätzlich zum Aromaten am Ru wurde eine Methlygruppe des Phosphins deprotoniert.

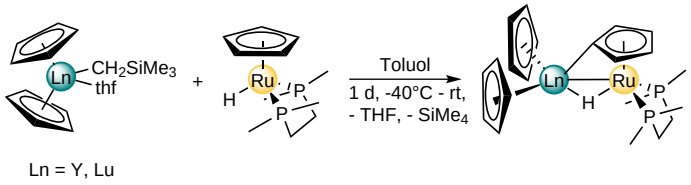

Schema 3. Synthese von $[Cp_2Ln(\mu\text{-}H)(\mu\text{-}\eta^1\text{:}\eta^5\text{-}C_5H_4)Ru(dmpe)]$.

Die Substitution der Carbonyl-Liganden in $[HRu(CO)_2Cp]$ durch ein elektonenreiches Phosphin veränderte die elektronischen Eigenschaften des neuen Komplexes dahinge-

hend, dass die Metall-Wasserstoff-Bindung gegenüber Seltenerd-Alkylen keine Reaktivität zeigte. Stattdessen zeigten Wasserstoffe am Cp-Liganden genügend Acidität, um mit Seltenerd-Alkylen zu reagieren. Es wurden folglich C-H-bindungsaktivierte Produkte erhalten. Um dieser Problematik entgegenzuwirken, wurden die Carbonyl-Liganden in $[HRu(CO)_2Cp]$ durch elektronenarme Phosphine ersetzt. Die elektronischen Eigenschaften sollten dabei denen der Ausgangsverbindung gleichen. Fluorierte Diphosphine fungieren als sperriges CO-Analogon. In erster Instanz wurde das leicht zugängliche (Perfluoroalkyl)phosphin dfmpf ausgewählt. Es wurden die Hydridkomplexe [HRu(dfmpf)Cp] (Schema 4) und $[HCo(dfmpf)(CO)_2]$ dargestellt. Vorläufige Reaktivitätsstudien zeigten, dass $[HCo(dfmpf)(CO)_2]$ eine höhere Reaktivität gegenüber Seltenerd-Alkylen aufweist als [HRu(dfmpf)Cp]. Dies steht in Einklang mit DFT-Rechnungen, welche eine schwächere Metall-Wasserstoff-Bindung in $[HCo(dfmpf)(CO)_2]$ vorhersagen.

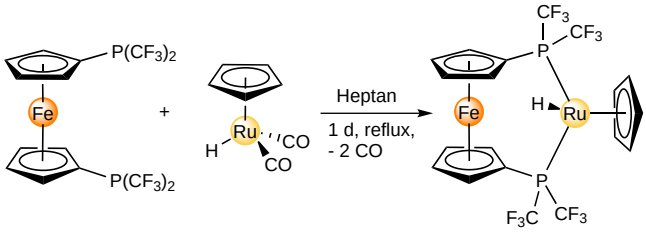

Schema 4. Synthese von [HRu(dfmpf)Cp].

2

Introduction

Bonds are the very heart of chemistry and have always fascinated chemists. It is almost a century ago when Lewis introduced in 1916 the idea of electron pairing and sharing.[1] A decade later it were Heitler and London who provided theoretical evidence that covalent bond formation is the result of electron pairing and sharing.[2,3] Several years later in 1931 Pauling reported in his pioneering work on the nature of the chemical bond.[4] Based on the work of his predecessors Lewis, Heitler and London he expanded the valence bond theory and introduced the concept of orbital hybridization. The challenging field of metal-metal bonded molecular compounds became an intensely studied field of inorganic chemistry during the last decades. Recent efforts shifted towards molecular compounds containing unsupported metal-metal bonds and new types of metal-metal linkages.[5] While metal-metal bonding in the d- and p-blocks is common and well understood, the metal-metal bonding chemistry of the f-block elements is in its infancy.[6] The hard and electropositive f-elements prefer hard, Lewis basic ligands. Thus, it is not surprising that the vast majority of f-element complexes consists of carbon, nitrogen, oxygen or halide based ligands. In comparison the use of metalloligands in f-element chemistry is underdeveloped.

The fundamental understanding of bonding phenomena in RE-TM complexes is important with respect to the general understanding of bonding theory and new reactivities. Beyond that an improved understanding of unsupported RE-TM bonds[5] seems very important as RE-TM bonding determines many of the characteristics of the related intermetallic compounds. These solid-state intermetallic compounds play an important role in our daily life. In particular, these compounds are represented in high-performance permanent magnets[7] and used as hydrogen storage materials[8,9] or in batteries of hybrid cars. Molecular analogues of such intermetallic compounds might become interesting alternatives for these applications and others.

The nature of the RE-TM bond is mostly highly polar as could be supported by numerous theoretical calculations.[10] This strong bond polarity generates metal centers which can be regarded as nucleophilic or electrophilic. Given this it seems natural to apply synthetic strategies known from organic syntheses.[11] This offers the possibility to synthesize larger aggregates in a controlled and rational fashion. One could imagine to

built up aggregates of increasing size starting from bimetallic compounds to nanosized materials.

Until recently, molecular compounds featuring unsupported bonds between rare-earth and transition metals were almost unknown. Beletskaya and coworkers reported in the early 1990's on the synthesis of $[Cp(CO)_2RuLuCp_2(thf)]$[12] (Figure 1, left) by salt elimination, the first structurally authenticated molecular compound[13] featuring such a bond. However, it was not before 2008 that the Kempe group reported on further examples of such compounds and showed that alkane elimination can be used to selectively form RE-TM bonds.[10a] Introduction of the $[Cp_2Re]$ moiety into RE-TM bonding had enormous impact on further progress in RE-TM bonding.

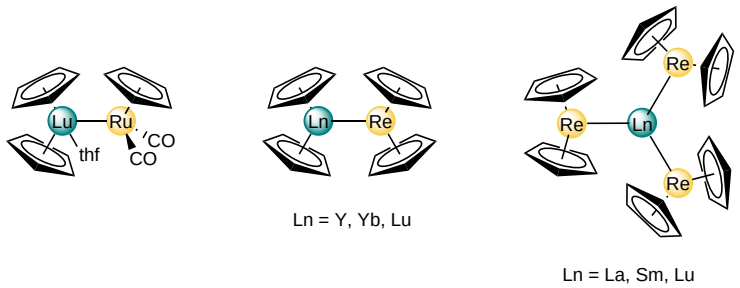

Figure 1. Selected examples[10a,10c,12b] of compounds featuring unsupported rare-earth–transition metal bonds.

Following their initial report on bismetallocenes $[Cp_2LnReCp_2]$[10a] (Figure 1, center) Kempe and coworkers reported on the model compound $[(2,6\text{-}t\text{Bu}_2C_6H_3O)Lu(CH_2SiMe_3)ReCp_2]$ to get insight into the reactivity of RE-TM bonds.[10e] Upon warming in toluene this complex decomposes to yield a molecular RE-TM cluster compound through C-H bond activation by the polar Lu-Re-bond. This cluster features a very interesting bonding situation. It shows highly polar three-center two-electron $ReLu_2$ units which can be conceptually situated between a localized two-center two-electron metal-metal bond as in bimetallic compounds and intermetallic compounds having a rather high degree of electron delocalization.

The same authors could also show that by use of the $[Cp_2Re]$ moiety it is possible to synthesize molecular compounds of the type $[Ln\{ReCp_2\}_3]$ containing RE solely bonded to TM atoms (Figure 1, right).[10c] Comparison of the electronic structure of the tetrametallic core in $[La\{ReCp_2\}_3]$ with the structurally related YRe_3 unit in the intermetallic compound Y_2ReB_6 revealed marked similarities in both compounds. Thus, the intermetalloids $[Ln\{ReCp_2\}_3]$ can be regarded as the link between molecular and intermetallic RE-TM compounds.

Besides Kempe's reports on RE-TM bonding with trivalent RE the authors could successfully employ the $[Cp_2Re]$ moiety in RE-TM bonding with divalent lanthanoids like ytterbium.[10d] The alkane elimination route provides an efficient protocol to these bimetallic compounds. However, as Kempe and coworkers reported recently, in the syntheses of bismetallocenes the rate of the reaction strongly depends on the employed lanthanoid and the steric bulk of the ligands.[10g] Salt metathesis can be an attractive

alternative for the synthesis of bismetallocenes featuring small lanthanoids like ytterbium or lutetium.

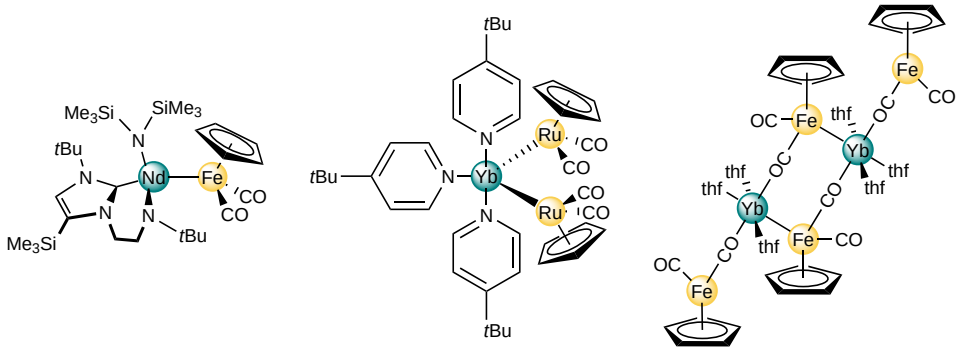

Figure 2. Selected examples[10b,10d,14] of compounds with Fp- or Rp-fragments featuring unsupported rare-earth–transition metal bonds.

Apart from Kempe's studies with the $[Cp_2Re]$ moiety only two more transition metal fragments are known to form unsupported bonds towards rare-earth metals: the carbonyl containing metalloligands Fp and Rp (Fp = $[CpFe(CO)_2]$, Rp = $[CpRu(CO)_2]$).[10b,10d,12b,14,15] Only few examples of complexes with such ligands were reported so far: Beletskaya's already mentioned compound $[Cp(CO)_2RuLuCp_2(thf)]$,[12] a neodymium-iron compound (Figure 2, left) reported by Arnold and coworkers[10b] and a ytterbium-ruthenium complex (Figure 2, center) reported by Kempe and coworkers.[10d] The prevalence for carbonylates in early and only few later studies can be explained with the assumption to provide a suitable, strongly Lewis basic partner for the Lewis acidic rare-earth fragment. The negative charge in these electron-rich, 18-electron transition metal carbonylates is stabilized by backbonding of the carbonyl ligands. However the use of transition metal carbonylates offers the possibility of other binding modes than the desired unsupported RE-TM bonds. Among the RE–TM carbonyl complexes, the isocarbonyl bridged compounds represent the most abundant class. Recently Mountford and coworkers reported impressive examples (Figure 2, right) that feature both RE-TM bonding and isocarbonyl linkages.[14,15]

It seems remarkable that the ate complex $[Cp_2Re]^-$ acts as suitable metalloligand in RE-TM bonding being only ligated by Cp ligands. Thus, isocarbonyl linkage is not relevant. Keeping this in mind the pursuit of further carbonyl-free metalloligands remains challenging. The substitution of carbonyl ligands in known carbonylates by other neutral ligands appears to be a promising strategy to carbonyl free metalloligands. Carbon monoxide being one of the ligands with the most π-accepting character lacks possibilities to be tuned electronically or sterically. Unlike CO, phosphines can be modified sterically and electronically. The strong π-acidity of fluorophosphines and (perfluoroalkyl)phosphines makes them a bulky mimic of CO.[16,17]

The goal of this thesis was to identify further transition metal hydrides suitable for metal-metal bonding. One possibility to achieve this could be by applying the strategies described above.

References

[1] G. N. Lewis, *J. Am. Chem. Soc.* **1916**, *38*, 762–785.

[2] W. Heitler, F. London, *Z. Phys.* **1927**, *44*, 455–472.

[3] F. London, *Z. Phys.* **1928**, *46*, 455–477.

[4] L. Pauling, *J. Am. Chem. Soc.* **1931**, *53*, 1367–1400.

[5] See, for example: (a) I. Resa, E. Carmona, E. Gutierrez-Puebla, A. Monge, *Science* **2004**, *305*, 1136–1138; (b) T. Nguyen, A. D. Sutton, M. Brynda, J. C. Fettinger, G. J. Long, P. P. Power, *Science* **2005**, *310*, 844–847; (c) S. P. Green, C. Jones, A. Stasch, *Science* **2007**, *318*, 1754–1757; (d) A. Grirrane, I. Resa, A. Rodriguez, E. Carmona, E. Alvarez, E. Gutierrez-Puebla, A. Monge, A. Galindo, D. del Río, R. A. Andersen, *J. Am. Chem. Soc.* **2007**, *129*, 693–703; (e) A. Noor, G. Glatz, R. Müller, M. Kaupp, S. Demeshko, R. Kempe, *Nat. Chem.* **2009**, *1*, 322–325; (f) F. R. Wagner, A. Noor, R. Kempe, *Nat. Chem.* **2009**, *1*, 529–536; (g) P. P. Power, *Nature* **2010**, *463*, 171–177; (h) A. Stasch, C. Jones, *Dalton Trans.* **2011**, *40*, 5659–5672.

[6] (a) S. T. Liddle, *Proc. R. Soc. A* **2009**, *465*, 1673–1700; (b) S. T. Liddle, D. P. Mills, *Dalton Trans.* **2009**, *9226*, 5592–5605; (c) D. Patel, S. T. Liddle, *Rev. Inorg. Chem.* **2012**, *32*, 1–22; (d) B. Oelkers, M. V. Butovskii, R. Kempe, *Chem. Eur. J.* **2012**, *18*, 13566–13579.

[7] D. Goll, H. Kronmüller, *Naturwissenschaften* **2000**, *87*, 423–438.

[8] L. Schlapbach, A. Züttel, *Nature* **2001**, *414*, 353–358.

[9] E. David, *J. Mater. Process. Technol.* **2005**, *162-163*, 169–177.

[10] (a) M. V. Butovskii, O. L. Tok, F. R. Wagner, R. Kempe, *Angew. Chem. Int. Ed.* **2008**, *47*, 6469–6472; (b) P. L. Arnold, J. McMaster, S. T. Liddle, *Chem. Commun.* **2009**, 818–820; (c) M. V. Butovskii, C. Döring, V. Bezugly, F. R. Wagner, Y. Grin, R. Kempe, *Nat. Chem.* **2010**, *2*, 741–744; (d) C. Döring, A.-M. Dietel, M. V. Butovskii, V. Bezugly, F. R. Wagner, R. Kempe, *Chem. Eur. J.* **2010**, *16*, 10679–10683; (e) M. V. Butovskii, O. L. Tok, V. Bezugly, F. R. Wagner, R. Kempe, *Angew. Chem. Int. Ed.* **2011**, *50*, 7695–7698; (f) T. Bauer, F. R. Wagner, R. Kempe, *Chem. Eur. J.* **2013**, *19*, 8732–8735; (g) M. V. Butovskii, B. Oelkers, T. Bauer, J. M. Bakker, V. Bezugly, F. R. Wagner, R. Kempe, *Chem. Eur. J.* **2014**, *20*, 2804–2811.

[11] L. H. Gade, *Angew. Chem. Int. Ed.* **1993**, *32*, 24–40.

[12] (a) G. K.-I. Magomedov, A. Z. Voskoboynikov, E. B. Chuklanova, A. I. Gusev, I. P. Beletskaya, *Metalloorg. Khim.* **1990**, *3*, 706–707; (b) I. P. Beletskaya, A. Z. Voskoboynikov, E. B. Chuklanova, N. I. Kirillova, A. K. Shestakova, I. N. Parshina, A. I. Gusev, G. K.-I. Magomedov, *J. Am. Chem. Soc.* **1993**, *115*, 3156–3166.

[13] Polymeric structures that contain both isocarbonyl-linked and direct RE-TM interactions were reported shortly afterwards: (a) H. Deng, S. G. Shore, *J. Am. Chem. Soc.* **1991**, *113*, 8538–8540; (b) H. Deng, S.-H. Chun, P. Florian, P. J. Grandinetti, S. G. Shore, *Inorg. Chem.* **1996**, *35*, 3891–3896.

[14] M. P. Blake, N. Kaltsoyannis, P. Mountford, *J. Am. Chem. Soc.* **2011**, *133*, 15358–15361.

[15] M. P. Blake, N. Kaltsoyannis, P. Mountford, *Chem. Commun.* **2013**, *49*, 3315–3317.

[16] J. Apel, J. Grobe, *Z. Anorg. Allg. Chem.* **1979**, *67*, 53–67.

[17] A. L. Fernandez, M. R. Wilson, A. Prock, W. P. Giering, *Organometallics* **2001**, *20*, 3429–3435.

3

Overview of Thesis Results

This thesis comprises four publications, which are presented in chapter 4-7.

3.1 Phenoxy Ligated Heteromultimetallic Hydride Complexes of Ruthenium and Rare-Earth Metals

Previous results showed that the alkane elimination reaction of $[Cp^*RuH_2]_2$ with $[Cp_2Y(CH_2SiMe_3)(thf)]$ gave $[H(Cp^*Ru)_2H_2YCp_2]$. Motivated by this findings the reaction of $[Cp^*RuH_2]_2$ with two equivalents of the rare-earth bis(alkyl) complexes $[Ln(CH_2SiMe_3)_2(OC_6H_3tBu_2\text{-}2,6)(thf)_2]$ (Ln = Y, Lu) was explored. Chapter 4 deals with these reaction which were assumed to lead to products with unsupported metal-metal bonds. However in all cases the heteromultimetallic polyhydride complexes $[(Cp^*Ru)_3(\mu\text{-}H)_4Ln(OC_6H_3tBu_2\text{-}2,6)(\mu\text{-}H)_2RuCp^*]$ (Ln = Y, Lu) were isolated regardless the stoichiometry (0.5-2.0 equiv $[Cp^*RuH_2]_2$; Scheme 1).

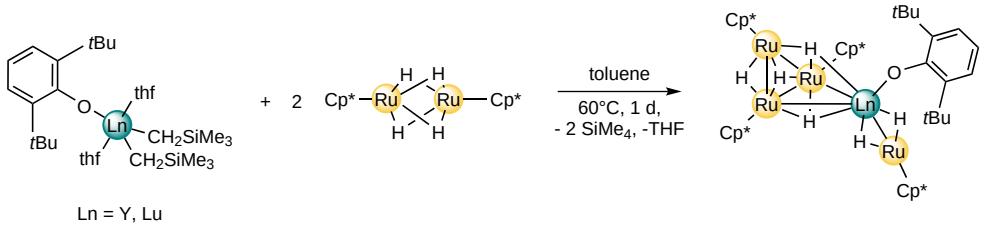

Scheme 1. Synthesis of $[(Cp^*Ru)_3(\mu\text{-}H)_4Ln(OC_6H_3tBu_2\text{-}2,6)(\mu\text{-}H)_2RuCp^*]$.

XRD analysis showed that both compounds are isostructural (Figure 1). The core structure consists of one rare-earth atom and four ruthenium atoms. These metal atoms are bridged by six hydride ligands. The ^1H NMR spectra show a signal for each hydride ligand. In case of the yttrium compound four signals show additional Y-H coupling, thus indicating an interaction of four of the hydride ligands with the yttrium metal.

A reaction mechanism for the formation of $[(Cp^*Ru)_3(\mu\text{-}H)_4Lu(OC_6H_3tBu_2\text{-}2,6)(\mu\text{-}H)_2RuCp^*]$ was suggested and supported on the basis of DFT calculations. The overall

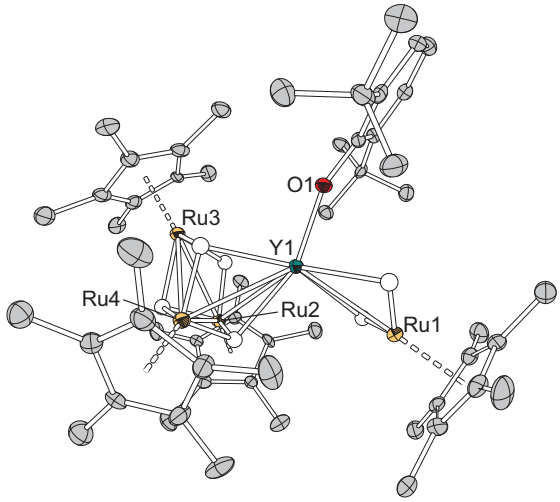

Figure 1. Solid state structure of $[(Cp^*Ru)_3(\mu\text{-}H)_4Y(OC_6H_3tBu_2\text{-}2,6)(\mu\text{-}H)_2RuCp^*]$.

formation process of $[(Cp^*Ru)_3(\mu\text{-}H)_4Lu(OC_6H_3tBu_2\text{-}2,6)(\mu\text{-}H)_2RuCp^*]$ was calculated to be exergonic by -34.2 kcal mol^{-1}.

3.2 Alkane Elimination Reactions between Yttrium Alkyls and Tungsten Hydrides

As the reaction of transition metal polyhydride complexes with rare-earth alkyls resulted in the formation of heteromultimetallic polyhydride complexes further studies focused on transition metal monohydride complexes. Chapter 5 deals with the alkane elimination reaction between yttrium alkyls and tungsten monohydrides.

Yttrium monoalkyls were investigated first as the formation of a bimetallic complex by alkane elimination would be expected. The reaction of equimolar amounts of the tungsten monohydride $[HW(CO)_3Cp]$ with the yttrium monoalkyl $[Cp_2Y(CH_2SiMe_3)(thf)]$ in THF did not give the expected bimetallic complex. Instead $[\{CpW(CO)_2(\mu\text{-}CO)\}_2Y\text{-}Cp(thf)_3]$ was obtained in 88% yield. As determined by XRD analyses the six-coordinate yttrium atom exhibits two $Y(\mu\text{-}OC)W$ linkages. Interestingly, the reaction in THF is accompanied by the loss of one Cp ligand at the original Cp_2Y moiety and the subsequent formation of $[Cp_3Y]$ as a byproduct. The ligand redistribution could be explained by the formation of two energetically preferred products instead of a binuclear compound.

To avoid the observed ligand redistribution the same reaction was examined in acetonitrile. Reaction of equimolar amounts of $[HW(CO)_3Cp]$ and $[Cp_2Y(CH_2SiMe_3)(thf)]$ in acetonitrile gave the binuclear compound $[\{CpW(CO)_2(\mu\text{-}CO)\}YCp_2(NCMe)_2]$ in 82% yield. As shown by XRD analyses this compound exhibits a five-coordinate yttrium atom with an isocarbonyl linkage towards tungsten.

The use of a phenoxy-substituted yttrium dialkyl should offer stable ancillary ligand bonding to the metal. The reaction of $[HW(CO)_3Cp]$ with $[Y(CH_2SiMe_3)_2(OC_6H_3tBu_2\text{-}$

2,6)(thf)$_2$] in toluene gave a solid polymeric product in 92% yield with the empirical formula [{CpW(CO)$_2$(μ-CO)}$_2$Y(OC$_6$H$_3$*t*Bu$_2$-2,6)]$_n$. This could be cleaved in THF to give the molecular compound [{CpW(CO)$_2$(μ-CO)}$_2$Y(OC$_6$H$_3$*t*Bu$_2$-2,6)(thf)$_3$]. Reaction of [HW(CO)$_3$Cp] with [Y(CH$_2$SiMe$_3$)$_2$(OC$_6$H$_3$*t*Bu$_2$-2,6)(thf)$_2$] in THF gave the same molecular compound in 80% yield. XRD analyses showed a six coordinate yttrium atom with two isocarbonyl linkages towards the tungsten moieties.

To offer a more Lewis basic ligand than the phenolate, [Ap*Y(CH$_2$SiMe$_3$)$_2$(thf)] was chosen as reaction partner. Reaction of [HW(CO)$_3$Cp] with [Ap*Y(CH$_2$SiMe$_3$)$_2$(thf)] in THF unexpectedly led to the formation of [{CpW(CO)$_2$(μ-CO)}$_3$Y(thf)$_5$]. Interestingly, here [HW(CO)$_3$Cp] protonates the amido ligand Ap*. The reaction of an yttrium trialkyl with the tungsten hydrido complex should also lead to the formation of [{CpW(CO)$_2$(μ-CO)}$_3$Y(thf)$_5$]. Treatment of [Y(CH$_2$SiMe$_3$)$_3$(thf)$_2$] with three equivalents of [HW(CO)$_3$Cp] led straightforward to [{CpW(CO)$_2$(μ-CO)}$_3$Y(thf)$_5$] in 91% yield (Scheme 2).

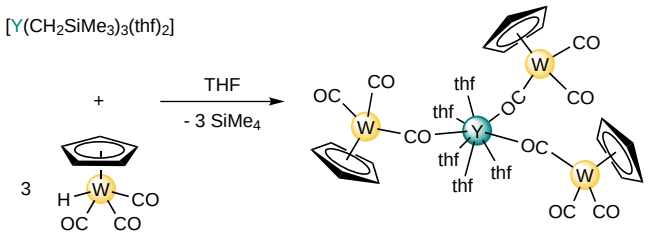

Scheme 2. Synthesis of [{CpW(CO)$_2$(μ-CO)}$_3$Y(thf)$_5$].

The molecular structure as determined by XRD analysis showed an eight-coordinate yttrium atom which exhibits square antiprismatic geometry with three isocarbonyl-bonded tungsten moieties and five coordinated thf molecules (Figure 2).

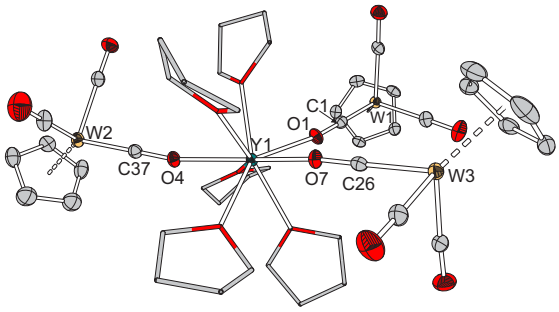

Figure 2. Solid state structure of [{CpW(CO)$_2$(μ-CO)}$_3$Y(thf)$_5$].

3.3 Heterometallic Hydride Complexes of Rare-Earth Metals and Ruthenium through C-H Bond Activation

Since carbonyl containing metalloligands are likely to form isocarbonyl linkages to rare-earth metal fragments further studies focused on new non-carbonyl transition metal fragments. The most prominent parent fragment, $[Ru(CO)_2Cp]$, has been chosen and the carbonyl ligands were replaced by a chelating phosphine ligand, thus identifying [HRu(dmpe)Cp] as a possible candidate for the formation of unsupported rare-earth–transition metal bonds by alkane elimination. Chapter 6 deals with the investigation of the reactivity of [HRu(dmpe)Cp] towards different rare-earth alkyls. However, [HRu(dmpe)Cp] was found to react with rare-earth alkyls to form C-H bond activated products by deprotonation of the Cp ligand on Ru. Various heterometallic hydride complexes of rare-earth metals and ruthenium were obtained.

The reaction of rare-earth monoalkyl complexes $[Cp_2Ln(CH_2SiMe_3)(thf)]$ (Ln = Y, Lu) with the ruthenium hydride complex [HRu(dmpe)Cp] gave the corresponding bimetallic hydride complexes $[Cp_2Ln(\mu\text{-H})(\mu\text{-}\eta^1{:}\eta^5\text{-}C_5H_4)Ru(dmpe)]$ (Ln = Y, Lu) in good yields (Scheme 3).

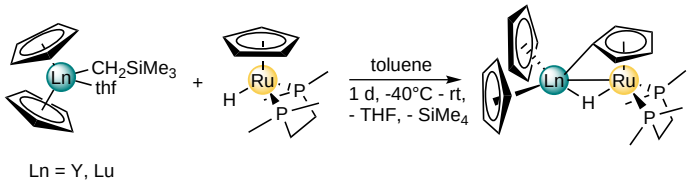

Scheme 3. Synthesis of $[Cp_2Ln(\mu\text{-H})(\mu\text{-}\eta^1{:}\eta^5\text{-}C_5H_4)Ru(dmpe)]$.

As revealed by NMR spectroscopy and XRD analyses (Figure 3) both metal centers are linked by a metal-metal bond which is bridged by a hydride and a $\mu\text{-}\eta^1{:}\eta^5$-bonded C_5H_4 ligand.

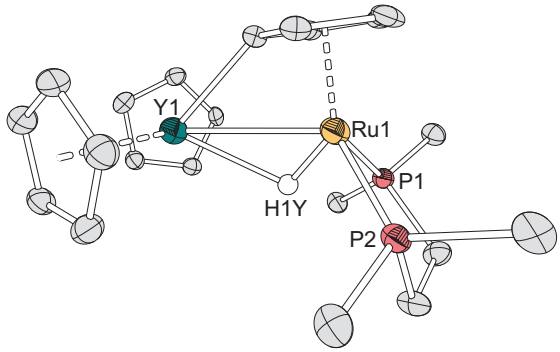

Figure 3. Solid state structure of $[Cp_2Y(\mu\text{-H})(\mu\text{-}\eta^1{:}\eta^5\text{-}C_5H_4)Ru(dmpe)]$.

Further the reactivity of the yttrium compound $[Cp_2Y(\mu\text{-H})(\mu\text{-}\eta^1{:}\eta^5\text{-}C_5H_4)Ru(dmpe)]$ was investigated. Reaction with diphenylacetylene led to the formation of $[Cp_2Y(\mu\text{-}$

H){μ-(Ph)CC(Ph)(C_5H_4)}Ru(dmpe)], by insertion of the alkyne into the highly reactive Y-C-σ-bond.

Due to the observed C-H bond activation of Cp ligands bound to Ru, the reactivity of the ruthenium hydride towards bis(alkyl) complexes was explored. In these sterically less crowded alkyls Ln-Ru bond formation could become relevant. The reaction of bis(alkyl) complexes [Ln(CH_2SiMe_3)$_2$(OC_6H_3tBu$_2$-2,6)(thf)$_2$] (Ln = Y, Lu) with [HRu(dmpe)Cp] gave the products [(OC_6H_3tBu$_2$-2,6)Ln(μ-H)(μ-η^1:η^5-C_5H_4){κ^3C,P,P'-CH_2(Me)P(CH_2)$_2$PMe_2}Ru]$_2$ (Ln = Y, Lu) by double C-H bond activation in moderate yields (Scheme 4). As in the cases described above the Cp ligand on Ru undergoes a C-H bond activation to form a Ln-C bond. Unexpectedly, a second C-H bond activation occurs at one of the aliphatic methyl groups of the phosphine ligand to form a second Ln-C bond.

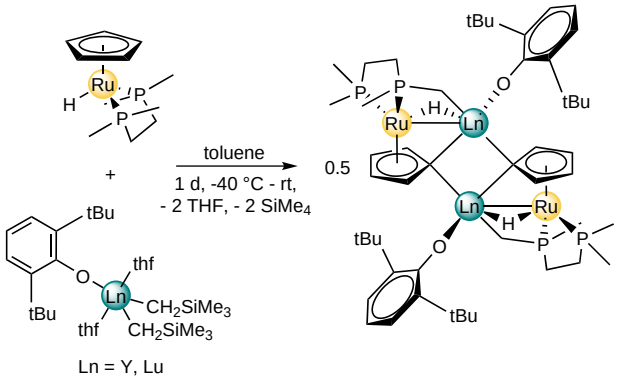

Scheme 4. Synthesis of [(OC_6H_3tBu$_2$-2,6)Ln(μ-H)(μ-η^1:η^5-C_5H_4){κ^{3}C,P,P'-CH_2(Me)P(CH_2)$_2$PMe_2}Ru]$_2$.

As revealed by XRD analyses these compounds show a dimeric structure. The formation of a dimer shows the greater demand for steric saturation at Y due to the less shielding phenoxide ligand in comparison to the two Cp ligands in [Cp_2Y(μ-H)(μ-η^1:η^5-C_5H_4)Ru(dmpe)]. Each Y-Ru pair is linked by a metal-metal bond which is significantly shorter than in [Cp_2Y(μ-H)(μ-η^1:η^5-C_5H_4)Ru(dmpe)]. This bond is bridged by a hydride, a μ-η^1:η^5-bonded C_5H_4 ligand, and the phosphine ligand's deprotonated methyl group.

3.4 Transition Metal Hydride Complexes of dfmpf

The substitution of carbonyl ligands in [HRu(CO)$_2$Cp] by the aliphatic diphosphine dmpe and examination of the resulting monohydride [HRu(dmpe)Cp] gave C-H bond activated rare-earth–transition metal hydride complexes. The electron-rich character of dmpe made the hydride not accessible for alkane elimination and favored instead C-H bond activation at the Cp ring. Chapter 7 deals with transition metal hydrides of the π-accepting phosphine dfmpf. Unlike CO, phosphines can be modified sterically and electronically. Fluorinated diphosphines serve as bidentate CO analogues. This makes

transition metal dfmpf complexes a bulky mimic of their carbonyl parent compounds and a promising candidate for the formation of unsupported bonds between rare-earth elements and transition metals. dfmpf was chosen as an easy to prepare, to purify and to handle (perfluoroalkyl)phosphine accessible on a multigram scale.

The reaction of the ruthenium monohydride [HRu(CO)$_2$Cp] with an excess of the fluorinated phosphine dfmpf gave the bimetallic hydride compound [HRu(dfmpf)Cp] in 38% yield (Scheme 5). [HRu(dfmpf)Cp] shows improved stability against air compared with its electron-rich phosphine congener [HRu(dmpe)Cp].

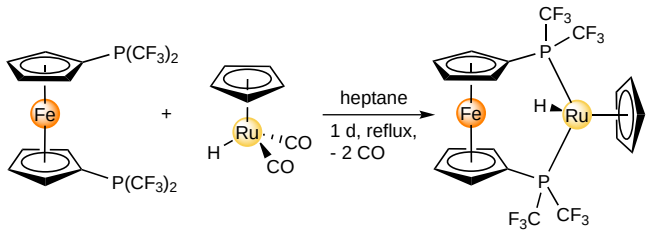

Scheme 5. Synthesis of [HRu(dfmpf)Cp].

The solid state structure of [HRu(dfmpf)Cp] (Figure 4) could be established by XRD analyses and was the basis for further DFT calculations. The optimized structure shows good agreement with the experimental data. Calculation showed a positive charged ruthenium and a negative charge on the ruthenium bonded hydrogen.

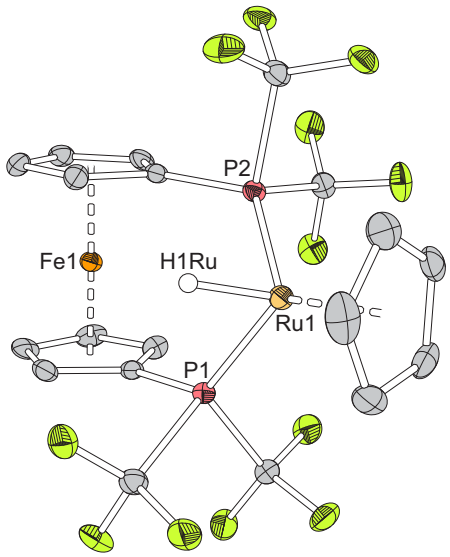

Figure 4. Solid state structure of [HRu(dfmpf)Cp].

The reaction of [HCo(CO)$_4$] with dfmpf yielded [HCo(dfmpf)(CO)$_2$] as moderately air sensitive solid. Geometry optimization starting from the experimentally obtained solid state structure is in agreement with the experimental data. Analysis of the MOs shows that the Co-H bond is weaker than the Ru-H bond in [HRu(dfmpf)Cp]. The de-

protonation energy is reduced compared to [HRu(dfmpf)Cp] and the cobalt atom shows a higher negative charge whereas the hydrogen atom is positively charged suggesting a protic character.

It appeared desirable to synthesize the heavier homologue of the cobalt compound $[HCo(dfmpf)(CO)_2]$ as well: a (perfluoroalkyl)phosphine Rh^I hydride. The reaction of $[Rh(COD)(\mu\text{-}Cl)]_2$ with dfmpf gave the substitution product $[Rh(dfmpf)(\mu\text{-}Cl)]_2$. XRD analyses revealed a dimeric structure. Since dimeric rhodium complexes are readily cleaved in acetonitrile this strategy was used on $[Rh(dfmpf)(\mu\text{-}Cl)]_2$. Treatment with two equivalents of $AgBF_4$ in acetonitrile gave the monomeric rhodium species $[Rh(dfmpf)(NCMe)_2][BF_4]$ by salt metathesis in nearly quantitative yield (Scheme 6). However, attempts failed to isolate the corresponding hydride complex.

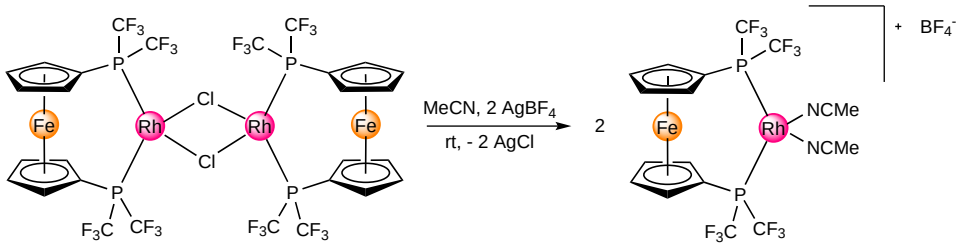

Scheme 6. Synthesis of $[Rh(dfmpf)(NCMe)_2][BF_4]$.

3.5 Individual Contribution to Joint Publications

The results presented in this thesis were obtained in collaboration with others and are published or are to be submitted as indicated below. In the following, the contributions of all the co-authors to the different publications are specified. The asterisk denotes the respective corresponding author.

Chapter 4

This work is to be submitted with the title

"Phenoxy Ligated Heteromultimetallic Hydride Complexes of Ruthenium and Rare-Earth Metals"
Adam P. Sobaczynski, Stefan Schwarz, Johannes Obenauf, and Rhett Kempe*

I synthesized and characterized all complexes in this work and carried out the NMR experiments. The X-ray analyses and crystal structure solutions were performed by Johannes Obenauf. Stefan Schwarz did the theoretical calculations on the obtained compounds and was involved in scientific discussions regarding the results. The manuscript was written by me with contribution of Stefan Schwarz. Rhett Kempe supervised this work and was involved in scientific discussions, comments and correction of the manuscript.

Chapter 5

This work is published in *Eur. J. Inorg. Chem.* **2014**, 1211–1217, with the title

"Alkane Elimination Reactions between Rare Earth Alkyls and Tungsten Hydrides"
Adam P. Sobaczynski, Johannes Obenauf, and Rhett Kempe*

I synthesized and characterized all complexes in this work and carried out the NMR experiments and IR measurements. The X-ray analyses and crystal structure solutions were performed by Johannes Obenauf. The manuscript was written by me. Rhett Kempe supervised this work and was involved in scientific discussions, comments and correction of the manuscript.

Chapter 6

This work is published in *Organometallics* **2013**, *32*, 1363–1369, with the title

"Heterometallic Hydride Complexes of Rare-Earth Metals and Ruthenium through C-H Bond Activation"
Adam P. Sobaczynski, Tobias Bauer, and Rhett Kempe*

I synthesized and characterized all complexes in this work and carried out the NMR experiments. The X-ray analyses and crystal structure solutions were performed by Tobias Bauer. The manuscript was written by me. Rhett Kempe supervised this work and was involved in scientific discussions, comments and correction of the manuscript.

Chapter 7

This work is to be submitted with the title

"Transition Metal Hydride Complexes of dfmpf"
Adam P. Sobaczynski, Stefan Schwarz, Johannes Obenauf, and Rhett Kempe*

I synthesized and characterized all complexes in this work and carried out the NMR experiments. I also did the IR measurements and the electrochemical experiments. The X-ray analyses and crystal structure solutions were performed by Johannes Obenauf. Stefan Schwarz did the theoretical calculations on the obtained compounds and was involved in scientific discussions regarding the results. The manuscript was written by me with contribution of Stefan Schwarz. Rhett Kempe supervised this work and was involved in scientific discussions, comments and correction of the manuscript.

4

Phenoxy Ligated Heteromultimetallic Hydride Complexes of Ruthenium and Rare-Earth Metals

Adam P. Sobaczynski, Stefan Schwarz, Johannes Obenauf, and Rhett Kempe*

Lehrstuhl Anorganische Chemie II, Universität Bayreuth, 95440 Bayreuth, Germany

To be submitted.

4.1 Abstract

The reaction of the phenoxy ligated rare-earth bis(alkyl) complexes [Ln(CH_2SiMe_3)$_2$(O-C_6H_3tBu$_2$-2,6)(thf)$_2$] (Ln = Y, Lu) with two equivalents of the binuclear ruthenium tetrahydride [Cp*RuH$_2$]$_2$ gave the heterometallic hexahydride complexes [(Cp*Ru)$_3$(μ-H)$_4$Ln(OC_6H_3-tBu$_2$-2,6)(μ-H)$_2$RuCp*] (**1a**: Ln = Y; **1b**: Ln = Lu) with evolution of tetramethylsilane. A reaction mechanism of the formation of **1b** is suggested and supported by DFT calculations. The complexes were characterized by NMR spectroscopy, X-ray crystal structure analysis (XRD) and elemental analyses.

4.2 Introduction

Metal hydrides are nowadays important in many catalytic and stoichiometric processes.[1] Of great interest appear heterometallic hydride complexes composed of rare-earth metals (RE) and transition metals (TM). The different electronic properties of these metals may lead to synergistic effects offering novel properties and reactivities not accessible for the homometallic species. While homometallic hydride compounds are widespread, heterometallic hydride complexes of RE and TM still lack in number, although first reports[2] already date back three decades. This may be due to missing efficient synthesis protocols. However, in recent years these compounds have received a great deal of attention. Intermetallic hydrides of RE and TM, for instance, are applied as hydrogen storage

materials[3] or in hybrid car batteries. Molecular analogues of such intermetalloids may become interesting alternatives for both of these applications and others.

The majority of the heteromultimetallic polyhydride complexes was synthesized using cyclopentadienyl based RE precursors. Their reactivity, however, remained limited, despite recent progress.[2,4–12] This woke the interest in cyclopentadienyl free RE precursors.[13–16] Changing the steric bulk of the ancillary ligands on the RE led to different reactivities from those observed in their cyclopentadienyl ligated analogues.[5,13] We report here on the synthesis of cyclopentadienyl free heteromultimetallic polyhydride complexes based on phenoxy ligated rare-earth moieties.

4.3 Results and Discussion

Motivated by our previous report on the synthesis of $[H(Cp^*Ru)_2H_2YCp_2]$[9] we assumed that the alkane elimination reaction of the formal dihydride $[Cp^*RuH_2]_2$ with two equivalents of a rare-earth bis(alkyl) should lead to products with unsupported metal-metal bonds by elimination of four equivalents of tetramethylsilane. The bimetallic tetrahydride $[Cp^*RuH_2]_2$ was reacted with two equivalents of the rare-earth bis(alkyls) $[Ln(CH_2SiMe_3)_2(OC_6H_3tBu_2\text{-}2,6)(thf)_2]$. However, in all cases the heteropentametallic polyhydride complexes $[(Cp^*Ru)_3(\mu\text{-}H)_4Ln(OC_6H_3tBu_2\text{-}2,6)(\mu\text{-}H)_2RuCp^*]$ (**1a**: Ln = Y; **1b**: Ln = Lu) were isolated. Regardless the chosen stoichiometry (0.5-2.0 equiv $[Cp^*RuH_2]_2$) the cluster compounds **1a**, **1b** were selectively obtained. The reaction with 2 equiv of $[Cp^*RuH_2]_2$ led to the formation of **1a** and **1b** as black, air sensitive solids in moderate yields of 46% and 58%, respectively (Scheme 1). **1a** and **1b** are sparingly soluble in benzene and toluene.

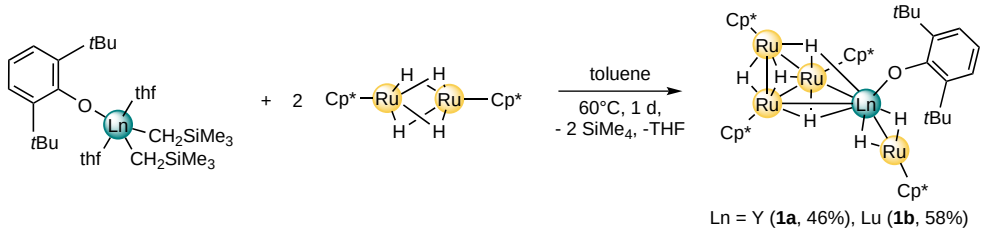

Scheme 1. Synthesis of $[(Cp^*Ru)_3(\mu\text{-}H)_4Ln(OC_6H_3tBu_2\text{-}2,6)(\mu\text{-}H)_2RuCp^*]$.

The ^{1}H NMR spectrum of **1a** displays four singlets at 1.69, 1.73, 2.01 and 2.02 ppm for the Cp* groups and a singlet at 1.84 ppm for the *tert*-butyl groups. The aromatic protons appear as triplet at 6.75 ppm with $J = 7.6$ Hz and as doublet at 7.20 ppm with $J = 7.6$ Hz. The six hydride ligands show one resonance each. Two singlet resonances at −22.00 and −7.30 ppm are assigned to hydrides located between ruthenium atoms. Four doublet resonances at −10.90 ($J = 11.3$ Hz), −8.63 ($J = 11.2$ Hz), −8.20 ($J = 14.0$ Hz) and −6.14 ($J = 12.5$ Hz) ppm featuring Y-H coupling are assigned to hydrides which are located between yttrium and ruthenium atoms. The ^{1}H NMR spectrum of **1b** shows the same signals at slightly altered chemical shifts, however the hydride signals

exhibit no coupling. Due to its poor solubility in aromatic solvents not all carbon atoms of **1a** could be assigned in the ^{13}C NMR spectrum. The spectrum shows four resonances at 12.8, 12.9, 13.1 and 13.1 ppm which are assigned to methyl groups of the Cp* ligands. The corresponding ring carbon atoms appear as signals at 81.5, 83.9, 85.8 and 94.8 ppm. The *tert*-butyl groups show two signals at 33.5 and 35.3 ppm for the quaternary carbons and the methyl groups. The ring carbon atoms of the phenoxy ligand could not be assigned. The ^{13}C NMR spectrum of the lutetium analogue **1b** shows a similar appearance, however, four signals in the aromatic region at 116.3, 125.6, 136.3 and 163.0 ppm are assigned to the ring carbon atoms of the phenoxy ligand.

The molecular structures of **1a** and **1b** were determined by XRD analyses. Figure 1 shows the solid state structure of **1a**. The Y-Ru distances span the range from 2.8738(9)-3.2589(9) Å. The bond length Y1–Ru1 (2.8738(9) Å) is the shortest in the series which can presumably be attributed to the two bridging hydride ligands across this bond. This bond is slightly shorter than the corresponding Y–Ru distance (2.9989(5) Å) in $[(Cp^*Ru)_4(C_5Me_3CH_2SiMe_3)Y(\mu\text{-}H)_7]$ reported by Hou and Shima.[17] The bond lengths Y1–Ru2 and Y1–Ru4 (3.1112(12), 3.0768(13) Å) are in the range of the sum of the atomic radii of Y (1.80 Å) and Ru (1.30 Å),[18] whereas the bond length Y1–Ru3 (3.2589(9) Å) is longer than this sum. The corresponding bond lengths in the Lu compound **1b** are as expected shorter (2.8284(6)-3.2439(6) Å) and follow the same trends as in **1a**. The hydride ligands could be located in **1a** and **1b**. The average Ru1–H distance in **1a** amounts

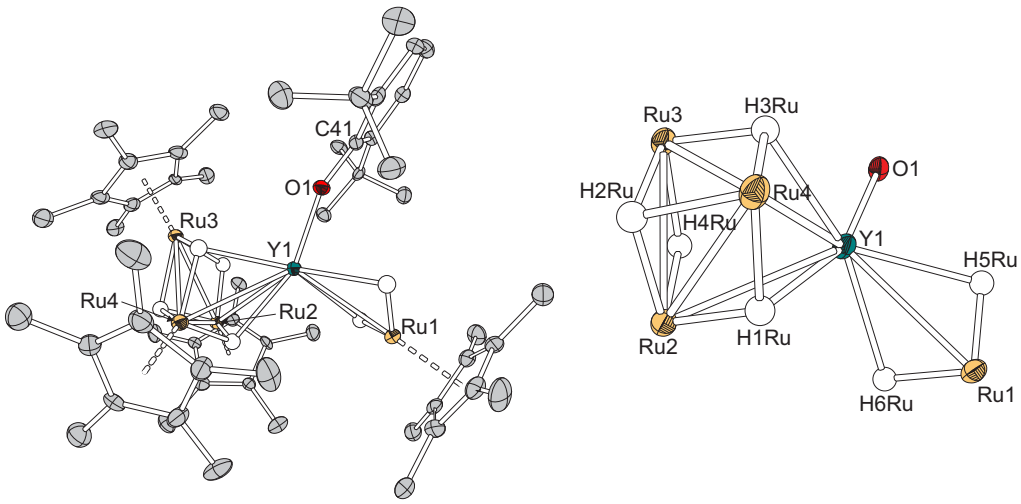

Figure 1. Solid state structure of **1a** with 30% thermal ellipsoids; complete structure (left) and metal hydride core (right). Hydrogen atoms except hydridic have been omitted for clarity. Selected bond lengths [Å], angles [°]: Y1–Ru1 2.8737(9), Y1–Ru2 3.1113(12), Y1–Ru3 3.2590(9), Y1–Ru4 3.0768(13), Y1–O1 2.072(5), Ru2–Ru3 2.7299(11), Ru2–Ru4 2.7635(11), Ru3–Ru4 2.7285(11), Y1–H1Ru 2.42(10), Y1–H3Ru 2.41(13), Y1–H5Ru 2.37(12), Y1–H6Ru 2.43(7), Ru1–H5Ru 1.44(12), Ru1–H6Ru 1.51(7), Ru1–$Cp_{centroid}$ 1.88, Ru(2-4)–$Cp_{centroid}$ 1.83 (average value); Y1–O1–C41 157.9, Ru1–Y1–O1 103.8, Y1–Ru1–$Cp_{centroid}$ 178.3.

to 1.48 Å which is shorter than in $[Cp^*RuH_2]_2$ (1.67 Å).[19] This suggests a stronger interaction of the bridging hydrides Y1–H–Ru1 with the ruthenium atom. The same effect was observed by Hou and Shima in their compound $[(Cp^*Ru)_4(C_5Me_3CH_2SiMe_3)Y(\mu\text{-}H)_7]$.[17] The angles Ru1–Y1–O1 and Y1–O1–C41 in **1a** were found to be 103.8° and 157.9°, respectively. Due to the smaller atomic radius of lutetium the analogous angles Ru3–Lu1–O1 and Lu1–O1–C23 in compound **1b** show smaller values of 102.4° and 147.7°, respectively. The corresponding Y–O–C angles in the bis(alkyl) complexes $[Ln(CH_2SiMe_3)_2(OC_6H_3tBu_2\text{-}2,6)(thf)_2]$ (Ln = Y, Lu) show in both cases values of 178.8°.[20] The deviation from nearly linear arrangement is attributed to steric repulsion of the Cp* ligand and the *tert*-butyl groups in **1a**, **1b**. The $[Cp^*Ru]_3$-portion of **1a**, **1b** is structurally related with the trinuclear complex $[\{Cp^*Ru(\mu\text{-}H)\}_3(\mu_3\text{-}H)_2]$.[21] The distances Ru2–Ru3, Ru2–Ru4, Ru3–Ru4 and the mean Ru-H distance (**1a**: 2.7299(11), 2.7635(11), 2.7285(11), 1.74; **1b**: 2.7410(6), 2.7547(8), 2.7410(6), 1.75) compare well with the corresponding distances (Ru-Ru 2.75 Å, Ru-H 1.80 Å) in $[\{Cp^*Ru(\mu\text{-}H)\}_3(\mu_3\text{-}H)_2]$.

Based on DFT calculations we suggest a reaction mechanism for the formation of **1b** (Figure 2). $[Lu(CH_2SiMe_3)_2(OC_6H_3tBu_2\text{-}2,6)(thf)_2]$ reacts in a first endergonic step with 1 equiv of $[Cp^*RuH_2]_2$ to form intermediate **A** which is 4.8 kcal mol^{-1} less stable than the starting materials. **A** is closely related to our previously reported heterotrinuclear complex $[H(Cp^*Ru)_2H_2YCp_2]$.[9] In the next exergonic step **A** reacts with one further equivalent of $[Cp^*RuH_2]_2$ to form the pentametallic intermediate **B**. Rearrangement of one ruthenium moiety and loss of a second thf molecule lead in a strongly exergonic reaction step to the final product **1b** which is −34.2 kcal mol^{-1} more stable than the starting materials. The calculated energy profile correlates with the reaction mechanism for the formation of $[(Cp^*Ru)_4(C_5Me_3CH_2SiMe_3)Y(\mu\text{-}H)_7]$ as postulated by Hou and Shima.[17]

4.4 Conclusion

To conclude, heteromultimetallic hydride complexes of rare-earth metals and ruthenium were synthesized. The reaction of rare-earth bis(alkyl) complexes $[Ln(CH_2SiMe)_2(OC_6H_3tBu_2\text{-}2,6)(thf)_2]$ (Ln = Y, Lu) with the ruthenium tetrahydride $[Cp^*RuH_2]_2$ leads to the formation of the heterometallic hexahydride complexes $[(Cp^*Ru)_3(\mu\text{-}H)_4Ln(OC_6H_3\text{-}tBu_2\text{-}2,6)(\mu\text{-}H)_2RuCp^*]$ (**1a**: Ln = Y; **1b**: Ln = Lu). These are formed regardless the employed amount of the ruthenium hydride (0.5-2 equiv). A reaction mechanism for the formation of **1b** was suggested and supported on the basis of DFT calculations. The overall formation process of **1b** was calculated to be exergonic by −34.2 kcal mol^{-1}.

4.5 Experimental Section

General Procedures. All manipulations were carried out under a dry and oxygen-free argon atmosphere using Schlenk techniques or in a nitrogen-filled glovebox (mBraun 120-G) with a high-capacity recirculator (below 0.1 ppm of O_2). Toluene was distilled

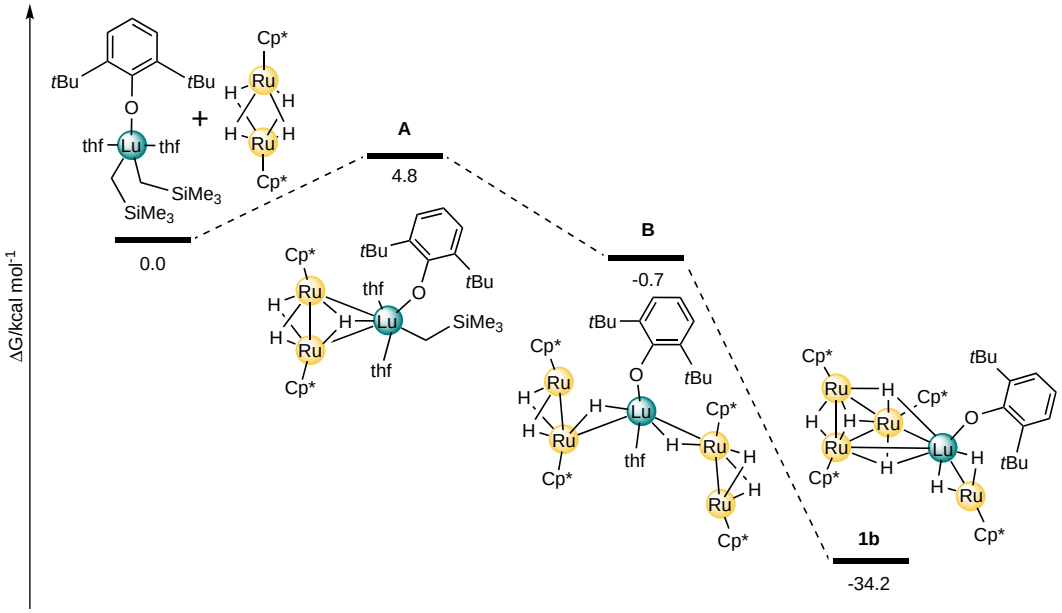

Figure 2. Calculated energy profile for the reaction of $[Lu(CH_2SiMe_3)_2(OC_6H_3tBu_2\text{-}2,6)(thf)_2]$ with $[Cp^*RuH_2]_2$ to form **1b**. Reaction proceeds from left to right. All free energies ΔG are given relative to the starting materials in kcal mol^{-1}.

from sodium benzophenone ketyl. Deuterated solvents were obtained from Cambridge Laboratories and were degassed, dried, and distilled prior to use. $[Cp^*RuH_2]_2$[19] and $[Lu(CH_2SiMe_3)_2(OC_6H_3tBu_2\text{-}2,6)(thf)_2]$[22] were prepared according to published procedures. $[Y(CH_2SiMe_3)_2(OC_6H_3tBu_2\text{-}2,6)(thf)_2]$[20] was prepared with minor modifications of the published procedure.

Instrumentation. ^{1}H and ^{13}C NMR spectra were recorded on Varian Unity 300 MHz and Bruker AC 300 MHz spectrometers. Chemical shifts are given in ppm being positive in the downfield. Signals for ^{1}H and ^{13}C are referenced to the residual solvent resonance. Elemental analyses were carried out using a Vario El III instrument. X-ray crystal structure analyses were performed by using a STOE-IPDS II diffractometer equipped with an Oxford Cryostream low-temperature unit. Structure solution and refinement was accomplished using SIR97,[23] SHELXL97,[24] and WinGX.[25] Crystallographic data for **1a** and **1b** are given in Table 1.

Synthesis of $[(Cp^*Ru)_3(\mu\text{-}H)_4Y(OC_6H_3tBu_2\text{-}2,6)(\mu\text{-}H)_2RuCp^*]$ (1a). A solution of $[Cp^*RuH_2]_2$ (285 mg, 600 μmol) and $[Y(CH_2SiMe_3)_2(OC_6H_3tBu_2\text{-}2,6)(thf)_2]$ (183 mg, 300 μmol) in toluene (5 mL) was stirred at 60 °C for 1 d. After filtration the reaction mixture was concentrated and stored at −35 °C for several days to give black X-ray-quality crystals of **1a** (175 mg, 141 μmol, 46%). ^{1}H NMR (300 MHz, [D$_8$]toluene, 296 K): δ = −22.00 (s, 1H, Ru*H*Ru), −10.90 (d, J_{HY} = 11.3 Hz, 1H, Y*H*Ru), −8.63

Table 1. Summary of crystallographic data.

	1a	**1b**
Formula	$C_{54}H_{87}ORu_4Y$	$C_{54}H_{87}LuORu_4$
M_r	1245.43	1331.49
Crystal system	monoclinic	monoclinic
Space group	$P2_1/c$	$P2_1/m$
a[Å]	18.2779(6)	11.7600(6)
b[Å]	11.9461(4)	18.9746(6)
c[Å]	24.2292(8)	13.2349(3)
α[°]	90.00	90.00
β[°]	90.131(3)	109.764(2)
γ[°]	90.00	90.00
V[Å^3]	5290.4(3)	2779.29(18)
Z	4	2
T[K]	133(2)	133(2)
μ[mm^{-1}] (Mo-K_α)	2.236	2.855
Rflns collected	8363	37785
Indep Reflections	8363	5409
GoF	1.093	0.929
R_1 [I>2σ(I)]	0.0458	0.0325
wR_2 (all data)	0.1248	0.0763

(d, J_{HY} = 11.2 Hz, 1H, Y*H*Ru), −8.20 (d, J_{HY} = 14.0 Hz, 1H, Y*H*Ru), −7.30 (s, 1H, Ru*H*Ru), −6.14 (d, J_{HY} = 12.5 Hz, 1H, Y*H*Ru), 1.69 (s, 15H, C_5Me_5), 1.73 (s, 15H, C_5Me_5), 1.84 (s, 18H, CMe_3), 2.01 (s, 15H, C_5Me_5), 2.02 (s, 15H, C_5Me_5), 6.75 (t, J_{HH} = 7.6 Hz, 1H, *p*-$C_{14}H_{21}O$), 7.20 (d, J_{HH} = 7.6 Hz, 2H, *m*-$C_{14}H_{21}O$) ppm. $^{13}C\{^1H\}$ NMR (75.4 MHz, [D$_8$]toluene, 296 K): δ = 12.8 (s, C_5Me_5), 12.9 (s, C_5Me_5), 13.1 (s, C_5Me_5), 13.1 (s, C_5Me_5), 33.5 (s, *C*Me$_3$), 35.3 (s, CMe_3), 81.4 (s, C_5Me$_5$), 83.5 (s, C_5Me$_5$), 85.8 (s, C_5Me$_5$), 94.4 (s, C_5Me$_5$) ppm. Anal. calcd for $C_{54}H_{87}ORu_4Y$ (1245.43): C, 48.71; H, 6.59. Found: C 48.45; H, 6.15.

Synthesis of [(Cp*Ru)$_3$(μ-H)$_4$Lu(OC$_6$H$_3$*t*Bu$_2$-2,6)(μ-H)$_2$RuCp*] (1b). In the same manner as described for **1a** [Cp*RuH$_2$]$_2$ (272 mg, 572 μmol) and [Lu(CH$_2$SiMe$_3$)$_2$(OC$_6$H$_3$*t*Bu$_2$-2,6)(thf)$_2$] (200 mg, 286 μmol) were reacted in toluene (5 mL). A concentrated reaction mixture was stored at −35 °C for several days to give black cubes of **1b** (224 mg, 168 μmol, 58%) suitable for X-ray analysis. ^{1}H NMR (300 MHz, [D$_8$]toluene, 296 K): δ = −22.33 (s, 1H, Ru*H*Ru), −10.05 (s, 1H, Lu*H*Ru), −9.35 (s, 1H, Lu*H*Ru), −7.30 (s, 1H, Ru*H*Ru), −6.96 (s, 1H, Ru*H*Ru), −4.88 (s, 1H, Lu*H*Ru), 1.73 (s, 15H, C_5Me_5), 1.75 (s, 15H, C_5Me_5), 1.80 (s, 18H, CMe_3), 1.98 (s, 15H, C_5Me_5), 2.02 (s, 15H, C_5Me_5), 6.71 (t, J_{HH} = 7.7 Hz, 1H, *p*-$C_{14}H_{21}O$), 7.21 (d, J_{HH} = 7.7 Hz, 2H, *m*-$C_{14}H_{21}O$) ppm. $^{13}C\{^1H\}$ NMR (75.4 MHz, [D$_8$]toluene, 296 K): δ = 11.6 (s, C_5Me_5), 12.8 (s, C_5Me_5), 13.1 (s, C_5Me_5), 13.5 (s, C_5Me_5), 33.9 (s, CMe_3), 35.4 (s, *C*Me$_3$), 81.5 (s, C_5Me$_5$), 83.9 (s, C_5Me$_5$), 85.8 (s, C_5Me$_5$), 94.8 (s, C_5Me$_5$), 116.3 (s, *p*-$C_{14}H_{21}O$), 125.6 (s, *m*-$C_{14}H_{21}O$), 136.3 (s, *o*-$C_{14}H_{21}O$), 163.0 (s, *ipso*-$C_{14}H_{21}O$) ppm. Anal. calcd for $C_{54}H_{87}LuORu_4$ (1331.49): C, 52.08; H, 7.04. Found: C 52.09; H, 6.89.

Computational methods. Density functional theory (DFT) calculations were performed with the TURBOMOLE[26] program package. The RI-DFT method[27–29] applying the B-P86 functional[30–33] with the default grid was used for all calculations. Initial structures were derived from the X-ray crystal structures of the starting materials. Geometry optimization and calculation of vibrational frequencies and thermodynamic data was performed with the split-valence basis set def2-SV(P)[34] used for all atoms. The effective core potential def-ecp was applied to Lu[35] and Ru.[36]

Corresponding Author *E-mail: kempe@uni-bayreuth.de

Acknowledgments Financial support by the Deutsche Forschungsgemeinschaft (DFG) (KE 756/21-1) is gratefully acknowledged.

4.6 References

[1] See, for example: (a) H. Nakazawa, M. Itazaki, *Top. Organomet. Chem.* **2011**, *33*, 27–81; (b) C. Deutsch, N. Krause, *Chem. Rev.* **2008**, *108*, 2916–2927; (c) C. Lau, S. Ng, G. Jia, Z. Lin, *Coord. Chem. Rev.* **2007**, *251*, 2223–2237; (d) S. E. Clapham, A. Hadzovic, R. H. Morris, *Coord. Chem. Rev.* **2004**, *248*, 2201–2237; (e) R. Noyori, *Angew. Chem. Int. Ed.* **2002**, *41*, 2008–2022; (f) M. Ephritikhine, *Chem. Rev.* **1997**, *97*, 2193–2242.

[2] W. J. Evans, J. H. Meadows, T. P. Hanusa, *J. Am. Chem. Soc.* **1984**, *106*, 4454–4460.

[3] L. Schlapbach, A. Züttel, *Nature* **2001**, *414*, 353–358.

[4] A. P. Sobaczynski, T. Bauer, R. Kempe, *Organometallics* **2013**, *32*, 1363–1369.

[5] T. Shima, Z. Hou, *Chem. Eur. J.* **2013**, *19*, 3458–3466.

[6] T. Shima, Y. Luo, T. Stewart, R. Bau, G. J. McIntyre, S. A. Mason, Z. Hou, *Nat. Chem.* **2011**, *3*, 814–820.

[7] Y. Takenaka, Z. Hou, *Organometallics* **2009**, *28*, 5196–5203.

[8] T. Shima, Z. Hou, *Chem. Lett.* **2008**, *37*, 298–299.

[9] M. V. Butovskii, O. L. Tok, F. R. Wagner, R. Kempe, *Angew. Chem. Int. Ed.* **2008**, *47*, 6469–6472.

[10] N. S. Radu, P. K. Gantzel, T. D. Tilley, *J. Chem. Soc. Chem. Commun.* **1994**, 1175–1176.

[11] D. Alvarez, K. G. Caulton, W. J. Evans, J. W. Ziller, *Inorg. Chem.* **1992**, *31*, 5500–5508.

[12] D. J. Alvarez, K. G. Caulton, W. J. Evans, J. W. Ziller, *J. Am. Chem. Soc.* **1990**, *112*, 5674–5676.

[13] W. W. N. O, X. Kang, Y. Luo, Z. Hou, *Organometallics* **2014**, *33*, 1030–1043.

[14] T. Bauer, F. R. Wagner, R. Kempe, *Chem. Eur. J.* **2013**, *19*, 8732–8735.

[15] D. M. Michaelidou, M. L. Green, A. K. Hughes, P. Mountford, A. N. Chernega, A. K. Hughes, *Polyhedron* **1995**, *14*, 2663–2675.

[16] M. L. H. Green, A. K. Hughes, D. M. Michaelidou, P. Mountford, *J. Chem. Soc. Chem. Commun.* **1993**, 591–593.

[17] T. Shima, Z. Hou, *Organometallics* **2009**, *28*, 2244–2252.

[18] J. C. Slater, *J. Chem. Phys.* **1964**, *41*, 3199–3204.

[19] H. Suzuki, H. Omori, D. H. Lee, Y. Yoshida, M. Fukushima, M. Tanaka, Y. Morooka, *Organometallics* **1994**, *11*, 1129–1146.

[20] W. J. Evans, R. N. R. Broomhall-Dillard, J. W. Ziller, *Organometallics* **1996**, *15*, 1351–1355.

[21] H. Suzuki, T. Kakigano, K.-i. Tada, M. Igarashi, K. Matsubara, A. Inagaki, M. Oshima, T. Takao, *Bull. Chem. Soc. Jpn.* **2005**, *78*, 67–87.

[22] M. V. Butovskii, O. L. Tok, V. Bezugly, F. R. Wagner, R. Kempe, *Angew. Chem. Int. Ed.* **2011**, *50*, 7695–7698.

[23] A. Altomare, M. C. Burla, M. Camalli, G. L. Cascarano, C. Giacovazzo, A. Guagliardi, A. G. G. Moliterni, G. Polidori, R. Spagna, *J. Appl. Crystallogr.* **1999**, *32*, 115–119.

[24] G. M. Sheldrick, *Acta Crystallogr. A.* **2008**, *A64*, 112–122.

[25] L. J. Farrugia, *J. Appl. Crystallogr.* **1999**, *32*, 837–838.

[26] TURBOMOLE V6.5 2013, a development of University of Karlsruhe and Forschungszentrum Karlsruhe GmbH, 1989-2007, TURBOMOLE GmbH, since 2007; available from `http://www.turbomole.com`.

[27] K. Eichkorn, O. Treutler, H. Öhm, M. Häser, R. Ahlrichs, *Chem. Phys. Lett.* **1995**, *240*, 652–660.

[28] K. Eichkorn, F. Weigend, O. Treutler, R. Ahlrichs, *Theor. Chem. Acc.* **1997**, *97*, 119–124.

[29] M. Sierka, A. Hogekamp, R. Ahlrichs, *J. Chem. Phys.* **2003**, *118*, 9136–9148.

[30] P. A. M. Dirac, *Proc. R. Soc. A* **1929**, *123*, 714–733.

[31] J. C. Slater, *Phys. Rev.* **1951**, *81*, 385–390.

[32] S. H. Vosko, L. Wilk, M. Nusair, *Can. J. Phys.* **1980**, *58*, 1200–1211.

[33] A. D. Becke, *Phys. Rev. A* **1988**, *38*, 3098–3100.

[34] F. Weigend, R. Ahlrichs, *Phys. Chem. Chem. Phys.* **2005**, *7*, 3297–3305.

[35] X. Cao, M. Dolg, *J. Chem. Phys.* **2001**, *115*, 7348–7355.

[36] D. Andrae, U. Häußermann, M. Dolg, H. Stoll, H. Preuß, *Theor. Chim. Acta* **1990**, *77*, 123–141.

5

Alkane Elimination Reactions between Rare Earth Alkyls and Tungsten Hydrides

Adam P. Sobaczynski, Johannes Obenauf, and Rhett Kempe*

Lehrstuhl Anorganische Chemie II, Universität Bayreuth, 95440 Bayreuth, Germany

Published in *Eur. J. Inorg. Chem.* **2014**, 1211-1217.

5.1 Abstract

Alkane elimination of the yttrium monoalkyl [$Cp_2Y(CH_2SiMe_3)(thf)$] (Cp = cyclopentadienyl, thf = tetrahydrofuran, Me = methyl) with the tungsten hydrido carbonyl complex [$HW(CO)_3Cp$] in THF gave rise to the trinuclear complex [{$CpW(CO)_2(\mu$-$CO)\}_2YCp(thf)_3$] (**1**). In the course of the reaction, one Cp ligand per yttrium was redistributed, thus leading to the formation of [Cp_3Y] as a side product. To avoid the observed ligand redistribution, other solvents were investigated. The reaction of [$Cp_2Y(CH_2SiMe_3)(thf)$] with [$HW(CO)_3Cp$] in acetonitrile afforded the dinuclear complex [{$CpW(CO)_2(\mu$-$CO)\}YCp_2(NCMe)_2$] (**2**). The reaction of the yttrium dialkyl complex [$Y(CH_2SiMe_3)_2(OC_6H_3tBu_2$-2,6)$(thf)_2$] with [$HW(CO)_3Cp$] in toluene gave the polymeric compound [{$CpW(CO)_2(\mu$-$CO)\}_2Y(OC_6H_3tBu_2$-2,6)$]_n$ (**3**), whereas reaction in THF gave the molecular compound [{$CpW(CO)_2(\mu$-$CO)\}_2Y(OC_6H_3tBu_2$-2,6)$(thf)_3$] (**4**). The reaction of the yttrium trialkyl complex [$Y(CH_2SiMe_3)_3(thf)_2$] with [$HW(CO)_3$-Cp] in THF led to the formation of [{$CpW(CO)_2(\mu$-$CO)\}_3Y(thf)_5$] (**5**). Reaction of [(Ap*)$Y(CH_2SiMe_3)_2(thf)$] {Ap*H = (2,6-diisopropylphenyl)-[6-(2,4,6-triisopropylphenyl)pyridin-2-yl]amine} with [$HW(CO)_3Cp$] in THF was unexpectedly accompanied by the loss of the Ap* ligand and resulted in the formation of **5** too. Isocarbonyl linkage is the dominating interaction between the Y and the W complex moieties. All compounds were characterized by NMR and IR spectroscopy as well as elemental analysis. Complexes **1**, **2**, **4**, and **5** were additionally characterized by X-ray crystal structure analysis (X-ray diffraction).

5.2 Introduction

Unsupported bonds between rare-earth elements (RE)[1] and transition metals (TM) have received a great deal of attention recently.[2,3] Until 2008, only one molecular compound[4] featuring such a bond had been described in the literature, [$Cp(CO)_2Ru$-$Lu(Cp)_2(thf)$] (Cp = cyclopentadienyl), reported by Beletskaya et al.[5] A significant further development of RE-TM bonding took place through the introduction of the Cp_2Re moiety, a well-suited transition-metal partner to form unsupported bonds with RE.[6] This moiety allowed access to complexes with RE atoms bonded solely to transition metals,[7] to metal-metal bonding between divalent lanthanoids and TMs,[8] as well as to the controlled formation of RE-TM clusters by means of multiple C-H bond-activation steps.[9,10] The progress observed in RE-TM bonding by the use of the Cp_2Re moiety mainly resulted from two aspects: (1) alkane elimination starting from [Cp_2ReH] can be used as an efficient protocol to synthesize bimetallic compounds, and (2) the Cp_2Re moiety[6,7,9] is, unlike the Fp and Rp fragments {Fp = [$CpFe(CO)_2$], Rp = [$CpRu(CO)_2$]},[5b,8,11–13] carbonyl-free and isocarbonyl linkage is not relevant. The development of further carbonyl-free TM hydride precursors suitable for forming unsupported bonds towards RE by alkane elimination remains challenging. We recently studied the replacement of the carbonyl ligands of the Rp moiety by phosphane ligands.[14] Unfortunately, the hydride ligand of [Cp(dmpe)RuH] (dmpe = 1,2-bis(dimethylphosphanyl)-ethane) is unreactive, and C-H bond activation at the Cp ligand takes place rather than metal-metal bond formation. Inspired by some impressive work of the Mountford group,[12,13] who introduced carbonyl complexes for metal-metal bonding between alkaline earth elements and TM, we shifted our attention towards group 6 metal carbonyl hydrides. In the course of our search for new transition metal hydrido complexes for RE-TM bond formation by alkane elimination, we investigated the reactivity of [$HW(CO)_3Cp$] towards yttrium alkyls. The results obtained are discussed here.

Among the RE-TM carbonyl complexes, the isocarbonyl bridged compounds represent the most numerous class. The first reports on isocarbonyl bridged RE-TM compounds date back to the early 1970s.[15] Their identity was claimed by means of IR spectroscopy. In 1981, Andersen and Tilley reported on the synthesis of [$Cp^*_2Yb(\mu$-$CO)Co(CO)_3(thf)$] (Cp^* = pentamethylcyclopentadienyl), which was the first compound of this type to be analyzed by X-ray single-crystal structure analysis (XRD).[16] Several synthetic approaches towards isocarbonyl-bridged RE-TM complexes were established over the past four decades. Adduct formation, reduction of transition-metal carbonyls with divalent rare-earth complexes[17] or rare-earth amalgams,[18] salt elimination,[19] and transmetalation[20] are the most common routes to these complexes. The resulting complexes offer the potential to be used as catalysts in Fischer-Tropsch reactions[21] or as starting materials for perovskite-type oxides, which are used as methane oxidation catalysts.[22] Extensive work has been done by the Shore group, who were able to demonstrate that isocarbonyl- and isocyanide- bridged RE-TM systems are precursors for superior bimetallic heterogeneous catalysts for a variety of important processes such as the reduction of nitrogen oxides, vapor-phase hydrogenation of phenol, and hydrodechlorination of chlorobenzenes.[23]

5.3 Results and Discussion

Reaction of [HW(CO)$_3$Cp] with Yttrium Monoalkyls. We began our investigation with yttrium monoalkyls as the formation of a binuclear complex by alkane elimination would be expected. The reaction of equimolar amounts of the tungsten monohydride [HW(CO)$_3$Cp] and the yttrium monoalkyl [Cp$_2$Y(CH$_2$SiMe$_3$)(thf)] in THF did not give the expected binuclear complex. Instead [{CpW(CO)$_2$(μ-CO)}$_2$YCp(thf)$_3$] (**1**) was obtained as a yellow, air- and moisture-sensitive solid in 88% isolated yield (based on tungsten; Scheme 1). The product features two tungsten moieties, each with an isocarbonyl bridge towards yttrium. Interestingly, the reaction in THF is accompanied by the loss of one Cp ligand at the original Cp$_2$Y moiety and the subsequent formation of [Cp$_3$Y] as byproduct. The ligand redistribution could be explained by the formation of two energetically preferred products instead of a binuclear compound. [Cp$_3$Y] is thermodynamically preferred, and the oxophilic character of the yttrium atom favors a second isocarbonyl linkage. In agreement with Pearson's concept,[24] the hard yttrium center prefers the hard carbonyl oxygen atoms over the tungsten center (metal-metal bonding) that is clearly the weaker nucleophile or Lewis base.

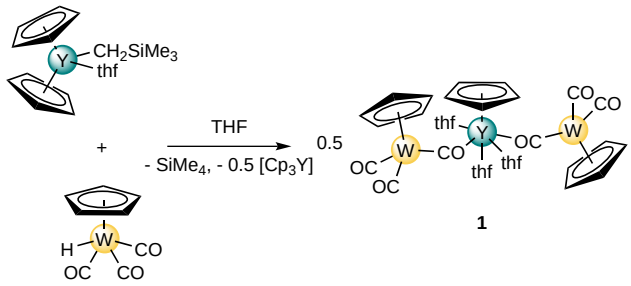

Scheme 1. Synthesis of **1**.

In the ^{1}H NMR spectrum of **1**, the Cp ligands on tungsten and yttrium show sharp singlets at δ = 5.23 and 6.06 ppm, respectively. The ^{13}C NMR spectrum shows single resonances for the Cp ligands on yttrium at δ = 111.8 ppm and at δ = 87.3 ppm for the Cp ligand on tungsten, respectively. The signal for the carbonyl ligands appears as broad resonance at δ = 228.5 ppm. The IR spectrum of 1 shows ν(CO) bands at 2024, 1934, 1910, 1808, and 1608 cm^{-1}, of which the last two were assigned as stretching modes of bridging carbonyls.

The molecular structure of **1** was determined by XRD and is presented in Figure 1. Compound **1** crystallizes in the monoclinic space group $P2_1/c$ with one thf molecule in the asymmetric unit. The six-coordinate yttrium atom exhibits a strongly distorted octahedral coordination sphere with two Y(μ-OC)W linkages and two thf ligands in the equatorial positions and a thf and Cp ligand in the axial positions. The geometry at the tungsten atoms is approximately tetrahedral. The structure shows a transoid conformation of the isocarbonyl bridged tungsten moieties. The two isocarbonyl linkages differ strongly in their Y–O–C angles. Y1–O1–C1 amounts to 142.9°, whereas Y1–O4–C26 amounts to 159.1°. The deviation from linearity of the Y–O–C motif is common in such systems.[19b,25] The values of the linking carbonyls for the C1–O1 and C26–O4 distances

amount to 1.237(12) and 1.206(12) Å, respectively. This shows an increase in the bond lengths relative to the mean C–O distance in the terminal carbonyls, which amounts to 1.177 Å. Concomitantly, the distances W1–C1 [1.876(12) Å] and W2–C26 [1.887(12) Å] are shortened relative to the mean distance for the terminal W–C linkages (1.934 Å). Both the bridging and terminal distances C–O are significantly shorter than in carbonyl W^0 complexes without Cp ligands, which is attributed to a weaker trans influence of the Cp ligand.[25] The different C–O separations in the terminal versus the bridging positions are in accordance with the more carbenoid character of the isocarbonyls.

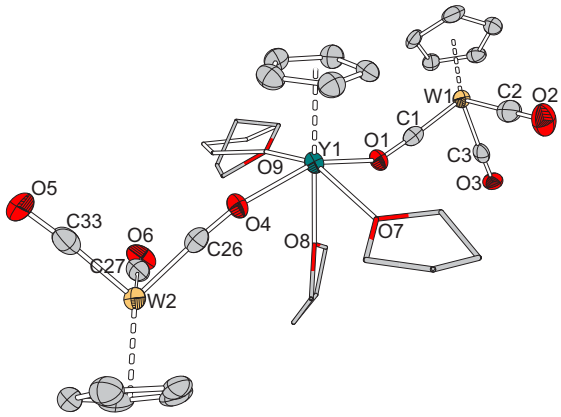

Figure 1. Molecular structure of **1**. Relevant atoms are depicted as 30% thermal ellipsoids. Hydrogen atoms and a thf molecule in the asymmetric unit have been omitted for clarity. One thf ligand shows disorder. Selected bond lengths [Å] and angles [°]: Y1–O1 2.262(6), Y1–O4 2.287(7), Y1–O7 2.363(6), Y1–O8 2.402(7), Y1–O9 2.339(7), Y1–$Cp_{centroid}$ 2.364, W1–$Cp_{centroid}$ 2.047, W2–$Cp_{centroid}$ 2.040, W1–C1 1.876(12), W1–C2 1.874(11), W1–C3 1.944(12), W2–C26 1.887(12), W2–C27 1.930(13), W2–C33 1.964(13), C1–O1 1.237(12), C2–O2 1.199(14), C3–O3 1.175(12), C26–O4 1.206(12), C27–O6 1.177(14), C33–O5 1.155(13); Y1–O1–C1 143.0, Y1–O4–C26 159.2, O1–Y1–O4 154.4.

To avoid the observed ligand redistribution, we examined the same reaction in acetonitrile. When the reaction of the tungsten monohydride $[HW(CO)_3Cp]$ with one equivalent of the yttrium monoalkyl $[Cp_2Y(CH_2SiMe_3)(thf)]$ was performed in acetonitrile, the binuclear compound $[\{CpW(CO)_2(\mu\text{-}CO)\}YCp_2(NCMe)_2]$ (**2**) could be isolated as a beige, air and moisture-sensitive solid in 82% yield (Scheme 2). In contrast to **1**, the formation of **2** proceeded without Cp ligand loss at the Cp_2Y moiety. The yttrium atom is coordinated by two additional molecules of acetonitrile. The solvate molecules seem to be bonded weakly as **2** loses its acetonitrile ligands upon prolonged exposure to vacuum.

The ^{1}H NMR spectrum displays the expected resonances for the two different types of Cp ligands at $\delta = 5.13$ and 6.04 ppm in a 1:2 ratio as well as the coordinating acetonitrile at $\delta = 1.92$ ppm. The ^{13}C NMR spectrum shows resonances at $\delta = 86.2$ and 111.4 ppm for the Cp ligands. The signals for coordinated acetonitrile were overlapped by the signals of the solvent. The IR spectrum shows ν(CO) stretches at 2024 and 1904 cm^{-1} for terminal carbonyls and at 1803 and 1660 cm^{-1} for bridging carbonyls. The latter appears at higher wavenumbers than in **1** (1608 cm^{-1}).

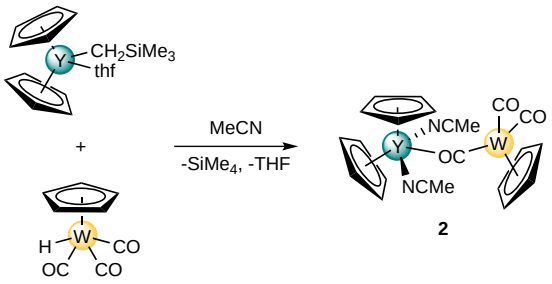

Scheme 2. Synthesis of **2**.

The solid-state structure of **2** was determined by XRD and is presented in Figure 2. The compound crystallizes in the monoclinic space group $P2_1/c$. Compound **2** exhibits a five-coordinate yttrium atom and an approximately tetrahedral geometry at the tungsten atom. The Y1–O1–C1 angle amounts to 136.0°, which is more acute than the Y–O–C angles (143.0, 159.2°) in **1**. As in the case of **1**, the bridging carbonyl C1–O1 exhibits an increased C–O bond length of 1.199(8) Å relative to the terminal carbonyls C2–O2 [1.152(8) Å] and C3–O3 [1.149(8) Å]. At the same time, the bond length W1–C1 [1.895(6) Å] is shortened relative to the distances W1–C2 [1.944(7) Å] and W1–C3 [1.958(7) Å]. This again compares well with the distances reported by Bruno and co-workers.[19a] The $Cp_{centroid}$–Y1–$Cp_{centroid}$ angle (128.7°) shows a slightly larger value than the mean of structurally characterized Cp_2Y moieties (124.6°).[26]

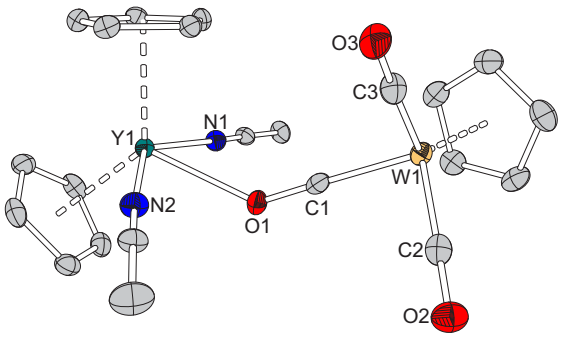

Figure 2. Molecular structure of **2**. Relevant atoms are depicted as 30% thermal ellipsoids. Hydrogen atoms have been omitted for clarity. Selected bond lengths [Å] and angles [°]: Y1–O1 2.349(4), Y1–N1 2.461(6), Y1–N2 2.459(5), $Cp_{centroid}$–Y1 2.351 (average value), W1–$Cp_{centroid}$ 2.035, W1–C1 1.895(6), W1–C2 1.944(7), W1–C3 1.958(7), C1–O1 1.199(8), C2–O2 1.153(8), C3–O3 1.149(8); $Cp_{centroid}$–Y1–$Cp_{centroid}$ 128.7, Y1–O1–C1 136.0.

Reaction of [HW(CO)$_3$Cp] with Yttrium Di- and Trialkyls. We decided to use a phenoxy-substituted yttrium dialkyl to offer stable ancillary ligand bonding to the metal. We first investigated the reaction in toluene. The reaction of the tungsten monohydride [HW(CO)$_3$Cp] (2 equiv) with [Y(CH$_2$SiMe$_3$)$_2$(OC$_6$H$_3$*t*Bu$_2$-2,6)(thf)$_2$] in toluene gave a solid polymeric product with the empirical formula [{CpW(CO)$_2$(μ-

CO)}$_2$Y(OC$_6$H$_3$(*t*Bu)$_2$-2,6)]$_n$ (**3**) in 92% isolated yield (Scheme 3). Compound **3** is sparingly soluble in toluene and insoluble in hexane. Upon exposure to air, compound **3** decomposes immediately. Attempts to obtain single crystals of **3** were not successful. When **3** was dissolved in THF, the molecular compound **4** was obtained. Therefore, we assume a polymeric structure for **3**. We explain the formation of a polymeric product in toluene with the lack of coordinating solvent molecules and therefore formation of intermolecular interactions to saturate the Lewis acidic yttrium atom.

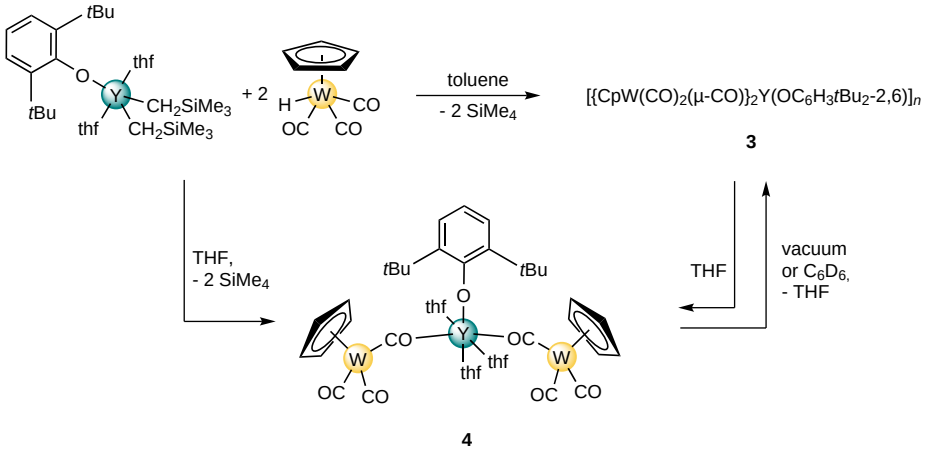

Scheme 3. Synthesis of **3** and **4**.

However, **3** could be analyzed by NMR spectroscopy. The ^{1}H NMR spectrum exhibits two sharp resonances for the *tert*-butyl groups and the Cp ligands at δ = 1.36 and 4.49 ppm, respectively. The aromatic protons show the expected signals, which resolve into a doublet of doublets at δ = 6.86 ppm and a doublet at δ = 7.19 ppm. The ^{13}C NMR spectrum exhibits two signals for the *tert*-butyl groups at δ = 30.4 and 34.4 ppm. The Cp ligand on tungsten shows one resonance at δ = 87.3 ppm. The carbonyls could not be detected. The IR spectrum shows ν(CO) bands at 2025, 1924, 1778, 1720, and 1658 cm^{-1}. The low-energy stretching compares well with the one in **2**.

Reaction of the tungsten monohydride [HW(CO)$_3$Cp] (2 equiv) with [Y(CH$_2$SiMe$_3$)$_2$-(OC$_6$H$_3$*t*Bu$_2$-2,6)(thf)$_2$] in THF gave the molecular compound [{CpW(CO)$_2$(μ- CO)}$_2$-Y(OC$_6$H$_3$*t*Bu$_2$-2,6)(thf)$_3$] (**4**) as a yellow, air- and moisture-sensitive solid in 80% isolated yield (Scheme 3). Under vacuum or when dissolved in C$_6$D$_6$, compound **4** loses its thf ligands and forms the polymeric compound **3**. In the ^{1}H NMR spectrum of **4**, the signal of the *tert*-butyl groups appears at δ = 1.36 ppm. The Cp ligands give rise to a single resonance at δ = 5.59 ppm. The protons of the coordinating thf molecules give signals at δ = 1.67 and 3.53 ppm, respectively. The aromatic protons give a triplet at δ = 6.65 ppm and a doublet at δ = 7.04 ppm. All resonances appear downfield-shifted relative to **3**. In the ^{13}C NMR spectrum of **4**, the *tert*-butyl groups give signals at δ = 30.7 and 35.2 ppm. The carbon atoms of the Cp ligand resonate at δ = 88.7 ppm. Additional resonances for the thf molecules appear at δ = 26.4 and 68.2 ppm. In contrast to **3**, the *ipso*-carbon atom of the phenolate in **4**, which appears at δ = 162.2 ppm, splits

into a doublet with $^2J_{CY} = 5.6$ Hz. The chemical shifts are slightly shifted to lower field relative to their counterparts in **3**. The carbonyls were detected as broad signal at $\delta =$ 228.2 ppm. The IR spectrum exhibits ν(CO) stretches at 2024, 1934, 1811, 1727, 1650, and 1608 cm^{-1}. The low-energy band for the bridging carbonyls is identical to that in **1**.

The solid-state structure of **4** was determined by XRD and is presented in Figure 3. The complex crystallizes in the monoclinic space group $C2/c$. Compound **4** shows a distorted octahedral geometry at the yttrium atom comparable to that of **1**. The tungsten moieties are isocarbonyl-linked to the yttrium atom and exhibit tetrahedral coordination. Their cisoid conformation is contrary to the transoid one for **1** and is presumably caused by steric repulsion with the *tert*-butyl groups. The angle Y1–O4–C1 was found to be 161.5° and is thus more obtuse than complexes **1** and **2**. The C1–O4 distance of the bridging carbonyl amounts to 1.289(9) Å and is elongated relative to the terminal carbonyls C2–O6 and C3–O5 (1.195(9) and 1.199(9) Å, respectively). Simultaneously, the distance W1–C1 [1.806(8) Å] is shortened relative to the distances W1–C2 and W1–C3 [1.904(9), 1.912(10) Å] of the terminal carbonyls. These bonds appear shorter than their counterparts described by Bruno and co-workers.[19a] Owing to its $C2$ axis, compound **4** exhibits a linear arrangement of the atoms C15, O3, Y1, and O2.

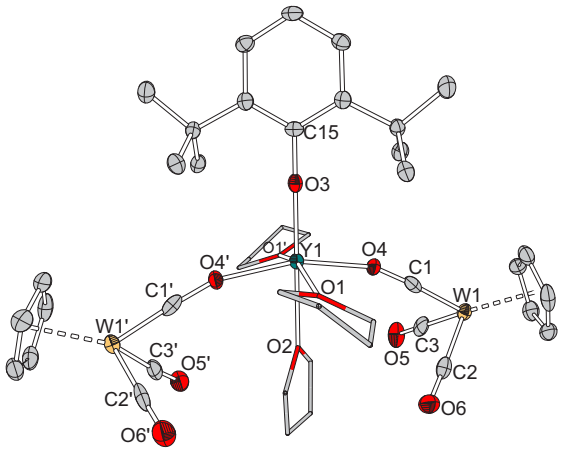

Figure 3. Molecular structure of **4**. Relevant atoms are depicted as 30% thermal ellipsoids. Hydrogen atoms have been omitted for clarity. Selected bond lengths [Å] and angles [°]: Y1–O1 2.308(4), Y1–O2 2.382(7), Y1–O3 2.063(7), Y1–O4 2.190(5), C1–O4 1.289(9), C2–O6 1.195(9), C3–O5 1.199(9), W1–C1 1.806(8), W1– C2 1.904(9), W1–C3 1.912(10), $Cp_{centroid}$–W1 2.040; Y1–O4–C1 161.6, O2–Y1–O3 180.0, O4–Y1–O4' 162.8.

To offer a more Lewis basic ligand than the phenolate, [(Ap*)Y(CH_2SiMe_3)$_2$(thf)] was chosen as reaction partner. Reaction of [HW(CO)$_3$Cp] (2 equiv) with [(Ap*)Y(CH_2SiMe_3)$_2$(thf)] (1 equiv) (Scheme 4) in THF unexpectedly led to the formation of [{CpW(CO)$_2$(μ-CO)}$_3$Y(thf)$_5$] (**5**).[27] The formation of **5** was, as in the case of **1**, accompanied by the loss of a ligand from the yttrium precursor. Interestingly, here [HW(CO)$_3$Cp] protonates the amido ligand Ap*. The reaction of an yttrium trialkyl with the tungsten hydrido complex should also lead to the formation of **5**.

To confirm this hypothesis, we treated $[Y(CH_2SiMe_3)_3(thf)_2]$ with three equivalents of $[HW(CO)_3Cp]$ to give **5**, which was obtained as a yellow, air- and moisture-sensitive solid in 91% isolated yield (Scheme 4).

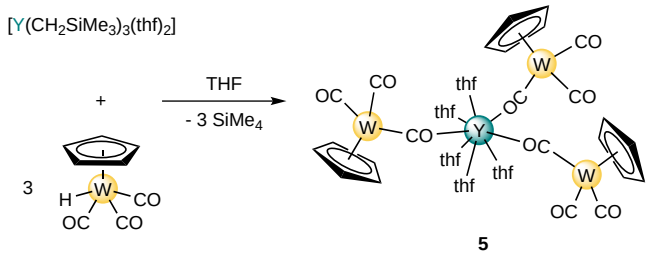

Scheme 4. Synthesis of **5**.

The ^1H NMR spectrum of **5** shows a resonance at $\delta = 5.28$ ppm assigned to the Cp ligands on tungsten and a set of two signals for the coordinated thf molecules at $\delta = 1.75$ and 3.60 ppm, respectively. The ^{13}C NMR spectrum exhibits signals at $\delta = 26.4$ and 68.2 ppm for the thf ligands and at $\delta = 87.6$ ppm for the Cp ligands. The carbonyls gave rise to a broad resonance at $\delta = 227.9$ ppm. The IR spectrum exhibits ν(CO) bands at 2025 and 1913 cm^{-1} for terminal carbonyls, and at 1811, 1726, and 1625 cm^{-1} for bridging ones. These bands compare with stretches at 2000, 1900, 1800, 1740, and 1660 cm^{-1} for the related $[\{CpMo(CO)_2(\mu\text{-}CO)\}_3La(thf)_5]$ reported by Beletskaya and co-workers.[28]

The solid-state structure of **5** was determined by XRD and is presented in Figure 4. The complex crystallizes in the triclinic space group $P\bar{1}$. $[\{CpW(CO)_2(\mu\text{-}CO)\}_3Y(thf)_5]$ is isostructural with $[\{CpMo(CO)_2(\mu\text{-}CO)\}_3La(thf)_5]$. The eight-coordinate yttrium atom exhibits square antiprismatic geometry with three isocarbonyl-bonded tungsten moieties and five coordinated thf molecules. The tungsten moieties show tetrahedral coordination. The angles Y–C–O amount to 169.5, 167.9, and 167.6°, which are the most obtuse in the series of compounds described herein. As in the compounds described above, the distances C–O [1.182(7), 1.200(6), 1.213(6) Å] of the bridging carbonyls are elongated relative to the mean distances C–O (1.148, 1.156, 1.151 Å) of the corresponding terminal carbonyls. The distances W–C of the bridging carbonyls [1.886(5), 1.890(5), 1.902(5) Å] are shortened relative to the mean value of their terminal (1.945, 1.947, 1.954 Å) counterparts. The W–C distances compare well with the ones reported by Bruno and co-workers.[19a]

5.4 Conclusion

We have shown that yttrium-tungsten bimetallic complexes can be synthesized in high yields by alkane elimination. Reaction of the tungsten hydrido complex $[HW(CO)_3Cp]$ with different yttrium alkyls readily gave di-, tri-, or tetranuclear complexes with the structures being dependent on the chosen alkyl complex and solvent. All obtained compounds exhibit no direct RE-TM interactions. Instead isocarbonyl linkages and zwitte-

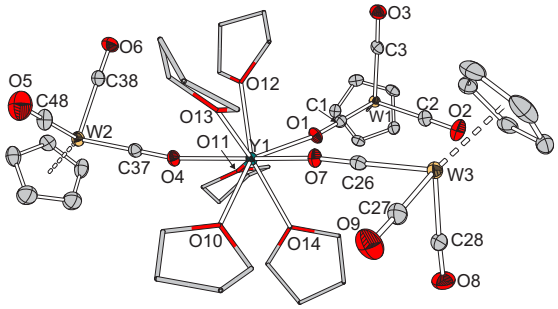

Figure 4. Molecular structure of **5**. Relevant atoms are depicted as 30% thermal ellipsoids. Hydrogen atoms and a thf molecule in the asymmetric unit have been omitted for clarity. Selected bond lengths [Å] and angles [°]: O1–Y1 2.305(4), O4–Y1 2.261(3), O7–Y1 2.255(3), O10–Y1 2.376(4), O11–Y1 2.419(4), O12–Y1 2.363(4), O13–Y1 2.453(4), O14–Y1 2.414(4), C1–O1 1.182(7), C26–O7 1.200(6), C37–O4 1.213(6), C2–O2 1.142(7), C3–O3 1.153(7), C38–O6 1.137(8), C48–O5 1.167(8), C27–O9 1.150(7), C28–O8 1.157(7), C1–W1 1.902(5), C37–W2 1.890(5), C26–W3 1.886(5), $Cp_{centroid}$–W1 2.045, $Cp_{centroid}$–W2 2.033, $Cp_{centroid}$–W3 2.033; Y1–O1–C1 169.5, Y1–O4–C37 167.6, Y1–O7–C26 167.9, O1–Y1–O4 141.1, O1–Y1–O7 72.1, O4–Y1–O7 143.7.

rionic complexes are formed. The acidity of the hydride of $[HW(CO)_3Cp]$ is high enough to allow a fast alkane elimination reaction with RE alkyls. However, $[W(CO)_3Cp]^-$, or rather the tungsten center, did not show enough nucleophilicity to compete with the carbonyls as a Lewis basic partner to form unsupported RE-TM bonds. Other carbonyl-containing fragments – such as Fp and Rp, the prototypes of a TM metalloligand in polar metal-metal bonding – seem to have that nucleophilicity. They accumulate sufficient negative charge at the metal center (nucleophilicity) to compete with existing carbonyl oxygen atoms or solvent molecules that can coordinate.

5.5 Experimental Section

General Procedures: All manipulations were carried out under a dry and oxygen-free argon atmosphere using Schlenk techniques or in a nitrogen-filled glovebox (mBraun 120-G) with a high capacity recirculator (below 0.1 ppm O_2). THF, toluene, and hexane were distilled from sodium benzophenone ketyl. Acetonitrile was dried with CaH_2. Deuterated solvents were obtained from Cambridge Laboratories and were degassed, dried, and distilled prior to use. $[Y(CH_2SiMe_3)_3(thf)_2]$[29] and $[Cp_2Y(CH_2SiMe_3)(thf)]$[6] were prepared according to published procedures. $[Y(CH_2SiMe_3)_2(OC_6H_3tBu_2\text{-}2,6)(thf)_2]$[30] was prepared with slight modifications to literature procedures. $[HW(CO)_3Cp]$ (Aldrich) was used as received.

Instrumentation: ^1H and ^{13}C NMR spectra were recorded with a Varian Unity 300 MHz spectrometer. Chemical shifts are given in ppm, were measured at 25 °C, and are referenced to the residual solvent signals for ^1H and ^{13}C. IR spectra were recorded with a JASCO FT/IR-6100 FTIR spectrometer. Samples were prepared as Nujol mulls be-

Table 1. Summary of crystallographic data.

	1	**2**	**4**	**5**
Formula	$C_{33}H_{39}O_9W_2Y{\cdot}C_4H_8O$	$C_{22}H_{21}N_2O_3WY$	$C_{42}H_{55}O_{10}W_2Y$	$C_{44}H_{55}O_{14}W_3Y{\cdot}C_4H_8O$
M_r	1108.36	634.16	1176.45	1520.44
Crystal system	monoclinic	monoclinic	monoclinic	triclinic
Space group	$P2_1/c$	$P2_1/c$	$C2/c$	$P\bar{1}$
a[Å]	23.4226(14)	16.1157(9)	12.1450(5)	11.1251(4)
b[Å]	10.2452(5)	10.0259(6)	24.2930(7)	11.2405(4)
c[Å]	15.8493(9)	14.9015(9)	14.7240(7)	20.6473(7)
α[°]	90.00	90.00	90.00	97.403(3)
β[°]	96.733(5)	114.435(4)	97.317(4)	101.324(3)
γ[°]	90.00	90.00	90.00	92.520(3)
V[Å^3]	3777.1(4)	2192.1(2)	4308.8(3)	2504.23(15)
Z	4	4	4	2
T[K]	133(2)	133(2)	133(2)	133(2)
μ[mm^{-1}] (Mo-K_α)	7.655	7.902	6.716	8.081
Rflns collected	47869	33416	9034	40835
Indep rflns	7120	4949	4588	12003
GoF	0.947	1.004	0.993	1.019
R_1 [I>2σ(I)]	0.0490	0.0426	0.0337	0.0373
wR_2 (all data)	0.1144	0.1072	0.0573	0.0924

tween NaCl plates. Elemental analyses (CHN) were carried out with a Vario El III. X-ray crystal structure analyses were performed with a STOE-IPDS II diffractometer equipped with an Oxford Cryostream low-temperature unit. Structure solution and refinement was accomplished using SIR97,[31] SHELXL97,[32] and WinGX.[33] A summary of crystallographic data is given in Table 1.

CCDC-970791 (for **1**), -970792 (for **2**), -970793 (for **4**), and -970794 (for **5**) contain the supplementary crystallographic data for this paper. These data can be obtained free of charge from The Cambridge Crystallographic Data Centre `via www.ccdc.cam.ac.uk/data_request/cif.`

[{CpW(CO)$_2$(μ-CO)}$_2$YCp(thf)$_3$] (1): [Cp$_2$Y(CH$_2$SiMe$_3$)(thf)] (95 mg, 250 μmol) and [HW(CO)$_3$Cp] (84 mg, 250 μmol) were dissolved at –40 °C in THF (3 mL). The reaction mixture was stirred and warmed slowly to room temperature. The resulting golden solution was filtered, concentrated, and stored at –35 °C to give [{CpW(CO)$_2$(μ-CO)}$_2$YCp(thf)$_3$] (**1**) (115 mg, 111 μmol, 88% based on tungsten) as a yellow solid. Single crystals of **1** suitable for X-ray analysis were grown from a concentrated THF solution at –35 °C. ^{1}H NMR (300 MHz, [D$_8$]THF): δ = 1.68 (br s, 12 H, β-H thf), 3.53 (br s, 12 H, α-H thf), 5.23 (s, 10H, W-C$_5H_5$), 6.06 (s, 5H, Y-C$_5H_5$) ppm. ^{13}C{^{1}H} NMR (75.4 MHz, [D$_8$]THF): δ = 26.4 (s, β-C thf), 68.3 (s, α-C thf), 87.3 (s, C_5H$_5$), 111.8 (s, C_5H$_5$), 228.5 (br s, CO) ppm. IR (Nujol): ν = 2024, 1934, 1910, 1808, 1608 [all ν(CO)] cm^{-1}. $C_{33}H_{39}O_9W_2Y$ (1036.24): calcd. C 38.25, H 3.79; found C 38.17, H 3.63.

[{CpW(CO)$_2$(μ-CO)}YCp$_2$(NCMe)$_2$] (2): In the same manner as described for **1**, [Cp$_2$Y(CH$_2$SiMe$_3$)(thf)] (95 mg, 250 μmol) and [HW(CO)$_3$Cp] (84 mg, 250 μmol) were reacted in acetonitrile (3 mL). The resulting golden solution was filtered, concentrated, and stored at –35 °C to give [{CpW(CO)$_2$(μ-CO)}YCp$_2$(NCMe)$_2$] (**2**) (132 mg, 207 μmol, 82%) as beige X-ray-quality crystals. ^{1}H NMR (300 MHz, CD$_3$CN): δ = 1.92 (s, 6 H, CH_3), 5.13 (s, 5H, W-C$_5H_5$), 6.04 (s, 10H, Y-C$_5H_5$) ppm. ^{13}C{^{1}H} NMR (75.4 MHz, CD$_3$CN): δ = 86.2 (s, W-C_5H$_5$), 111.4 (s, Y-C_5H$_5$) ppm. IR (Nujol): ν = 2024, 1904, 1803, 1660 [all ν(CO)] cm^{-1}. C$_{22}$H$_{21}$N$_2$O$_3$WY (634.17): calcd. C 41.67, H 3.34, N 4.42; found C 39.38, H 3.00, N 4.00. The observed lower C value might be due to MeCN loss during drying.

[{CpW(CO)$_2$(μ-CO)}$_2$Y(OC$_6$H$_3$*t*Bu$_2$-2,6)]$_n$ (3): A mixture of [Y(CH$_2$SiMe$_3$)$_2$(OC$_6$H$_3$*t*Bu$_2$-2,6)(thf)$_2$] (77 mg, 125 μmol) and [HW(CO)$_3$Cp] (84 mg, 250 μmol) was dissolved at –40 °C in THF (3 mL). The reaction mixture was stirred and warmed slowly to room temperature. The resulting precipitate was separated by filtration, washed with toluene (5 mL) and hexane (5 mL), and dried under vacuum to give [{CpW(CO)$_2$(μ-CO)}$_2$Y(OC$_6$H$_3$*t*Bu$_2$-2,6)]$_n$ (**3**) (112 mg, 116 μmol, 92%) as an off-white solid. ^{1}H NMR (300 MHz, C$_6$D$_6$): δ = 1.36 (s, 18H, CH_3), 4.49 (s, 10H, W-C$_5H_5$), 6.86 (dd, $^3J_{HH}$ = 7.5, $^3J_{HH}$ = 8.1 Hz, 1 H, *p*-C$_{14}$H$_{21}$O), 7.19 (d, $^3J_{HH}$ = 7.5Hz, 2 H, *m*-C$_{14}$H$_{21}$O) ppm. ^{13}C{^{1}H} NMR (75.4 MHz, C$_6$D$_6$): δ = 30.4 (s, *C*Me$_3$), 34.4 (s, *C*Me$_3$), 88.5 (s, C_5H$_5$), 120.4 (s, *p*-C$_{14}$H$_{21}$O), 125.4 (s, *m*-C$_{14}$H$_{21}$O), 136.1 (s, *o*-C$_{14}$H$_{21}$O), 154.3 (s, *i*-C$_{14}$H$_{21}$O) ppm. IR (Nujol): ν = 2025, 1924, 1778, 1720, 1658 [all ν(CO)] cm^{-1}. C$_{30}$H$_{31}$O$_7$W$_2$Y (960.15): calcd. C 37.53, H 3.25; found C 37.02, H 3.17.

[{CpW(CO)$_2$(μ-CO)}$_2$Y(OC$_6$H$_3$*t*Bu$_2$-2,6)(thf)$_3$] (4): In the same manner as described for **3**, [Y(CH$_2$SiMe$_3$)$_2$(OC$_6$H$_3$*t*Bu$_2$-2,6)(thf)$_2$] (77 mg, 125 μmol) and [HW(CO)$_3$Cp] (84 mg, 250 μmol) were reacted in THF (3 mL). The resulting golden solution was filtered, concentrated, and stored at –35 °C to give [{CpW(CO)$_2$(μ-CO)}$_2$Y(OC$_6$H$_3$*t*Bu$_2$-2,6)(thf)$_3$] (**4**) (119 mg, 101 μmol, 80%) as a yellow solid. Single crystals of **4** suitable for X-ray analysis were grown from a concentrated THF solution at room temperature. ^{1}H NMR (300 MHz, [D$_8$]THF): δ = 1.36 (s, 18H, CH_3), 1.67 (br s, 12 H, β-H thf), 3.53 (br s, 12H, α-H thf), 5.59 (s, 10H, C$_5H_5$), 6.65 (t, $^3J_{HH}$ = 7.8 Hz, 1 H, *p*-C$_{14}$H$_{21}$O), 7.04 (d, $^3J_{HH}$ = 7.8 Hz, 2 H, *m*-C$_{14}$H$_{21}$O) ppm. ^{13}C{^{1}H} NMR (75.4 MHz, [D$_8$]THF): δ = 26.4 (s, β-C thf), 30.7 (s, C*Me*$_3$), 35.2 (s, *C*Me$_3$), 68.2 (s, α-C thf), 88.7 (s, C_5H$_5$), 117.8 (s, *p*-C$_{14}$H$_{21}$O), 125.4 (s, *m*-C$_{14}$H$_{21}$O), 139.9 (s, *o*-C$_{14}$H$_{21}$O), 162.2 (d, $^2J_{CY}$ = 5.6 Hz, *i*-C$_{14}$H$_{21}$O), 228.2 (br s, *C*O) ppm. IR (Nujol): ν = 2024, 1934, 1811, 1727, 1650, 1608 [all ν(CO)] cm^{-1}. C$_{38}$H$_{47}$O$_9$W$_2$Y (**4**–thf, 1104.36): calcd. C 41.33, H 4.29; found C 41.40, H 4.25.

[{CpW(CO)$_2$(μ-CO)}$_3$Y(thf)$_5$] (5): A mixture of [Y(CH$_2$SiMe$_3$)$_3$(thf)$_2$] (74 mg, 150 μmol) and [HW(CO)$_3$Cp] (150 mg, 450 μmol) was dissolved at –40 °C in THF (5 mL). The reaction mixture was stirred and warmed slowly to room temperature. The resulting yellow solution was filtered, concentrated, and stored at –35 °C to give

[{$CpW(CO)_2(\mu$-CO)}$_3$Y(thf)$_5$] (**5**) (198 mg, 137 μmol, 91%) as yellow crystals. Single crystals of **5** suitable for X-ray analysis were obtained by slowly cooling a hot saturated THF solution of **5** to ambient temperature. ^{1}H NMR (300 MHz, [D$_8$]THF): δ = 1.75 (br s, 20 H, β-H thf), 3.60 (br s, 20 H, α-H thf), 5.27 (s, 15H, C_5H_5) ppm. ^{13}C{^{1}H} NMR (75.4 MHz, [D$_8$]THF): δ = 26.4 (s, β-C thf), 68.2 (s, α-C thf), 87.6 (s, C_5H$_5$), 227.9 (br s, *C*O) ppm. IR (Nujol): ν = 2025, 1913, 1811, 1726, 1625 [all ν(CO)] cm^{-1}. $C_{40}H_{47}O_{13}W_3Y$ (**5**–thf, 1376.22): calcd. C 34.91, H 3.44; found C 34.66, H 3.34.

Supporting Information (see footnote on the first page of this article): CIF files for compounds **1**, **2**, **4**, and **5**.

Acknowledgments Financial support by the Deutsche Forschungsgemeinschaft (DFG) (KE 756/21-1) is gratefully acknowledged.

5.6 References

[1] The term RE describes the group 3 elements scandium, yttrium, lanthanum and the 14 lanthanoids (Ce to Lu).

[2] For a key paper of ligand-supported RE-TM bonding, see: A. Spannenberg, M. Oberthür, H. Noss, A. Tillack, P. Arndt, R. Kempe, *Angew. Chem.* **1998**, *110*, 2190–2192.

[3] (a) D. Patel, S. T. Liddle, *Rev. Inorg. Chem.* **2012**, *32*, 1–22; (b) B. Oelkers, M. V. Butovskii, R. Kempe, *Chem. Eur. J.* **2012**, *18*, 13566–13579.

[4] Polymeric structures that contain both isocarbonyl-linked and direct RE-TM interactions were reported shortly afterwards: (a) H. Deng, S. G. Shore, *J. Am. Chem. Soc.* **1991**, *113*, 8538–8540; (b) H. Deng, S.-H. Chun, P. Florian, P. J. Grandinetti, S. G. Shore, *Inorg. Chem.* **1996**, *35*, 3891–3896.

[5] (a) G. K.-I. Magomedov, A. Z. Voskoboynikov, E. B. Chuklanova, A. I. Gusev, I. P. Beletskaya, *Metalloorg. Khim.* **1990**, *3*, 706–707; (b) I. P. Beletskaya, A. Z. Voskoboynikov, E. B. Chuklanova, N. I. Kirillova, A. K. Shestakova, I. N. Parshina, A. I. Gusev, G. K.-I. Magomedov, *J. Am. Chem. Soc.* **1993**, *115*, 3156–3166.

[6] M. V. Butovskii, O. L. Tok, F. R. Wagner, R. Kempe, *Angew. Chem. Int. Ed.* **2008**, *47*, 6469–6472.

[7] M. V. Butovskii, C. Döring, V. Bezugly, F. R. Wagner, Y. Grin, R. Kempe, *Nat. Chem.* **2010**, *2*, 741–744.

[8] C. Döring, A.-M. Dietel, M. V. Butovskii, V. Bezugly, F. R. Wagner, R. Kempe, *Chem. Eur. J.* **2010**, *16*, 10679–10683.

[9] M. V. Butovskii, O. L. Tok, V. Bezugly, F. R. Wagner, R. Kempe, *Angew. Chem. Int. Ed.* **2011**, *50*, 7695–7698.

[10] T. Bauer, F. R. Wagner, R. Kempe, *Chem. Eur. J.* **2013**, *19*, 8732–8735.

[11] P. L. Arnold, J. McMaster, S. T. Liddle, *Chem. Commun.* **2009**, 818–820.

[12] M. P. Blake, N. Kaltsoyannis, P. Mountford, *J. Am. Chem. Soc.* **2011**, *133*, 15358–15361.

[13] M. P. Blake, N. Kaltsoyannis, P. Mountford, *Chem. Commun.* **2013**, *49*, 3315–3317.

[14] A. P. Sobaczynski, T. Bauer, R. Kempe, *Organometallics* **2013**, *32*, 1363–1369.

[15] See, for example: (a) A. E. Crease, P. Legzdins, *J. Chem. Soc. Dalt. Trans.* **1973**, 1501–1507; (b) A. E. Crease, P. Legzdins, *J. Chem. Soc. Chem. Commun.* **1972**, 268–269.

[16] T. D. Tilley, R. A. Andersen, *J. Chem. Soc. Chem. Commun.* **1981**, 985–986.

[17] See, for example: (a) J. M. Boncella, R. A. Andersen, *Inorg. Chem.* **1984**, *23*, 432–437; (b) T. D. Tilley, R. Andersen, *J. Am. Chem. Soc.* **1982**, *104*, 1772–1774; (c) A. Recknagel, A. Steiner, S. Brooker, D. Stalke, F. T. Edelmann, *Chem. Ber.* **1991**, *124*, 1373–1375; (d) A. C. Hillier, S. Y. Liu, A. Sella, O. Zekria, M. R. Elsegood, *J. Organomet. Chem.* **1997**, *528*, 209–215.

[18] I. Beletskaya, G. Suleimanov, R. Shifrina, R. Mekhdiev, T. Agdamskii, V. N. Khandozhko, N. Kolobova, *J. Organomet. Chem.* **1986**, *299*, 239–244.

[19] See, for example: (a) P. N. Hazin, C. Lakshminarayan, L. S. Brinen, J. L. Knee, J. W. Bruno, W. E. Streib, K. Folting, *Inorg. Chem.* **1988**, *27*, 1393–1400; (b) P. N. Hazin, J. C. Huffman, J. W. Bruno, *J. Chem. Soc. Chem. Commun.* **1988**, 1473–1474.

[20] See, for example: G. Z. Suleimanov, V. N. Khandozhko, L. T. Abdullaeva, R. R. Shifrina, K. S. Khalilov, N. E. Kolobova, I. P. Beletskaya, *J. Chem. Soc. Chem. Commun.* **1984**, 191–192.

[21] C. K. Rofer-DePoorter, *Chem. Rev.* **1981**, *81*, 447–474.

[22] See, for example: (a) O. Buassi-Monroy, C. Luhrs, A. Chávez-Chávez, C. Michel, *Mater. Lett.* **2004**, *58*, 716–718; (b) Y. Sadaoka, E. Traversa, M. Sakamoto, *J. Alloys Compd.* **1996**, *240*, 51–59; (c) A. Baiker, P. E. Marti, P. Keusch, E. Fritsch, A. Reller, *J. Catal.* **1994**, *146*, 268–276.

[23] See, for example: (a) S. Jujjuri, E. Ding, S. G. Shore, M. A. Keane, *Appl. Organomet. Chem.* **2003**, *17*, 493–498; (b) S. G. Shore, E. Ding, C. Park, M. A. Keane, *Catal. Commun.* **2002**, *3*, 77–84; (c) A. Rath, E. Aceves, J. Mitome, J. Liu, U. S. Ozkan, S. G. Shore, *J. Mol. Catal. A* **2001**, *165*, 103–111.

[24] R. G. Pearson, *J. Am. Chem. Soc.* **1963**, *85*, 3533–3539.

[25] K. Müller-Buschbaum, G. B. Deacon, C. M. Forsyth, *Eur. J. Inorg. Chem.* **2002**, *2002*, 3172–3177.

[26] For the calculation of the mean value, 109 Cp_2Y fragments were considered [CSD (Cambridge Structural Database) v. 5.31].

[27] N. M. Scott, R. Kempe, *Eur. J. Inorg. Chem.* **2005**, *2005*, 1319–1324.

[28] A. Pasynskii, I. L. Eremenko, G. Z. Suleimanov, Y. Nuriev, I. Beletskaya, V. E. Shklover, Y. T. Struchkov, *J. Organomet. Chem.* **1984**, *266*, 45–52.

[29] M. F. Lappert, R. Pearce, *J. Chem. Soc. Chem. Commun.* **1973**, 126.

[30] W. J. Evans, R. N. R. Broomhall-Dillard, J. W. Ziller, *Organometallics* **1996**, *15*, 1351–1355.

[31] A. Altomare, M. C. Burla, M. Camalli, G. L. Cascarano, C. Giacovazzo, A. Guagliardi, A. G. G. Moliterni, G. Polidori, R. Spagna, *J. Appl. Crystallogr.* **1999**, *32*, 115–119.

[32] G. M. Sheldrick, *Acta Crystallogr. A.* **2008**, *A64*, 112–122.

[33] L. J. Farrugia, *J. Appl. Crystallogr.* **1999**, *32*, 837–838.

6

Heterometallic Hydride Complexes of Rare-Earth Metals and Ruthenium through C-H Bond Activation

Adam P. Sobaczynski, Tobias Bauer, and Rhett Kempe*

Lehrstuhl Anorganische Chemie II, Universität Bayreuth, 95440 Bayreuth, Germany

Published in *Organometallics* **2013**, *32*, 1363-1369.

6.1 Abstract

The reaction of rare-earth monoalkyl complexes [$Cp_2Ln(CH_2SiMe_3)(thf)$ (Cp = cyclopentadienyl; Ln = Y, Lu) with the ruthenium hydride complex [HRu(dmpe)Cp] (dmpe = bis(dimethylphosphino)ethane) gave the corresponding bimetallic hydride complexes [$Cp_2Ln(\mu$-H)(μ-η^1:η^5-C_5H_4)Ru(dmpe)] (Ln = Y (**1a**), Lu (**1b**)). One carbon atom of the Ru-bound Cp ligand bridges to the Ln atom in these complexes. The linkage is formed via a C-H bond activation step. The reaction of **1a** with diphenylacetylene led to the formation of [$Cp_2Y(\mu$-H)$\{\mu$-(Ph)CC(Ph)(C_5H_4)$\}$Ru(dmpe)], which indicates that the Y–C σ-bond is significantly more reactive than the Y–H–Ru bond. The reaction of bis(alkyl) complexes [$Ln(CH_2SiMe_3)_2(OC_6H_3(tBu)_2$-2,6)$(thf)_2$] (Ln = Y, Lu, *t*Bu = *tert*-butyl) with [HRu(dmpe)Cp] gave the dimeric products [$(OC_6H_3(t$Bu$)_2$-2,6)Ln(μ-H)(μ-η^1:η^5-C_5H_4)$\{\kappa^3$C,P,P'-CH_2(Me)P(CH_2)$_2$P$Me_2\}$Ru]$_2$ (Ln = Y, Lu) by double C-H bond activation. The complexes were characterized by NMR spectroscopy, X-ray crystal structure analysis (XRD), and elemental analysis.

6.2 Introduction

Metal hydrides have become essential in a variety of catalytic processes.[1] In addition, heteromultimetallic hydride complexes are of interest due to promising novel properties and reactivity not accessible for the homometallic species. These may arise from the synergetic effect of the two different metals. Although rare-earth-metal–transition-metal hydride complexes were first explored almost three decades ago, their number still remains limited. This could be explained by the lack of efficient synthetic strategies as well as difficulties in characterizing and handling such compounds. In terms of characterization, the Ln-based paramagnetism restricts NMR studies and the hydride ligands are difficult to localize via X-ray crystal structure analysis (XRD) in the presence of the heavily diffracting Ln atoms. However, intermetallic hydrides of rare-earth metals and transition metals play an important role in our daily life. In particular, these compounds are used as hydrogen storage materials[2] or in batteries.[3] Molecular analogues of such intermetallic compounds might become interesting alternatives for both of these applications and others.

The first report on a rare-earth-metal–transition-metal hydride complex dates back to 1984, when Evans and coworkers described the synthesis of the heterotrimetallic complex $[\{(CH_3C_5H_4)_2YH\}_2\{(CH_3C_5H_4)_2ZrH\}H]$ by reaction of the dimeric hydride $[(CH_3C_5H_4)_2YH(thf)]_2$ with 0.5 equiv of the zirconium dihydride $[(CH_3C_5H_4)ZrH_2]_2$.[4] In 1990, the groups of Caulton and Evans reported on the synthesis of the first structurally authenticated rare-earth-metal–transition-metal hydride complexes.[5] Reacting $[Cp_2LnMe(thf)]$ (Ln = Y, Lu) with $[Re_2H_8(PMe_2Ph)_4]$ yielded $[Cp_2Y(thf)Re_2H_7(PMe_2Ph)_4]$ or $[Cp_2LuRe_2H_7(PMe_2Ph)_4]$ by methane elimination. However, the hydrides were not located in the XRD analysis. Two years later, the same authors reported on the synthesis of $[Cp_2Y(thf)H_6Re(PPh_3)_2]$ by reacting $[Cp_2YMe(thf)]$ with $[ReH_7(PPh_3)_2]$ following the same synthetic protocol.[6] The product was structurally characterized by X-ray analysis, including location of the hydride ligands. Green and co-workers reported on the synthesis of rare-earth-metal–transition-metal hydride complexes containing divalent ytterbium.[7,8] Treatment of YbI_2 with 2 equiv of the potassium salts $K[(PMe_3)_3WH_5]$ and $K[Cp_2NbH_2]$ resulted in the formation of $[\{(PMe_3)_3WH_5\}_2Yb(diglyme)]$ and $[(Cp_2NbH_2)_2Yb(diglyme)]$ (diglyme = $(MeOCH_2CH_2)_2O$), respectively. Tilley and co-workers reported on the synthesis of rare-earth-metal-tungsten heterobimetallic complexes by H_2 elimination.[9] Reaction of 0.5 equiv of $[LnCp^*_2H]_2$ (Ln = Y, Sm, Cp* = pentamethylcyclopentadienyl) with $[WCp_2H_2]$ led to the formation of $[Cp^*_2Ln(\mu\text{-}\eta^1{:}\eta^5\text{-}C_5H_4)H_2WCp]$, accompanied by C-H bond activation. In 2008 we used the alkane elimination route to obtain the heterotrimetallic trihydride $[H(Cp^*Ru)_2H_2YCp_2]$ by reacting $[Cp_2Y(CH_2SiMe_3)(thf)]$ with $[Cp^*RuH_2]_2$.[10] Hou and Shima reported on the synthesis of a variety of heteromultimetallic hydride complexes by alkane elimination from half-sandwich rare-earth-metal (bis)alkyl complexes with transition-metal polyhydrides.[11,12] Furthermore, Hou and Takenaka reported on the reaction of the metallocene hydride complexes $[(C_5Me_4SiMe_3)_2LnH(thf)]$ (Ln = Y, Dy, Lu) with $[Cp^*IrH_4]$, which gave the corresponding heterobimetallic trihydride complexes $[(C_5Me_4SiMe_3)_2LnH_3IrCp^*]$ (Ln =

Y, Dy, Lu) with evolution of H_2.[13] Very recently, Hou and co-workers reported that tetranuclear rare-earth-metal octahydride clusters react with transition-metal hydrides to give structurally well-defined heteromultimetallic polyhydride complexes.[14] Unprecedented insight into the hydrogen addition and release process of this family of complexes could be given.

So far heteromultimetallic hydride complexes combining rare-earth metals (RE) and transition metals (TM) have been prepared by alkane elimination,[5,6,10] salt elimination,[7,8] C-H activation,[9,11] and H_2 elimination.[9,13] Herein, we report on the syntheses of heterometallic hydride complexes containing the rare-earth metals Y and Lu and the transition metal Ru by C-H bond activation.

At this point only a few transition-metal fragments are known to form unsupported rare-earth-metal–transition-metal bonds,[15–18] namely, $[Ru(CO)_2Cp]$,[19,20] $[Fe(CO)_2Cp]$,[21–24] and $[ReCp_2]$.[10,20,25,26] The preference for carbonyl-containing transition-metal fragments can be explained by their Lewis basic character that allows the formation of metal-metal bonds with their Lewis acidic rare-earth counterparts. In addition to that, the carbonyl ligands were useful in structure determination by use of IR spectroscopy. However, unambiguous evidence of unsupported metal-metal bonds could only be provided by Xray structure analysis, as carbonyl-containing transition-metal fragments are likely to form isocarbonyl linkages to rare-earth-metal fragments.[20–22,24] Motivated by the success of the carbonyl-free fragment $[ReCp_2]$ in the formation of unsupported rare-earth-metal–transition-metal bonds,[10,20,25,26] we were looking for further non-carbonyl transition-metal fragments. We have chosen the most prominent fragment, $[Ru(CO)_2Cp]$, and decided to replace the carbonyl ligands by a chelating phosphine ligand, thus identifying [HRu(dmpe)Cp][27] as a possible candidate for the formation of unsupported rare-earth-metal–transition-metal bonds by alkane elimination. However, [HRu(dmpe)Cp] was found to react with rare-earth-metal alkyls to form C-H bond activated products by deprotonation of the Cp ligands.[9]

6.3 Results and Discussion

Reaction of $[Cp_2Ln(CH_2SiMe_3)(thf)]$ with the Ruthenium Hydride Complex [HRu(dmpe)Cp]. The reaction of the ruthenium monohydride [HRu(dmpe)Cp] with a slight excess of the monoalkyl complex $[Cp_2Y(CH_2SiMe_3)(thf)]$[10] in toluene at –40 °C with subsequent warming to ambient temperature gave the heterobimetallic monohydride species **1a** in 69% yield with liberation of tetramethylsilane (Scheme 1). The Cp ligand on Ru undergoes a C-H bond activation to form a Y-C bond in **1a**. The corresponding Lu analogue **1b** was prepared in the same manner in 63% yield. During the formation of **1a**, **1b** amorphous, insoluble byproducts are formed, which can be separated by filtration.

The ^{1}H NMR spectra of **1a** and the Lu counterpart **1b** exhibit a single resonance due to two equivalent Cp ligands on Ln and two singlets due to a mirror-symmetric Ru-bonded C_5H_4 ligand. **1a** shows a doublet of triplets pattern at –16.19 ppm with $^1J_{HY}$ = 17.2 Hz and $^2J_{HP}$ = 26.7 Hz in the hydride region, whereas the lutetium compound **1b** shows a triplet at −15.04 ppm with $^2J_{HP}$ = 25.2 Hz. The six-line pattern for **1a** and the

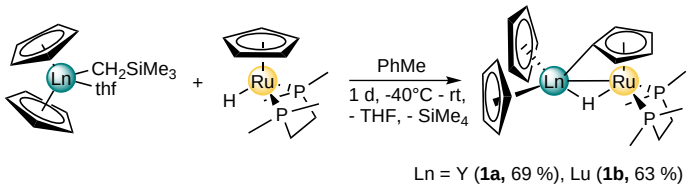

Scheme 1. Synthesis of **1a**, **1b**.

smaller $^2J_{HP}$ coupling constant in **1a** compared to $^2J_{HP}$ = 36.9 Hz in [HRu(dmpe)Cp] are consistent with a bridging hydride between the two metal centers. The $^{31}P\{^1H\}$ NMR spectra[28] of **1a**, **1b** both show a doublet with $^2J_{PH}$ = 24.4 Hz and $^2J_{PH}$ = 22.6 Hz, respectively. **1a** shows no P-Y coupling.

The solid-state structure of **1a** was determined by XRD and is presented in Figure 1. Both metal centers are linked by a metal-metal bond which is bridged by a hydride and a μ-η^1:η^5-bonded C_5H_4 ligand. The Y-Ru distance amounts to 3.1107(12) Å, which is slightly longer than the hydride-bridged Y-Ru bonds in $[Cp_2Y(thf)H_6Re(PPh_3)_2]$[6] (3.088(1) Å) and in $[H(Cp^*Ru)_2H_2YCp_2]$[10] (3.046 Å; average value). The bridging Y1–C2 bond amounts to 2.410(10) Å and is bent downward by 40.4° with respect to the plane of the C_5H_4 ligand. The C_5H_4 ligand itself is tilted by 5.8° out of the horizontal plane of the Ru-Y connecting line. The bridging hydride is slightly out of the plane spanned by C2, Y1, and Ru1 (C2–Y1–Ru1–H1Y = 166.2°), which can be explained by the twisted arrangement of the phosphine featuring two different Y–P distances. The two Cp ligands on Y adopt an eclipsed conformation. The angle $(Cp_{centroid})$–Y–$(Cp_{centroid})$ of 128.7° is larger than in $[H(Cp^*Ru)_2H_2YCp_2]$[10] (124.5°) and also larger than the mean angle in literature-known, structurally characterized Cp_2Y moieties[29] (124.6°). This shows the demand for steric saturation at the Y atom.

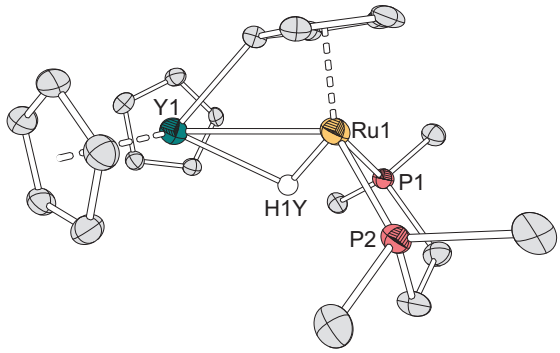

Figure 1. ORTEP drawing of **1a** with 50% thermal ellipsoids. Hydrogen atoms, except the bridging hydride, have been omitted for clarity. Selected bond lengths (Å), angles (deg), and torsion angles (deg): Ru1–Y1 = 3.1107(12), C2–Y1 = 2.410(10), Y1–H1Y = 2.4875(9), Ru1–H1Y = 1.4721(7), $Cp_{centroid}$–Ru1 = 1.871, $Cp_{centroid}$–Y1 = 2.368 (average value); $Cp_{centroid}$–Y1–$Cp_{centroid}$ = 128.7, Ru1–Y1–$Cp_{centroid}$ = 84.2, $Cp_{centroid}$–C2–Y1 = 139.6, Ru1–H1Y–Y1 = 100.4; C2–Y1–Ru1–H1Y = 166.2.

The formation of **1a** by reacting equimolar amounts of [$Cp_2Y(CH_2SiMe_3)(thf)$] and [HRu(dmpe)Cp] in C_6D_6 at room temperature was monitored by ^1H NMR spectroscopy, resulting in the diagram depicted in Figure 2. A significant amount of Y-containing byproducts is formed and can be withdrawn from the reaction mixture by precipitation; thus, unreacted [HRu(dmpe)Cp] remains. The reaction can be regarded as complete after about 120 min. **1a** decomposes slowly in solution. After some weeks the concentration of **1a** decreases while the concentration of Cp_3Y increases.

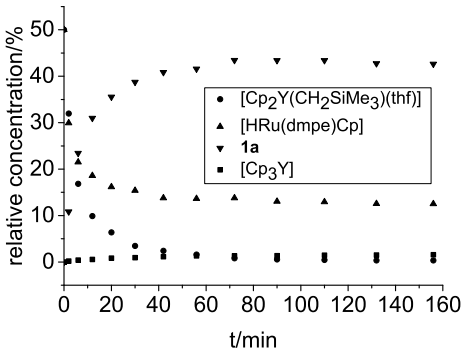

Figure 2. Time-dependent plot for the formation of **1a**.

In order to determine the origin of the bridging hydride in **1a**, we decided to prepare [DRu(dmpe)Cp] and elucidate whether or not an intermediate with an unsupported metal-metal bond is involved in the formation of **1a**. Reaction of [ClRu(dmpe)Cp][30] with sodium in CD_3OD gave the deutero complex [DRu(dmpe)Cp] (deuterium incorporation 85%).[31] The reaction proceeds via formation of the alkoxide followed by deuteride abstraction with release of the corresponding aldehyde.[32] [DRu(dmpe)Cp] was also synthesized in a second pathway in which in situ generated [$HRu(CO)_2Cp$][33] was treated with D_2[34] followed by substitution of the carbonyl ligands with dmpe (deuterium incorporation 90%).

Treatment of [$Cp_2Y(CH_2SiMe_3)(thf)$] with [DRu(dmpe)Cp] afforded the deuterated compound **1ad** and revealed that the bridging hydride comes from the Ru-bonded hydride. The C-H activation does not take place via Ln-Ru bond formation and subsequent C-H activation of the Cp ring. The reaction pathway via Ln-Ru bond formation would eliminate DCH_2SiMe_3, and compound **1a** should be the product. Mixtures of **1a** and **1a**d would indicate the relevance of both reaction pathways.

In order to investigate its reactivity, **1a** was treated with diphenylacetylene at ambient temperature. This led to the insertion of the alkyne into the Y-C bond to yield **2a** (Scheme 2). We believe that the strained Y-C bond is responsible for the observed reactivity.

The ^1H NMR spectrum of **2a** exhibits a doublet of triplets pattern at –14.97 ppm with $^1J_{HY}$ = 18.9 Hz and $^2J_{HP}$ = 28.5 Hz in the hydride region. The $^{31}P\{^1H\}$ NMR spectrum shows two doublets with $^2J_{PH}$ = 26.5 Hz and $^2J_{PH}$ = 32.1 Hz; however, no P-Y coupling was observed as in the case of **1a**.

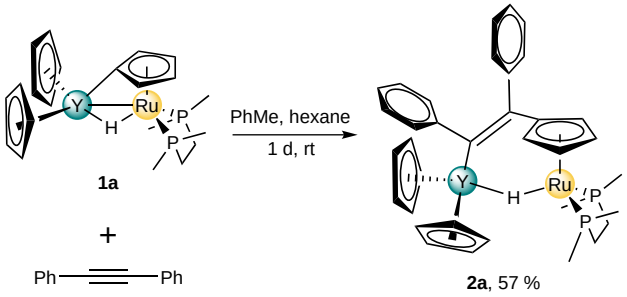

Scheme 2. Synthesis of **2a**.

The structure of **2a** was determined by XRD and is presented in Figure 3. The Ru–Y distance is lengthened to 3.3720(5) Å. The C6–C7 distance amounts to 1.351(4) Å and is in agreement with a C-C double bond. The sums of angles around C6 and C7 are 359.9 and 357.9°, respectively, indicating an almost planar environment around these carbon atoms. The torsion angle C30–C6–C7–Y1 (160.3°) is smaller than C4–C6–C7–C8 (171.9°); thus, the C7–Y1 bond is slightly out of plane.

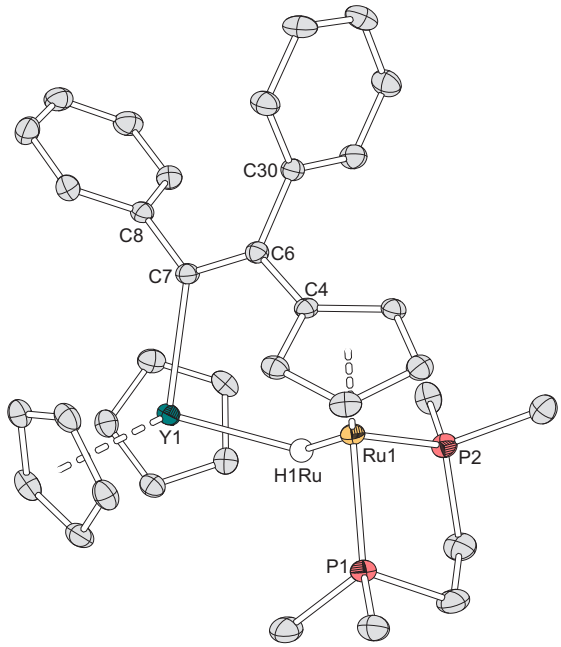

Figure 3. ORTEP drawing of **2a** with 50% thermal ellipsoids. Hydrogen atoms, except the bridging hydride, have been omitted for clarity. Selected bond lengths (Å), angles (deg), and torsion angles (deg): Ru1–Y1 = 3.3720(5), Ru1–H1Ru = 1.479, Y1–H1Ru = 2.355, $Cp_{centroid}$–Y1 = 2.395 (average value), Y1–C7 = 2.454(3), $Cp_{centroid}$–Ru1 = 1.889, C6–C7 = 1.351(4); $Cp_{centroid}$–Y1–$Cp_{centroid}$ = 122.6, Ru1–H1Ru–Y1 = 121.5; C30–C6–C7–Y1 = 160.3, C4–C6–C7–C8 = 171.9.

Reaction of [Ln(CH$_2$SiMe$_3$)$_2$(OC$_6$H$_3$(*t*Bu)$_2$-2,6)(thf)$_2$] with the Ruthenium Hydride Complex [HRu(dmpe)Cp]. Because we observed C-H bond activation of Cp ligands bound to Ru, we became interested in what would happen if we reacted the ruthenium hydride with bis(alkyl) complexes. In these sterically less crowded alkyls Ln-Ru bond formation could become relevant. The reaction of the ruthenium hydride [HRu(dmpe)Cp] with an equimolar amount of the bis(alkyl) complexes [Ln(CH$_2$SiMe$_3$)$_2$(OC$_6$H$_3$(*t*Bu)$_2$-2,6)(thf)$_2$] (Ln = Y, Lu)[26] in toluene at –40 °C with subsequent warming to ambient temperature and workup at low temperatures afforded the tetrametallic dihydride complexes **3a**, **3b** in 55% and 44% yields, respectively (Scheme 3). The Cp ligand undergoes a C-H bond activation to form a Ln-C bond. Unexpectedly, a second C-H bond activation occurs at one of the aliphatic methyl groups of the phosphine ligand to form a second Ln-C bond.

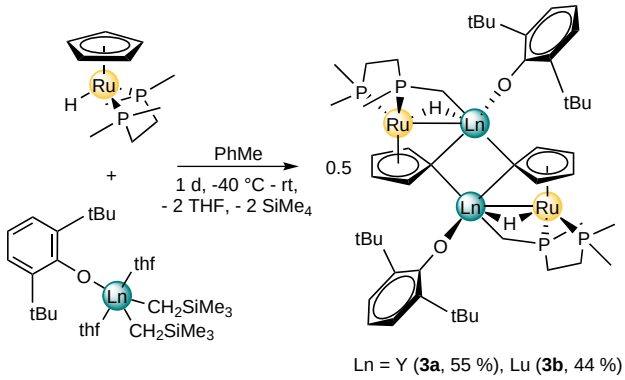

Scheme 3. Synthesis of **3a**, **3b**.

The ^{1}H NMR spectrum of **3a** gives rise to a six-line pattern in the hydride region at –13.38 ppm with $^1J_{HY}$ = 18.8 Hz and $^2J_{HP}$ = 31.2 Hz. The lutetium analogue **3b** shows a triplet at –12.17 ppm with $^2J_{HP}$ = 31.7 Hz. The ^{31}P{^{1}H} NMR spectra of **3a**, **3b** exhibit two resonances each, with additional P-Y coupling for **3a**, which amounts to 7.9 Hz. This is in contrast to the case for **1a** and can be explained by coupling via the bridging methylene group of **3a**.

The dimeric structure of **3a** was determined by XRD and is presented in Figure 4. The two units of the molecule are linked by a central rectangle which is spanned by Y1, Y1', C5, and C5'. This structural motif is related to one of our previously reported C-H activated products, [Cp$_2$ReLa(thf)CpReC$_5$H$_4$]$_2$. The formation of a dimer shows the greater demand for steric saturation at Y due to the less shielding phenoxide ligand in comparison to the two Cp ligands in **1a**. Y1 and Ru1 are linked by a metal-metal bond which amounts to 2.9283(10) Å and which is significantly (0.183 Å) shorter than in **1a**. This bond is bridged by a hydride, a μ-η^1:η^5-bonded C$_5$H$_4$ ligand, and the phosphine ligand's deprotonated methyl group. The bridging Y1–C5 bond length in **3a** is 0.190 Å longer than in **1a**. Simultaneously the C$_5$H$_4$ ligand is tilted by 3.3° out of the horizontal plane defined by the Y-Ru bond, thus facing away from Y. The distance Y1–C5' (2.479(8) Å) is significantly shorter than Y1–C5 (2.595(8) Å) and lies within

the expected range for a Y-C bond. The torsion angle Ru1–Y1–C5–Y1' is 164.9°. The torsion angle C5–Y1–Ru1–H1Ru (123.3°) shows that the phosphine moiety is twisted around the Y–Ru bond. The angle between the Cp plane and the plane spanned by Y1, Y1', C5, and C5' is 76.2°. The coordination environment about ruthenium is similar to that for [HRu(dmpe)Cp].

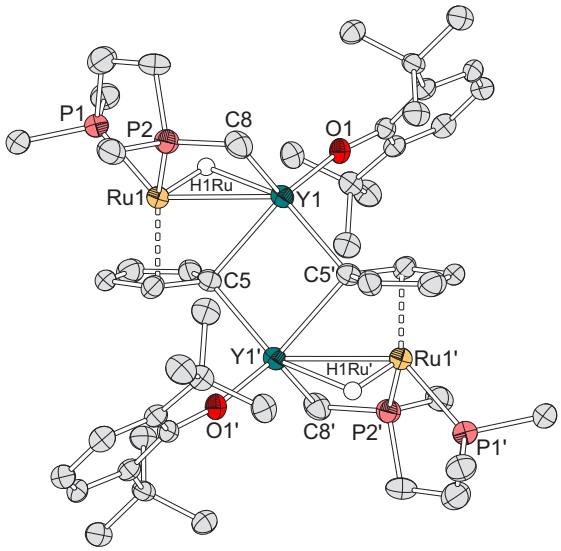

Figure 4. ORTEP drawing of **3a** with 50% thermal ellipsoids. Hydrogen atoms, except the bridging hydride, have been omitted for clarity. Selected bond lengths (Å), angles (deg), and torsion angles (deg): Ru1–Y1 = 2.9283(10), C5–Y1 = 2.595(8), C5'–Y1 = 2.479(8), C8–Y1 = 2.399(7), O1–Y1 = 2.066(5), H1Ru–Y1 = 2.329, H1Ru–Ru1 = 1.448, $Cp_{centroid}$–Ru1 = 1.869; Y1–Ru1–$Cp_{centroid}$ = 93.3, Y1–O1–C = 24168.1(5), O1–Y1–C8 = 117.9(3), O1–Y1–Ru1 = 118.20(14), C8–Y1–C5 = 105.6(3), C5'–Y1–C8 = 107.1(3), C5–Y1–O1 = 130.4(2), C5–Y1–Ru1 = 132.12(19), C5– Y1–C5' = 87.0(3), Y1–C5–Y1' = 93.0(3); Ru1–Y1–C5–Y1' = 164.9, C5–Y1–Ru1–H1Ru = 123.3.

6.4 Conclusion

In summary, we have demonstrated that [HRu(dmpe)Cp] can serve as a building block for the synthesis of heterometallic hydride complexes containing both rare-earth metals and transition metals. The reaction of $[Cp_2Ln(CH_2SiMe_3)(thf)]$ (Ln = Y, Lu) with [HRu(dmpe)Cp] leads to heterometallic hydrides. The formation of these hydrides proceeds via direct attack of an aromatic C-H bond. The formation of transient unsupported Ln–Ru bonds is not relevant. Reactivity studies revealed a highly reactive Cp-Ln σ-bond. The reaction of $[Ln(CH_2SiMe_3)_2(OC_6H_3(t\mathrm{Bu})_2\text{-}2,6)(thf)_2]$ (Ln = Y, Lu) with [HRu(dmpe)Cp] proceeds via multiple C-H bond activations.

Table 1. Summary of crystallographic data.

	1a	2a	3a	3b
Formula	$C_{21}H_{31}P_2RuY$	$C_{35}H_{41}P_2RuY$	$C_{50}H_{82}O_2P_4Ru_2Y_2$	$C_{50}H_{80}Lu_2O_2P_4Ru_2{\cdot}3C_7H_8$
M_r	1108.36	634.16	1176.45	1520.44
Crystal system	monoclinic	triclinic	monoclinic	triclinic
Space group	$P2_1/c$	$P\bar{1}$	$P2_1/n$	$P\bar{1}$
a[Å]	15.2280(6)	12.4160(5)	9.7450(7)	15.0930(7)
b[Å]	7.3090(3)	12.5160(5)	25.8100(19)	15.5230(8)
c[Å]	19.6230(8)	13.7560(5)	11.9330(9)	18.3880(8)
α[°]	90.00	103.685(3)	90.00	97.095(4)
β[°]	96.902(3)	113.818(3)	113.074(6)	112.040(3)
γ[°]	90.00	105.650(3)	90.00	110.461(4)
V[Å^3]	2168.24(15)	1732.21(14)	2761.3(4)	3576.8(3)
Z	4	2	2	2
T[K]	133(2)	133(2)	133(2)	133(2)
μ[mm^{-1}] (Mo-K_α)	3.509	2.215	2.768	3.280
Rflns collected	15567	6432	9116	12016
Indep rflns	4097	4627	4627	12016
GoF	1.193	0.797	0.613	0.742
R_1 [I>2σ(I)]	0.0636	0.0275	0.0395	0.0372
wR_2 (all data)	0.1778	0.0555	0.0844	0.0803

6.5 Experimental Section

General Procedures. All manipulations were carried out under a dry and oxygen-free argon atmosphere using Schlenk techniques or in a nitrogen-filled glovebox (mBraun 120-G) with a high-capacity recirculator (below 0.1 ppm of O_2). THF, toluene, diethyl ether, hexane, and heptane were distilled from sodium benzophenone ketyl. Dichloromethane was dried over CaH_2, methanol was dried over magnesium, and acetone was dried over K_2CO_3. Deuterated solvents were obtained from Cambridge Laboratories and were degassed, dried, and distilled prior to use. [Lu(CH$_2$SiMe$_3$)$_2$(OC$_6$H$_3$(*t*Bu)$_2$-2,6)(thf)$_2$],[26] Ru_3CO_{12}[35] and [ClRu(PPh$_3$)$_2$Cp][36] were prepared according to published procedures. [Y(CH$_2$SiMe$_3$)$_2$(OC$_6$H$_3$(*t*Bu)$_2$-2,6)(thf)$_2$][37] and [HRu(dmpe)Cp][27] were prepared with minor modifications of these procedures. [Cp$_2$Lu(CH$_2$SiMe$_3$)(thf)][38] was prepared according to the alkane elimination route described by Butovskii et al., starting from [Lu(CH$_2$SiMe$_3$)$_3$(thf)$_2$].[10] [ClRu(dmpe)Cp][39] was prepared by the method of Treichel using dmpe.[30] [DRu(dmpe)Cp] was synthesized according to Chinn and Heinekey[31] as well as by adapting the procedure from Casey and coworkers.[34] YCl_3 (Strem), dmpe (Strem), and D_2 (Air Liquide) were used as received.

Instrumentation. ^{1}H, ^{13}C, and ^{31}P NMR spectra were recorded on Varian Unity 300 MHz and Varian Unity 400 MHz spectrometers. Chemical shifts are given in ppm, measured at 26 °C, and referenced to the residual solvent signals for ^{1}H and ^{13}C. Elemental analyses were carried out using a Vario El III instrument. X-ray crystal structure analyses were performed by using a STOE-IPDS II diffractometer equipped with an

Oxford Cryostream low-temperature unit. Structure solution and refinement was accomplished using SIR97,[40] SHELXL97,[41] and WinGX.[42] Crystallographic data for **1a**, **2a**, and **3a**, **3b** are given in Table 1.

Modified Synthesis of [ClRu(dmpe)Cp]. [ClRu(dmpe)Cp] was prepared following a literature procedure using dmpe. A mixture of [ClRu(PPh_3)$_2$Cp] (2.66 g, 3.66 mmol) and dmpe (1.04 g, 6.90 mmol) in 500 mL of toluene was refluxed for 20 h. After removal of all volatiles the orange oil was dissolved in a minimal amount of CH_2Cl_2 and placed on a column packed with neutral alumina. PPh_3 was eluted with CH_2Cl_2, followed by elution of the product as a yellow band using acetone. Collecting this band and evaporating the solvent gave a solid residue, which was taken up in diethyl ether. After filtration the volume of the solution was reduced, and it was stored overnight at –20 °C to give [ClRu(dmpe)Cp] (608 mg, 1.73 mmol, 47%) as orange needles. ^{1}H NMR (300 MHz, C_6D_6): δ (ppm) 0.87-1.60 (m, 16H, dmpe), 4.41 (s, 5H, C_5H_5). ^{13}C{^{1}H} NMR (75.4 MHz, C_6D_6): δ(ppm) 15.8 (m, PCH_3), 20.9 (m, PCH_3), 29.8 (m, PCH_2), 77.3 (s, C_5H_5). ^{31}P{^{1}H} NMR (161.9 MHz, C_6D_6): δ (ppm) 55.1 (s).

Modified Synthesis of [DRu(dmpe)Cp]. *Method a.* To [ClRu(dmpe)Cp] (112 mg, 318 μmol) in 2 mL of CD_3OD was added sodium (45 mg, 1.96 mmol). The mixture was heated to 70 °C for 2 h. Meanwhile its color changed from orange to light yellow and NaCl precipitated. After filtration and reduction of the volume of the solution, storage overnight at −20 °C gave [DRu(dmpe)Cp] (64.6 mg, 204 μmol, 64%) as pale yellow needles. ^{1}H NMR (300 MHz, C_6D_6): δ (ppm) 1.13-1.20 (m, 4H, CH_2), 1.20-1.23 (m, 6H, CH_3), 1.35-1.39 (m, 6H, CH_3), 4.82 (s, 5H, C_5H_5). ^{13}C{^{1}H} NMR (75.4 MHz, C_6D_6): δ (ppm) 24.2 (m, PCH_3), 28.0 (m, PCH_3), 32.5 (m, PCH_2), 77.1 (s, C_5H_5). ^{31}P{^{1}H} NMR (161.9 MHz, C_6D_6): δ (ppm) 60.6 (d).

Method b. A solution of Ru_3CO_{12} (80 mg, 125 μmol) and cyclopentadiene (0.35 mL, 4.16 mmol) in 20 mL of heptane was refluxed. After ca. 2 h the initially red solution turned light yellow, indicating the formation of [HRu(CO)$_2$Cp]. The reaction mixture was degassed by three freeze-pump-thaw cycles. D_2 (0.6 bar) was added successively three times to the frozen mixture, which was then warmed to ambient temperature. A solution of dmpe (81 mg, 540 μmol) in 5 mL of heptane was added to the reaction mixture, and refluxing was continued for 30 min. After removal of all volatiles the residue was recrystallized from CD_3OD to give [DRu(dmpe)Cp] (62.1 mg, 197 μmol, 52%) as beige needles.

Synthesis of [Cp$_2$Y(μ-H)(μ-η^1:η^5-C$_5$H$_4$)Ru(dmpe)] (1a). A mixture of [Cp$_2$Y(CH$_2$SiMe$_3$)(thf)] (94 mg, 248 μmol) and [HRu(dmpe)Cp] (71 mg, 223 μmol) was slurried at −40 °C in 3 mL of toluene. The reaction mixture was warmed to ambient temperature overnight. After filtration the solvent was stripped off at –40 °C to afford [Cp$_2$Y(μ-H)(μ-η^1:η^5-C$_5$H$_4$)Ru(dmpe)] (**1a**; 92 mg, 172 μmol, 69%) as a yellow solid. Single crystals of **1a** suitable for Xray analysis were grown from a concentrated toluene solution at –20 °C. ^{1}H NMR (300 MHz, C_6D_6): δ (ppm) –16.19 (dt, $^1J_{HY}$ = 17.2 Hz, $^2J_{HP}$ = 26.6 Hz, 1H,

μ-H), 0.93 (d, 4H, CH_2), 1.11-1.14 (m, 6H, CH_3), 1.24-1.27 (m, 6H, CH_3), 4.33 (s, 2H, C_5H_4), 4.79 (s, 2H, C_5H_4), 6.35 (s, 10H, C_5H_5). $^{13}C\{^1H\}$ NMR (75.4 MHz, C_6D_6): δ (ppm) 22.8 (m, PCH$_3$), 26.3 (m, PCH$_3$), 32.5 (m, PCH$_2$), 81.3 (s, C_5H_4), 82.2 (s, C_5H_4), 110.3 (s, C_5H_5). $^{31}P\{^1H\}$ NMR (161.9 MHz, C_6D_6): δ (ppm) 54.8 (d, J = 24.4 Hz). Anal. Calcd for $C_{21}H_{31}P_2RuY$ (535.38): C, 47.11; H, 5.84. Found: C, 46.61; H, 5.86.

Synthesis of [Cp$_2$Y(μ-D)(μ-η^1:η^5-C$_5$H$_4$)Ru(dmpe)] (1ad). A J. Young valve NMR tube was charged with [Cp$_2$Y(CH$_2$SiMe$_3$)(thf)] (18.9 mg, 50 μmol), [DRu(dmpe)Cp] (17.5 mg, 50 μmol), and 0.6 mL of C_6D_6. The reaction mixture was kept at room temperature and monitored by ^{1}H NMR spectroscopy. The signals for [Cp$_2$Y(CH$_2$SiMe$_3$)(thf)] and [DRu(dmpe)Cp] disappeared and the formation of **1a**d was observed. No new signals were observed in the hydride region. ^{1}H NMR (300 MHz, C_6D_6): δ (ppm) 0.93 (d, 4H, CH_2), 1.11-1.14 (m, 6H, CH_3), 1.23-1.27 (m, 6H, CH_3), 4.33 (s, 2H, C_5H_4), 4.79 (s, 2H, C_5H_4), 6.35 (s, 10H, C_5H_5).

Synthesis of [Cp$_2$Lu(μ-H)(μ-η^1:η^5-C$_5$H$_4$)Ru(dmpe)] (1b). Following the procedure for **1a**, [Cp$_2$Lu(CH$_2$SiMe$_3$)(thf)] (116 mg, 250 μmol) was reacted with [HRu(dmpe)Cp] (79 mg, 250 μmol) in 3 mL of toluene. [Cp$_2$Lu(μ-H)(μ-η^1:η^5-C$_5$H$_4$)Ru(dmpe)] (**1b**; 98 mg, 158 μmol, 63%) was isolated as a yellow solid. Single crystals of **1b** suitable for X-ray analysis were grown from a concentrated toluene solution at –20 °C. ^{1}H NMR (300 MHz, C_6D_6): δ (ppm) –15.04 (t, $^2J_{HP}$ = 25.2 Hz, 1H, μ-H), 0.90 (d, 4H, CH_2), 1.09-1.11 (m, 6H, CH_3), 1.21-1.24 (m, 6H, CH_3), 4.38 (s, 2H, C_5H_4), 4.74 (s, 2H, C_5H_4), 6.33 (s, 10H, C_5H_5). $^{13}C\{^1H\}$ NMR (75.4 MHz, C_6D_6): δ (ppm) 22.5 (m, PCH$_3$), 25.7 (m, PCH$_3$), 32.4 (m, PCH$_2$), 83.2 (s, C_5H_4), 84.0 (s, C_5H_4), 110.0 (s, C_5H_5), 133.9 (s, C_5H_4). $^{31}P\{^1H\}$ NMR (161.9 MHz, C_6D_6): δ (ppm) 54.8 (d, J = 22.6 Hz). Anal. Calcd for $C_{21}H_{31}LuP_2Ru$: C, 40.59; H, 5.03. Found: C, 40.84; H, 5.24.

Synthesis of [Cp$_2$Y(μ-H){μ-(Ph)CC(Ph)(C$_5$H$_4$)}Ru(dmpe)] (2a). A solution of **1a** in toluene, prepared as described above from [Cp$_2$Y(CH$_2$SiMe$_3$)(thf)] (94 mg, 248 μmol) and [HRu(dmpe)Cp] (64 mg, 200 μmol), was layered at room temperature with a solution of diphenylacetylene (54 mg, 300 μmol) in 3 mL of hexane. The reaction mixture was allowed to stand overnight, causing a color change from yellow to orange. After the volume of the solution was reduced, it was kept at –35 °C to afford orange X-ray-quality crystals of **2a** (82 mg, 115 μmol, 57%). ^{1}H NMR (300 MHz, C_6D_6): δ (ppm) –14.97 (dt, $^1J_{HY}$ = 19.2 Hz, $^2J_{HP}$ = 28.5 Hz, 1H, μ-H), 0.82 (d, 4H, CH_2), 1.17-1.20 (m, 6H, CH_3), 1.34-1.37 (m, 6H, CH_3), 4.78 (s, 2H, C_5H_4), 4.90 (s, 2H, C_5H_4), 6.25 (s, 10H, C_5H_5), 6.84-7.23 (m, 10H, Ph). $^{13}C\{^1H\}$ NMR (75.4 MHz, C_6D_6): δ (ppm) 22.1 (m, CH$_2$), 26.9 (m, CH$_3$), 32.2 (m, CH$_3$), 76.4 (m, C_5H_4), 79.8 (m, C_5H_4), 110.4 (C_5H_5), 120.0 (s, Ph), 121.3 (s, Ph), 124.9 (s, Ph), 125.6 (s, Ph), 126.2 (s, Ph), 129.2 (s, Ph), 130.8 (s, Ph), 138.9 (s, C_5H_4), 140.6 (s, *ipso*-Ph), 140.8 (s, *ipso*-Ph), 152.8 (s, PhCC$_5$H$_4$). $^{31}P\{^1H\}$ NMR (161.9 MHz, C_6D_6): δ (ppm) 54.7 (d, J = 26.5 Hz), 58.9 (d, J = 32.1 Hz). Anal. Calcd for $C_{35}H_{41}P_2RuY$ (713.60): C, 58.91; H, 5.79. Found: C, 58.62; H, 5.86.

Synthesis of [{OC$_6$H$_3$(*t*Bu)$_2$-2,6}Y(μ-H)(μ-η^1:η^5-C$_5$H$_4$){κ^{3}C,P,P-CH$_2$(Me)P(CH$_2$)$_2$PMe$_2$}Ru]$_2$ (3a). [Y(CH$_2$SiMe$_3$)$_2$(OC$_6$H$_3$(*t*Bu)$_2$-2,6)(thf)$_2$] (153 mg, 250 μmol) and [HRu(dmpe)Cp] (79 mg, 250 μmol) were slurried at –40 °C in 5 mL of toluene. The reaction mixture was warmed to ambient temperature overnight. After filtration the volume of the solution was reduced and it was kept overnight at –20 °C to give [{OC$_6$H$_3$(*t*Bu)$_2$-2,6}Y(μ-H)(μ-η^1:η^5-C$_5$H$_4$){κ^3C,P,P'-CH$_2$(Me)P(CH$_2$)$_2$PMe$_2$}Ru]$_2$ (**3a**; 97 mg, 70 μmol, 55%) as a colorless microcrystalline solid. Single crystals of **3a** suitable for X-ray analysis were grown from a concentrated toluene solution after several days at room temperature. ^{1}H NMR (300 MHz, C$_6$D$_6$): δ (ppm) –13.38 (dt, $^1J_{HY}$ = 18.0 Hz, $^2J_{HP}$ = 31.2 Hz, 2H, μ-H), 0.82-1.03 (m, 20H, dmpe), 1.67 (s, 36H, OC$_6$H$_3$(C*Me*$_3$)$_2$), 4.54 (m, 4H, C$_5$*H*$_4$), 5.29 (m, 4H, C$_5$*H*$_4$), 6.82 (t, J_{HH} = 7.7 Hz, 2H, *p*-OC$_6$*H*$_3$(CMe$_3$)$_2$), 7.36 (d, J_{HH} = 7.7 Hz, 4H, *m*-OC$_6$*H*$_3$(CMe$_3$)$_2$). ^{13}C{^{1}H} NMR (75.4 MHz, C$_6$D$_6$): δ (ppm) 22.9 (m, P*C*H$_3$), 26.7 (m, P*C*H$_3$), 31.7 (s, C*Me*$_3$), 32.3 (m, P*C*H$_2$), 35.6 (s, *C*Me$_3$), 78.4 (s, C$_5$H$_4$), 81.9 (s, *C*$_5$H$_4$), 113.9 (s, *p*-C$_{14}$H$_{21}$O), 125.2 (s, *m*-C$_{14}$H$_{21}$O), 138.1 (s, *o*-C$_{14}$H$_{21}$O), 164.5 (d, $^2J_{CY}$ = 4.8 Hz, *ipso*-C$_{14}$H$_{21}$O). ^{31}P{^{1}H} NMR (161.9 MHz, C$_6$D$_6$): δ (ppm) 58.6 (dd, J_{PP} = 12.0 Hz, J_{PH} = 27.9 Hz), 61.0 (ddd, J_{PY} = 7.9 Hz, J_{PP} = 16.1 Hz, J_{PH} = 28.6 Hz). Anal. Calcd for C$_{50}$H$_{82}$O$_2$P$_4$Ru$_2$Y$_2$ (1219.00): C, 49.24; H, 6,78. Found: C, 49.65; H, 6.73.

Synthesis of [{OC$_6$H$_3$(*t*Bu)$_2$-2,6}Lu(μ-H)(μ-η^1:η^5-C$_5$H$_4$){κ^{3}C,P,P-CH$_2$(Me)P(CH$_2$)$_2$PMe$_2$}Ru]$_2$ (3b). Following the procedure for **3a**, [Lu(CH$_2$SiMe$_3$)$_2$(OC$_6$H$_3$(*t*Bu)$_2$-2,6)(thf)$_2$] (153 mg, 250 μmol) and [HRu(dmpe)Cp] (79 mg, 250 μmol) were reacted in 3 mL of toluene. [{OC$_6$H$_3$(*t*Bu)$_2$-2,6}Lu(μ-H)(μ-η^1:η^5-C$_5$H$_4$){κ^3C,P,P'-CH$_2$(Me)P(CH$_2$)$_2$PMe$_2$}Ru]$_2$ (**3b**; 78 mg, 56 μmol, 44%) was isolated as a colorless microcrystalline solid. Single crystals of **3b** suitable for X-ray analysis were grown from a concentrated toluene solution at –20 °C. ^{1}H NMR (300 MHz, C$_6$D$_6$): δ (ppm) –12.17 (t, $^2J_{HP}$ = 31.7 Hz, 2H, μ-H), 0.80-0.99 (m, 12H, C*H*$_3$), 0.93-0.96 (m, 8H, C*H*$_2$), 1.71 (s, 36H, OC$_6$H$_3$(C*Me*$_3$)$_2$), 4.79 (m, 4H, C$_5$*H*$_4$), 4.98 (m, 4H, C$_5$*H*$_4$), 6.84 (t, J_{HH} = 7.8 Hz, 2H, *p*-OC$_6$*H*$_3$(CMe$_3$)$_2$), 7.36 (d, J_{HH} = 7.8 Hz, 4H, *m*-OC$_6$*H*$_3$(CMe$_3$)$_2$). ^{13}C{^{1}H} NMR (75.4 MHz, C$_6$D$_6$): δ (ppm) 23.2 (m, P*C*H$_3$), 26.8 (m, P*C*H$_3$), 32.3 (m, P*C*H$_2$), 35.1 (s, C*Me*$_3$), 40.1 (s, *C*Me$_3$), 81.6 (s, *C*$_5$H$_4$), 83.5 (s, *C*$_5$H$_4$), 116.6 (s, *p*-C$_{14}$H$_{21}$O), 124.9 (s, *m*-C$_{14}$H$_{21}$O), 132.6 (s, *C*$_5$H$_4$), 138.0 (s, *o*-C$_{14}$H$_{21}$O), 165.6 (s, *ipso*- C$_{14}$H$_{21}$O). ^{31}P{^{1}H} NMR (161.9 MHz, C$_6$D$_6$): δ (ppm) 53.5 (d, *J* = 28.1 Hz), 66.0 (d, *J* = 27.5 Hz). Anal. Calcd for C$_{50}$H$_{82}$Lu$_2$O$_2$P$_4$Ru$_2$ (1389.09): C, 43.15; H, 5.94. Found: C, 43.03; H, 5.68.

Supporting Information CIF files giving crystallographic data for **1a**, **2a**, and **3a**, **3b**. This material is available free of charge via the Internet at `http://pubs.acs.org`.

Corresponding Author *E-mail: kempe@uni-bayreuth.de

Acknowledgments Financial support by the Deutsche Forschungsgemeinschaft (DFG) (KE 756/21-1) is gratefully acknowledged.

6.6 References

[1] See, for example: (a) H. Nakazawa, M. Itazaki, *Top. Organomet. Chem.* **2011**, *33*, 27–81; (b) C. Deutsch, N. Krause, *Chem. Rev.* **2008**, *108*, 2916–2927; (c) C. Lau, S. Ng, G. Jia, Z. Lin, *Coord. Chem. Rev.* **2007**, *251*, 2223–2237; (d) S. E. Clapham, A. Hadzovic, R. H. Morris, *Coord. Chem. Rev.* **2004**, *248*, 2201–2237; (e) R. Noyori, *Angew. Chem. Int. Ed.* **2002**, *41*, 2008–2022; (f) M. Ephritikhine, *Chem. Rev.* **1997**, *97*, 2193–2242.

[2] L. Schlapbach, A. Züttel, *Nature* **2001**, *414*, 353–358.

[3] For instance, the batteries of hybrid cars are based on such materials.

[4] W. J. Evans, J. H. Meadows, T. P. Hanusa, *J. Am. Chem. Soc.* **1984**, *106*, 4454–4460.

[5] D. J. Alvarez, K. G. Caulton, W. J. Evans, J. W. Ziller, *J. Am. Chem. Soc.* **1990**, *112*, 5674–5676.

[6] D. Alvarez, K. G. Caulton, W. J. Evans, J. W. Ziller, *Inorg. Chem.* **1992**, *31*, 5500–5508.

[7] M. L. H. Green, A. K. Hughes, D. M. Michaelidou, P. Mountford, *J. Chem. Soc. Chem. Commun.* **1993**, 591–593.

[8] D. M. Michaelidou, M. L. Green, A. K. Hughes, P. Mountford, A. N. Chernega, A. K. Hughes, *Polyhedron* **1995**, *14*, 2663–2675.

[9] N. S. Radu, P. K. Gantzel, T. D. Tilley, *J. Chem. Soc. Chem. Commun.* **1994**, 1175–1176.

[10] M. V. Butovskii, O. L. Tok, F. R. Wagner, R. Kempe, *Angew. Chem. Int. Ed.* **2008**, *47*, 6469–6472.

[11] T. Shima, Z. Hou, *Chem. Lett.* **2008**, *37*, 298–299.

[12] T. Shima, Z. Hou, *Organometallics* **2009**, *28*, 2244–2252.

[13] Y. Takenaka, Z. Hou, *Organometallics* **2009**, *28*, 5196–5203.

[14] T. Shima, Y. Luo, T. Stewart, R. Bau, G. J. McIntyre, S. A. Mason, Z. Hou, *Nat. Chem.* **2011**, *3*, 814–820.

[15] S. T. Liddle, *Proc. R. Soc. A* **2009**, *465*, 1673–1700.

[16] S. T. Liddle, D. P. Mills, *Dalton Trans.* **2009**, *9226*, 5592–5605.

[17] D. Patel, S. T. Liddle, *Rev. Inorg. Chem.* **2012**, *32*, 1–22.

[18] B. Oelkers, M. V. Butovskii, R. Kempe, *Chem. Eur. J.* **2012**, *18*, 13566–13579.

[19] I. P. Beletskaya, A. Z. Voskoboynikov, E. B. Chuklanova, N. I. Kirillova, A. K. Shestakova, I. N. Parshina, A. I. Gusev, G. K.-I. Magomedov, *J. Am. Chem. Soc.* **1993**, *115*, 3156–3166.

[20] C. Döring, A.-M. Dietel, M. V. Butovskii, V. Bezugly, F. R. Wagner, R. Kempe, *Chem. Eur. J.* **2010**, *16*, 10679–10683.

[21] H. Deng, S. G. Shore, *J. Am. Chem. Soc.* **1991**, *113*, 8538–8540.

[22] H. Deng, S.-H. Chun, P. Florian, P. J. Grandinetti, S. G. Shore, *Inorg. Chem.* **1996**, *35*, 3891–3896.

[23] P. L. Arnold, J. McMaster, S. T. Liddle, *Chem. Commun.* **2009**, 818–820.

[24] M. P. Blake, N. Kaltsoyannis, P. Mountford, *J. Am. Chem. Soc.* **2011**, *133*, 15358–15361.

[25] M. V. Butovskii, C. Döring, V. Bezugly, F. R. Wagner, Y. Grin, R. Kempe, *Nat. Chem.* **2010**, *2*, 741–744.

[26] M. V. Butovskii, O. L. Tok, V. Bezugly, F. R. Wagner, R. Kempe, *Angew. Chem. Int. Ed.* **2011**, *50*, 7695–7698.

[27] M. S. Chinn, D. M. Heinekey, *J. Am. Chem. Soc.* **1987**, *109*, 5865–5867.

[28] Note added in proof: as one reviewer pointed out correctly, the doublet appearance of the ^{31}P NMR signals should be attributed to the $^{2}J_{\mathrm{PH}}$ phosphorus coupling with the bridging hydride. This can be explained by the fact that the NMR apparatus' decoupling frequency bandwidth was adjusted in a manner not to include the frequency of the hydrides to be decoupled.

[29] For the calculation of the mean value, 109 Cp_2Y fragments were considered [CSD (Cambridge Structural Database) v. 5.31].

[30] P. M. Treichel, D. A. Komar, P. J. Vincenti, *Synth. React. Inorg. Met.-Org. Chem.* **1984**, *14*, 383–400.

[31] M. S. Chinn, D. M. Heinekey, *J. Am. Chem. Soc.* **1990**, *112*, 5166–5175.

[32] M. I. Bruce, M. G. Humphrey, A. G. Swincer, R. C. Wallis, *Aust. J. Chem.* **1984**, *37*, 1747–1755.

[33] A. P. Humphries, S. A. R. Knox, *J. Chem. Soc. Dalt. Trans.* **1975**, 1710–1714.

[34] C. P. Casey, J. B. Johnson, X. Jiao, S. E. Beetner, S. W. Singer, *Chem. Commun.* **2010**, *46*, 7915–7917.

[35] M. Fauré, C. Saccavini, G. Lavigne, *Chem. Commun.* **2003**, 1578–1579.

[36] M. I. Bruce, C. Hameister, A. G. Swincer, R. C. Swincer, *Inorg. Synth.* **1982**, *21*, 78–84.

[37] W. J. Evans, R. N. R. Broomhall-Dillard, J. W. Ziller, *Organometallics* **1996**, *15*, 1351–1355.

[38] H. Schumann, W. Genthe, N. Bruncks, *Angew. Chem. Int. Ed.* **1981**, *20*, 119–120.

[39] L. F. Szczepura, K. J. Takeuchi, *Inorg. Chem.* **1990**, *29*, 1772–1777.

[40] A. Altomare, M. C. Burla, M. Camalli, G. L. Cascarano, C. Giacovazzo, A. Guagliardi, A. G. G. Moliterni, G. Polidori, R. Spagna, *J. Appl. Crystallogr.* **1999**, *32*, 115–119.

[41] G. M. Sheldrick, *Acta Crystallogr. A.* **2008**, *A64*, 112–122.

[42] L. J. Farrugia, *J. Appl. Crystallogr.* **1999**, *32*, 837–838.

7

Transition Metal Hydride Complexes of dfmpf

Adam P. Sobaczynski, Stefan Schwarz, Johannes Obenauf, and Rhett Kempe*

Lehrstuhl Anorganische Chemie II, Universität Bayreuth, 95440 Bayreuth, Germany

To be submitted.

7.1 Abstract

New transition metal hydrides with the electron deficient diphosphine [Fe{η^5-C_5H_4P-$(CF_3)_2$}$_2$] (dfmpf) were synthesized. Carbonyl replacement by dfmpf in the ruthenium hydride [$HRu(CO)_2Cp$] or in the cobalt hydride [$HCo(CO)_4$] led to the (perfluoroalkyl)phosphine substituted hydride complexes [HRu(dfmpf)Cp] (**1**) or [HCo(dfmpf)-$(CO)_2$] (**2**). **1** and **2** were structurally optimized and investigated by DFT methods. Calculations revealed a more reactive metal-hydrogen bond in **2** than in **1**. Furthermore the rhodium complex [Rh(dfmpf)(μ-Cl)]$_2$ (**3**) was obtained by reaction of [Rh(COD)(μ-Cl)]$_2$ and dfmpf. Subsequent salt metathesis with $AgBF_4$ gave [Rh(dfmpf)$(NCMe)_2$][BF_4] (**4**). The obtained compounds were characterized by NMR and IR spectroscopy as well as by cyclic voltammetry and elemental analysis. X-ray crystal structure analyses (XRD) of all complexes except **4** were performed.

7.2 Introduction

Unsupported bonds between rare-earth elements (RE) and transition metals (TM) received a great deal of attention in recent years.[1] In the early 1990's Beletskaya reported on the synthesis of [$Cp(CO)_2RuLu(Cp)_2(thf)$],[2] the first molecular compound[3] featuring such a bond. However, it was not before 2008 that our group reported on further examples of such compounds and introduced the [Cp_2Re] moiety in RE-TM bonding.[4] This had enormous impact on further progress in RE-TM bonding. The [Cp_2Re] moiety allowed access to RE solely bonded to TM atoms as in [Sm{$ReCp_2$}$_3$],[5] metal-metal bonding between divalent lanthanoids and TM[6] as well as the controlled formation of

RE-TM clusters via multiple C-H bond activation steps.[7,8] The observed progress since introduction of the [Cp_2Re] moiety is based on two reasons: (i) Alkane elimination reactions of [Cp_2ReH] with rare-earth alkyls serve as an efficient route to the bimetallic compounds. (ii) The carbonyl-free [Cp_2Re] moiety[4,5,7,9] prevents isocarbonyl linkage, which is the most abundant type of linkages in RE-TM-compounds featuring carbonyl-containing moieties like Fp and Rp (Fp = [$CpFe(CO)_2$], Rp = [$CpRu(CO)_2$]).[2b,6,10] The [Cp_2Re] moiety represents the first and so far only carbonyl-free TM fragment capable of forming unsupported bonds toward RE. Despite the possibility of isocarbonyl linkages the carbonyls in Fp and Rp are essential to generate and stabilize a nucleophilic ate complex which may form unsupported bonds towards RE. Given this, it seems remarkable that the ate complex $[Cp_2Re]^-$ shows sufficient stability being only ligated by Cp ligands. Keeping this in mind the pursuit of further carbonyl-free metalloligands remains challenging. We recently studied the substitution of carbonyl ligands in [$HRu(CO)_2Cp$][11] by the aliphatic diphosphine 1,2-bis(dimethylphosphino)ethane (dmpe) and the subsequent reaction of [HRu(dmpe)Cp] with RE alkyls.[12] However this resulted in rare-earth–transition metal hydride complexes due to C-H bond activation. The electron-donating character of dmpe made the hydride inaccessible for alkane elimination and favored C-H bond activation at the Cp ring instead. Carbon monoxide being one of the ligands with the most π-accepting character lacks possibilities to be tuned electronically or sterically. The strong π-acidity of fluorophosphines and (perfluoroalkyl)phosphines makes them a bulky mimic of CO.[13,14] Unlike CO, phosphines can be modified sterically and electronically. However their high volatility renders PF_3 and $P(CF_3)_3$ difficult to prepare and to handle. Fluorinated diphosphines serve as bidentate CO analogues.[15] While not exhaustively explored, they were studied in more detail than the analogous monophosphines. In the past there were no convenient syntheses of fluorinated diphosphines. Therefore their number still remains limited. For most of them their coordination properties are unexplored. A lot of work has been done by Roddick and coworkers who mainly explored the coordination properties of $(C_2F_5)_2PCH_2CH_2P(C_2F_5)_2$ (dfepe)[15b,16] and $(CF_3)_2PCH_2CH_2P(CF_3)_2$ (dfmpe).[17] In 2005 Caffyn and coworkers reported on a general route to perfluoroalkyl mono- and diphosphines,[18] making a wide range of phosphines accessible in a convenient way. Later this method was extended by the same group to the synthesis of perfluoroalkyl substituted ferrocenyldiphosphines.[19] This made the (perfluoroalkyl)phosphine 1,1'-bis(bis(trifluoromethyl)phosphino)ferrocene (dfmpf) readily accessible on a multigram scale. Substitution of carbonyl ligands for sterically demanding dfmpf in [$M(CO)_2L_n$] systems should maintain their electronic properties providing low valent metalloligands. We report here on the synthesis of (perfluoroalkyl)phosphine analogues of [$CpRuL_2H$] and [$Co(CO)_{3-n}L_nH$] (L = PR_3).

7.3 Results and Discussion

Synthesis and Structural Characterization of [HRu(dfmpf)Cp]. The classical synthetic route to complexes of the type [$CpRuL_2H$] (L = PR_3) begins with [$CpRu(PPh_3)_2Cl$][20] which is a versatile reagent to access a wide range of substitution products with

mono- and bidentate phosphines or phosphites.[21] For the most part the resulting complexes [$CpRuL_2Cl$][21,22] are treated with sodium methoxide[22,23] to give the corresponding hydride complexes.[22] However this protocol seems to be confined to electron-rich phosphines. Roddick and coworkers described a general reluctance of [$CpRuL_2Cl$] to undergo halide displacement reactions with electron-poor, π-accepting phosphines.[17] A second synthetic approach to [$CpRuL_2H$] starts from in situ generated [$CpRu(CO)_2H$].[11] In this one pot reaction carbonyl replacement by mono- or diphosphines leads to the desired hydride compounds.[11,24] This reaction is not confined to donating phosphines as we could show by preparing complexes of the type [$CpRuL_2H$] with electron-poor (perfluoroalkyl)phosphines. Thus the reaction of the ruthenium monohydride [$HRu(CO)_2Cp$][11] with an excess of the fluorinated phosphine dfmpf[19] in refluxing heptane gave the bimetallic hydride compound [HRu(dfmpf)Cp] (**1**) as an orange solid in 38% isolated yield (Scheme 1). Due to the phosphine's electron-poor character prolonged reaction time (overnight) was necessary to substitute the carbonyls compared to electron-rich phosphine analogues (e.g. 0.5 h for [HRu(dmpe)Cp][24]). **1** shows good solubility in common aromatic and polar solvents like benzene, THF or acetonitrile and is less soluble in alkanes. Compared with its electron-rich phosphine congener [HRu(dmpe)Cp] which decomposes rapidly upon exposure to air **1** shows improved stability and can be handled in air without visible decomposition.

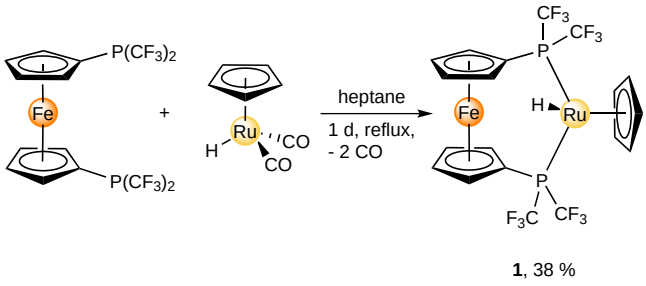

Scheme 1. Synthesis of **1**.

In the ^{1}H NMR spectrum the hydride exhibits a triplet of septets pattern with $^2J_{PH}$ = 35.1 Hz and $^4J_{FH}$ = 1.9 Hz. The corresponding IR band is observed at 1970 cm^{-1}. The protons of the ferrocenyl backbone give multiplets at 3.76 and 4.53 ppm in the ^{1}H NMR spectrum. The Cp ring on ruthenium gives a sharp singlet at 4.95 ppm. The ^{13}C NMR spectrum shows two doublets with $^3J_{PC}$ = 6.2 Hz and $^3J_{PC}$ = 7.7 Hz at 72.7 and 73.0 ppm, a broad resonance at 73.5 ppm and a doublet with $^2J_{CP}$ = 14 Hz at 74.5 ppm for the Cp rings on iron. The Cp ring on ruthenium gives a singlet at 82.6 ppm. The two trifluoromethyl groups at each phosphorus atom feature in the ^{13}C NMR spectrum a quartet of doublets with $^1J_{CF}$ = 324 Hz, $^1J_{CP}$ = 16 Hz at 125.2 ppm and a quartet with $^1J_{CF}$ = 324 Hz at 125.6 ppm, respectively. The ^{19}F NMR spectrum shows signals at –63.2 and –62.2 ppm with coupling constants of $^2J_{PF}$ = 71 Hz for each sort of trifluoromethyl groups. The ^{31}P NMR spectrum displays a AA'$X_6X'_6$ higher order pattern at 91.1 ppm with $^2J_{PP}$ = 30 Hz, $^2J_{PF}$ = 71 Hz and $^4J_{PF}$ = 0.8 Hz for the two phosphorus atoms (Figure 1a).

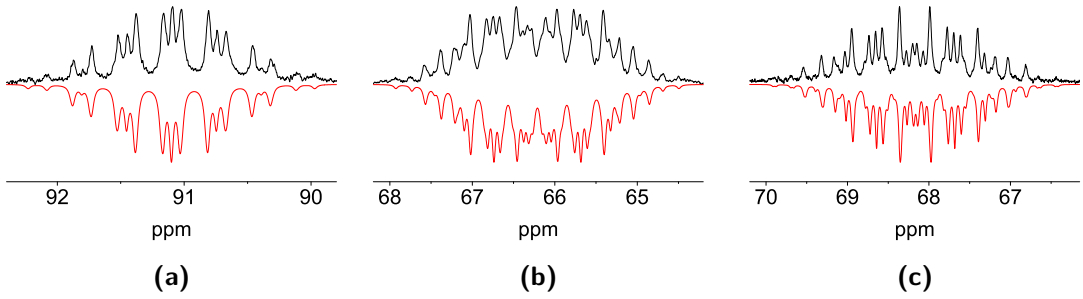

Figure 1. Proton decoupled $^{31}P\{^{1}H\}$ NMR spectra (202.5 MHz, 298 K) of **1** (**a**; C_6D_6), **3** (**b**; $[D_8]$THF) and **4** (**c**; CD_3CN); experimental black, simulated[25] red.

Single crystals of **1** suitable for an X-ray diffraction study were obtained after recrystallization from methanol which allowed to determine the solid-state structure of **1** (Figure 2). Compound **1** crystallizes in the orthorhombic space group $Pna2_1$. The geometry around the tetracoordinate ruthenium atom can be described as distorted trigonal pyramidal with the hydride ligand in the apical position. The distance Ru1–H1Ru amounts to 1.43(4) Å. This is in the same range as in comparable compounds of the same type[26] and significantly (ca. 0.10 Å) shorter than average bond lengths Ru–H (1.55 Å) in compounds with electron-rich phosphine ligands.[27] The same phenomenon can be observed with the bond lengths Ru–P which amount to 2.194 Å and are thus ca. 0.03-0.07 Å shorter than average bond lengths Ru–P (2.27 Å).[28] The Cp rings of the ferrocenyl backbone are synperiplanar staggered, their dihedral angle amounts to 2.4°.[29] The angle $Cp_{centroid}$–Fe1–$Cp_{centroid}$ was found to be 179.3°.

Computational analysis of complex **1** was performed using DFT methods. Geometry optimization starting from the experimental structure is in agreement with the experimental data (Table S1).[30–33] Analysis of the resulting molecular orbitals (MOs) shows two MOs involved in the Ru-H bond (Figure 3). The energy of the MO forming the Ru-H-σ-bond is 2.99 eV lower than the HOMO energy (Table S3). Additional electron density is contributed to the hydrogen by the dz^2-type orbital lobe located at the Ru atom in the HOMO. The calculated charge on ruthenium shows a small positive value; concomitantly the ruthenium-bound hydrogen carries a small negative charge pointing to the hydridic character of this atom. The calculated deprotonation energy amounts to 14.97 eV (Table S4). The IR stretch of the hydride is well reproduced by DFT (DFT: 1996 cm^{-1}, experiment: 1970 cm^{-1}).

Synthesis and Structural Characterization of [HCo(dfmpf)(CO)$_2$]. Beyond the complexes $[CpM(CO)_2H]$ (M = Fe, Ru) and their respective anions which proved successful in RE-TM bonding[2b,6,10] cobalt carbonyl fragments of the type $[Co(CO)_{3-n}L_n]$ (L = PR_3) were used in TM-5f elements bonding.[1b,34,35] However complexes featuring unsupported Co-4f bonds were not reported yet. Disproportionation of Co_2CO_8 in DMF followed by acidification with HCl gave in situ the cobalt monohydride $[HCo(CO)_4]$.[36] Addition of the hydride containing solution to a solution of dfmpf resulted in apparent

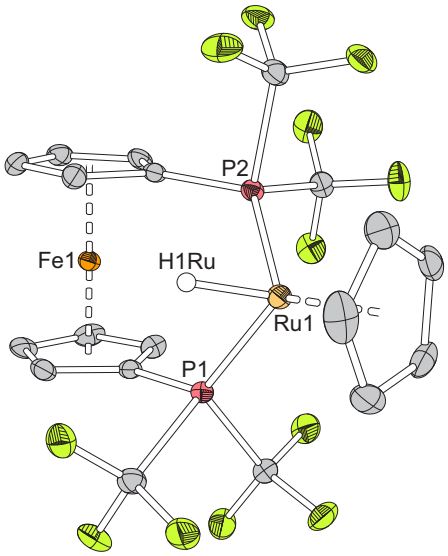

Figure 2. Molecular structure of **1** with 30% thermal ellipsoids. Hydrogen atoms except hydridic have been omitted for clarity. Selected bond lengths [Å] and angles [°]: Ru1–H1Ru 1.43(4), P1–Ru1 2.1992(10), P2–Ru1 2.1892(10), $Cp_{centroid}$–Ru1 1.882, $Cp_{centroid}$–Fe1 1.645 (average value), Fe1–Ru1 4.326; $Cp_{centroid}$–Fe1–$Cp_{centroid}$ 179.3, H1Ru–Ru1–$Cp_{centroid}$ 123.3, $Cp_{centroid}$–Ru1–P1 130.1, $Cp_{centroid}$–Ru1–P2 127.8, P1–Ru1–P2 96.0, P1–Ru1–H1Ru 76.9, P2–Ru1–H1Ru 85.7, P1–$Cp_{centroid}$–$Cp_{centroid}$–P2 26.4.

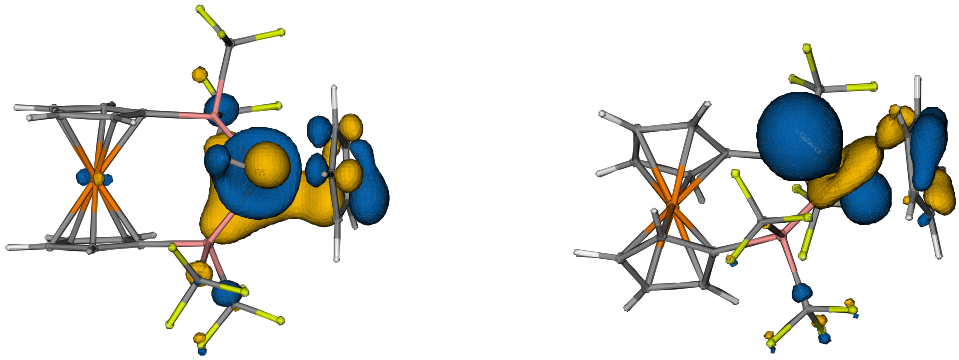

(a) **(b)**

Figure 3. HOMO (MO 149, –5.82 eV) of **1** (**a**) and the MO (MO 137, –8.93 eV) representing the Ru-H σ-bond (**b**).

liberation of carbon monoxide and a color change from orange to bright yellow. The bimetallic species [HCo(dfmpf)$(CO)_2$] (**2**) was isolated as a moderately air sensitive yellow solid (Scheme 2). In contrast to **1** the formation of **2** proceeded in short time and excellent yield. **2** serves as sterically demanding analogue of [$HCo(CO)_4$]. **2** shows good solubility in common aromatic and polar solvents as well as in alkanes.

The ^{1}H NMR spectrum displays in the hydride region a triplet at –12.56 ppm with

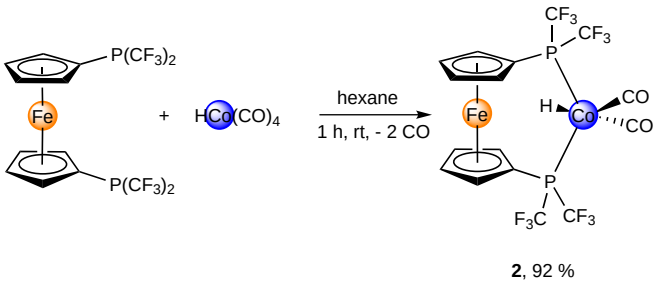

Scheme 2. Synthesis of **2**.

$^{2}J_{PH} = 36.9$ Hz. The aromatic protons give signals at 3.72 and 4.24 ppm. The ^{13}C NMR spectrum shows three doublet resonances for the Cp rings at 73.6 ($^{3}J_{PC} = 6.7$ Hz), 74.2 ($^{2}J_{CP} = 10.6$ Hz), and 75.2 ($^{1}J_{CP} = 17.8$ Hz) ppm. The trifluoromethyl groups appear as quartet of doublets at 125.5 ppm with $^{1}J_{CF} = 321$ Hz and $^{1}J_{CP} = 48$ Hz and unresolved ^{3}J carbon fluorine coupling. The carbonyls were located as a broad resonance at 202.7 ppm. In the ^{19}F NMR spectrum the trifluoromethyl groups exhibit a multiplet at –61.4 ppm with $^{2}J_{PF} = 80$ Hz. The ^{31}P NMR spectrum shows a single broad resonance at 71.2 ppm with no visible linesplitting due to the cobalt quadrupole.

The solid-state structure of **2** was determined by XRD and is presented in Figure 4. Compound **2** crystallizes in the monoclinic space group $P2_1/n$. The geometry at the pentacoordinate cobalt can be described as distorted trigonal bipyramidal with one carbonyl and the hydride in apical positions. The hydride ligand could be located and the distance Co1–H1Co was found to be 1.79(9) Å. This, however, seems not to be reliable as one would expect a shorter distance. The distance Co1–H1Co in **2** is significantly longer than the corresponding distance (1.58(4) Å) in [HCo(dippf)(CO)$_2$][37] and the calculated distance (1.49 Å, Table S2). The Co-P distances are as expected slightly shorter (ca. 0.06 Å) than in the electron-rich phosphine analogue [HCo(dippf)(CO)$_2$] (dippf = 1,1'-bis(diisopropylphosphino)ferrocene).[37] The Cp rings of the ferrocenyl backbone are synclinal staggered the dihedral angle amounts to 0.4°. The Cp$_{centroid}$–Fe1–Cp$_{centroid}$ angle was found to be 177.3°.

Structure optimization of **2** by DFT methods was performed in the same way as for compound **1**. The results of the geometry optimization were in good agreement with the experimental data (Table S2) except for the hydride-metal as mentioned above. Analysis of the MOs shows that only the overlap between the dz^2-type orbital lobe of Co and H contributes to the Co-H-bond (Figure 5). The energy of the corresponding MO is 2.45 eV lower than the HOMO energy (Table S3). Therefore the Co-H bond is about 20% weaker than the Ru-H bond in compound **1**. The deprotonation energy is reduced by 9% compared to **1** (Table S4). In contrast to **1** the cobalt atom shows a higher negative charge whereas the hydrogen atom is positively charged suggesting a protic character.

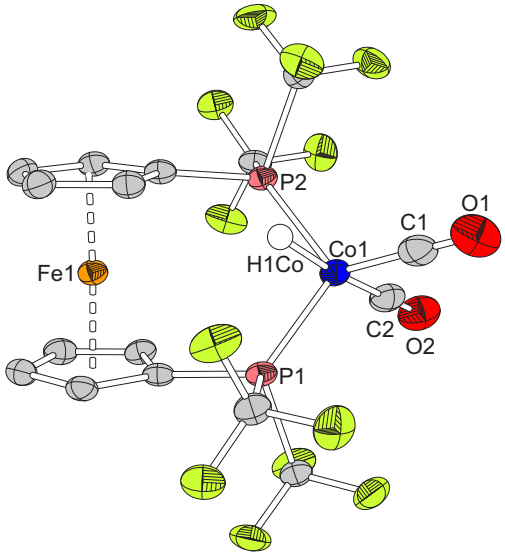

Figure 4. Solid state structure of **2** with 30% thermal ellipsoids. Hydrogen atoms except hydridic have been omitted for clarity. Selected bond lengths [Å] and angles [°]:Co1–H1Co 1.79(9), Co1–C1 1.748(8), Co1–C2 1.752(8), C1–O1 1.141(8), C2–O2 1.145(9), Co1–P1 2.1113(15), Co1–P2 2.1071(15), $Cp_{centroid}$–Fe1 1.650 (average value), Fe1–Co1 4.045; H1Co–Co1–C2 175.8, H1Co–Co1–C1 77.3, P1–Co1–P2 109.5, P1–Co1–H1Co 76.7, P2–Co1–H1Co 72.3, P1–Co1–C1 115.3, P1–Co1–C2 107.5, P2–Co1–C1 117.1, P2–Co1–C2 106.5, C1–Co1–C2, 100.1, $Cp_{centroid}$–Fe1–$Cp_{centroid}$ 177.3, P1–$Cp_{centroid}$–$Cp_{centroid}$–P2 39.6.

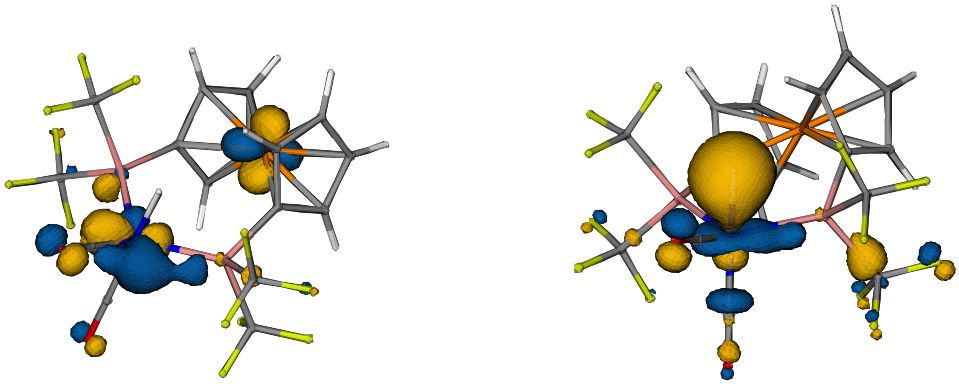

Figure 5. HOMO (MO 146, –6.45 eV) of **2** (**a**) and the MO (MO 135, –8.90 eV) representing the H-Co σ-bond (**b**).

Electrochemistry. In addition to the spectroscopic and structural characterization we examined the redox behavior of the complexes **1** and **2** by cyclic voltammetry. The cyclic voltammogram of **1** displays one reversible oxidative wave at approximately 0.7 V vs Fc/Fc^+ followed by a second irreversible oxidation at about 0.9 V (Figure 6a). According to the first reversible oxidation the HOMO of **1** was calculated to be –5.84 eV, which

correlates well with the DFT-calculated value of –5.82 eV (Table S3). Reductive waves were not observed as the reductive potential is limited by the solvent.

The cyclic voltammogram of compound **2** shows an irreversible oxidation at 0.25 V vs Fc/Fc^+ which is attributed to the oxidation of the ferrocenyl backbone (Figure 6b). A reversible oxidative couple at approximately 0.8 V vs Fc/Fc^+ is assigned to the oxidation of the cobalt center. This occurs at significantly more positive potential compared to the related compound $[HCo(dippf)(CO)_2]$.[37] Most likely this is attributed to the electron withdrawing potential of dfmpf which makes the cobalt less easy to oxidize. This reflects in the experimentally estimated energy of the HOMO of –5.96 eV (DFT: –6.45 eV; Table S3) which is at a significantly lower energy as in $[HCo(dippf)(CO)_2]$ (DFT: –5.42 eV).

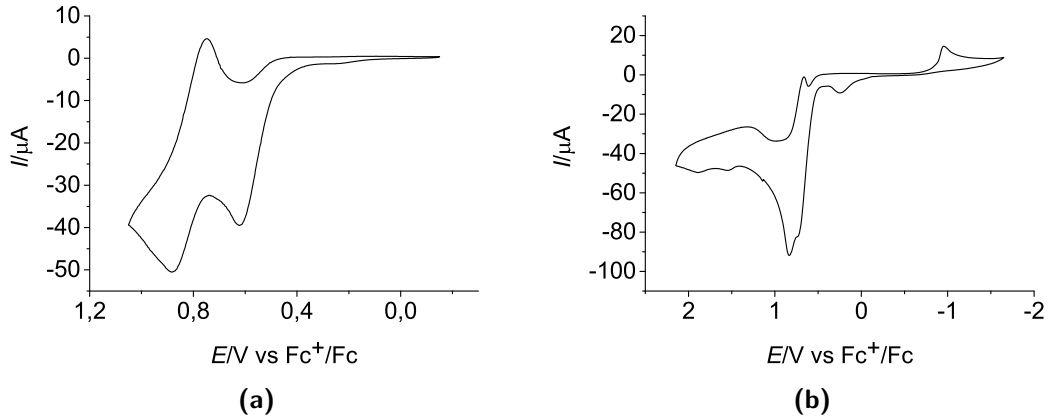

Figure 6. Cyclic voltammograms of **1** (**a**) and **2** (**b**) at a platinum electrode and scan rates of 50 $mV\,s^{-1}$ in CH_2Cl_2/0.1 M $[NBu_4][PF_6]$.

Synthesis of [Rh(dfmpf)(μ-Cl)]$_2$. As the heavier homologue of the cobalt compound **2** we became interested in the synthesis of a (perfluoroalkyl)phosphine Rh^I hydride. However the synthesis of such Rh compounds is not as straightforward as in the cases described above. A versatile starting material in rhodium chemistry is $[Rh(COD)(\mu\text{-}Cl)]_2$.[38] The reaction of $[Rh(COD)(\mu\text{-}Cl)]_2$ with dfmpf in refluxing THF overnight gave the substitution product $[Rh(dfmpf)(\mu\text{-}Cl)]_2$ (**3**) after workup as an orange air stable solid in 89% isolated yield (Scheme 3). **3** is sparingly soluble in aromatics and alkanes but shows good solubility in dichloromethane, acetonitrile and THF.

In the ^1H NMR spectrum the aromatic protons appear as broad signals at 4.77 and 4.88 ppm. The ^{13}C NMR spectrum shows doublets at 75.7 and 76.0 ppm with carbon phosphorus couplings of 11 and 7.7 Hz, respectively. The CF_3-groups appear as quartet of doublets at 122.7 ppm with coupling constants of $^1J_{CF} = 325$ Hz and $^1J_{CP} = 64$ Hz. In the ^{19}F NMR spectrum the trifluoromethyl groups appear at –53.3 ppm as multiplet with $^2J_{PF} = 73$ Hz. The ^{31}P NMR spectrum shows a AA'X_6X'$_6$Y higher order pattern at 66.2 ppm with $^1J_{PRh} = 213.5$ Hz, $^2J_{PP} = 39.5$ Hz, $^2J_{PF} = 73.0$ Hz (Figure 1b).

The solid-state structure of **3** was determined by XRD and revealed a dimeric structure (Figure 7). As one would expect the use of a bulky electron-poor ligand afforded

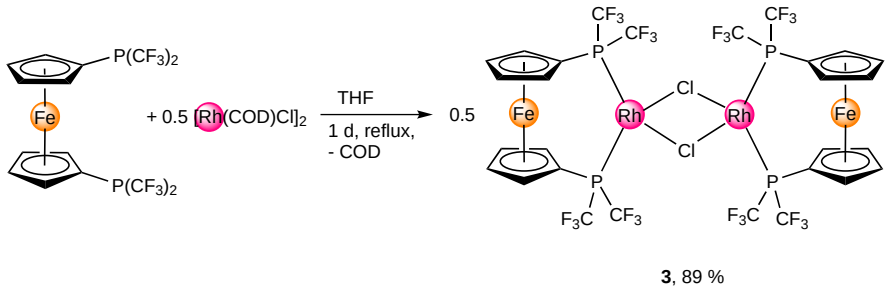

3, 89 %

Scheme 3. Synthesis of **3**.

a dimeric complex.[39] Compound **3** crystallizes in the monoclinic space group $P2_1/c$. The two rhodium atoms are bridged by two chloride ions. This Rh_2Cl_2-unit adopts a hinged conformation with a dihedral angle of 132°. This compares well with hinge angles of 128° and 124° for the parent compounds $[(dfepe)Rh(\mu\text{-}Cl)]_2$[38a] and $[(CO)_2Rh(\mu\text{-}Cl)]_2$,[40] respectively. The geometry around each of the four-coordinate rhodium atoms is approximately square planar. The Cp rings on Fe1 are synperiplanar staggered the dihedral angle amounts to 5.3°. The Cp rings on Fe2 are synperiplanar staggered with a dihedral angle of 2.2°. The $Cp_{centroid}$–Fe–$Cp_{centroid}$ angle were found to be 179.4 and 178.2°, respectively.

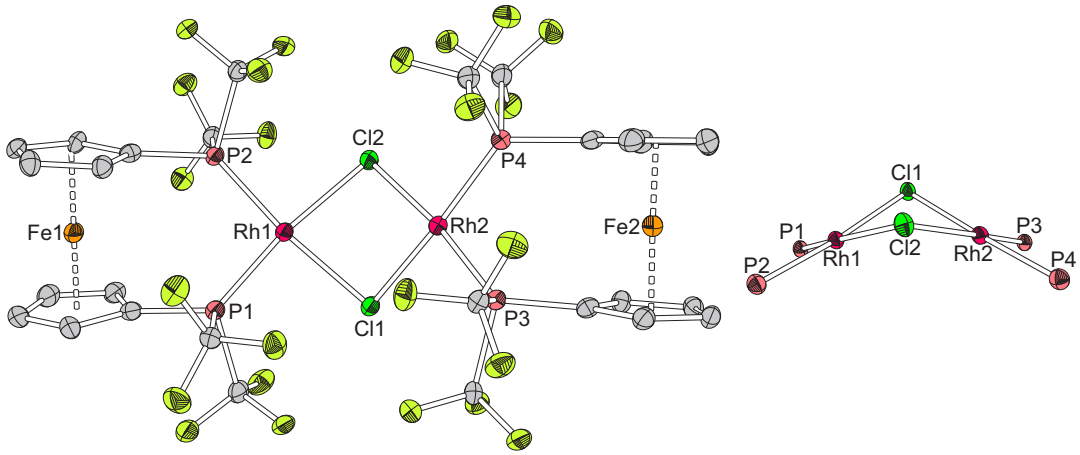

Figure 7. Solid state structure of **3** with 30% thermal ellipsoids; full structure (left), and core structure (right). Hydrogen atoms have been omitted for clarity. Selected bond lengths [Å] and angles [°]: Rh1–P1 2.1851(16), Rh1–P2 2.1821(15), Rh1–Cl1 2.3668(14), Rh1–Cl2 2.3738(14), Rh2–P3 2.1807(15), Rh2–P4 2.1850(16), Rh2–Cl1 2.3731(15), Rh2–Cl2 2.3817(14), $Cp_{centroid}$–Fe1 1.650 (average value), $Cp_{centroid}$–Fe2 1.650 (average value), Fe1–Rh1 4.329, Fe2–Rh2 4.292, Rh1–Rh2 3.285; P1–Rh1–P2 97.7, P3–Rh2–P4 94.1, Cl1–Rh1–Cl2 81.3, Cl1–Rh2–Cl2 81.0, P1–Rh1–Cl1 90.6, P2–Rh1–Cl2 90.8, P3–Rh2–Cl1 92.6, P4–Rh2–Cl2 92.5, Rh1–Cl1–Rh2 87.8, Rh1–Cl2–Rh2 87.4, $Cp_{centroid}$–Fe1–$Cp_{centroid}$ 179.4, $Cp_{centroid}$–Fe2–$Cp_{centroid}$ 178.2, P1–$Cp_{centroid}$–$Cp_{centroid}$–P2 31.0, P3–$Cp_{centroid}$–$Cp_{centroid}$–P4 14.9.

Synthesis of [Rh(dfmpf)(NCMe)$_2$][BF$_4$]. As dimeric rhodium complexes are readily cleaved in acetonitrile[41] we used this strategy on compound **3**. The dimeric compound **3** was treated in acetonitrile with two equivalents of $AgBF_4$ to give the monomeric rhodium species [Rh(dfmpf)(NCMe)$_2$][BF$_4$] (**4**) by salt metathesis as an ochre solid in nearly quantitative yield (Scheme 4). **4** is sparingly soluble in aromatics and of limited solubility in THF but is excellently soluble in acetonitrile.

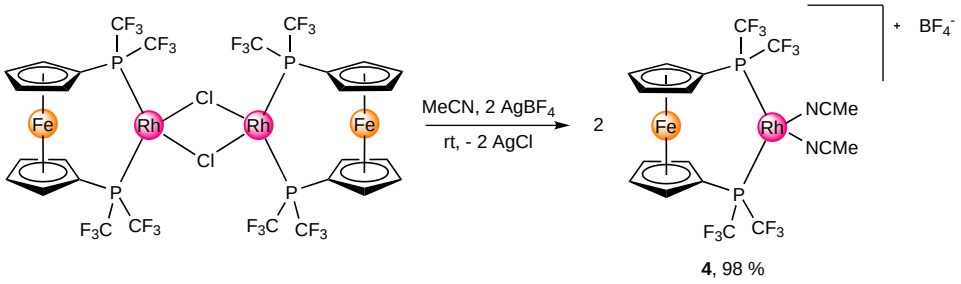

Scheme 4. Synthesis of **4**.

In the ^{1}H NMR spectrum the methyl groups of the coordinated acetonitrile give a singlet at 1.96 ppm. The aromatic protons give two signals at 4.87 and 4.89 ppm. The ^{11}B NMR spectrum displays a singlet at –1.1 ppm for the BF_4 ion. The ^{13}C NMR spectrum shows a resonance at 1.8 ppm for the methyl groups of acetonitrile. The Cp ring carbon atoms appear as doublets at 76.3 (J_{CP} = 11.9 Hz) and 77.7 ppm (J_{CP} = 8.4 Hz). The CF_3 groups appear at 122.6 ppm as quartet of doublets with coupling constants of $^1J_{CF}$ = 322 Hz and $^1J_{CP}$ = 63 Hz. The ^{19}F NMR spectrum shows as one would expect two signals, a multiplet at –54.1 ppm with $^2J_{PF}$ = 76.9 Hz for the trifluoromethyl groups and a singlet at –149.5 ppm for the tetrafluoroborate. The ^{31}P NMR spectrum shows a similar AA'X$_6$X'$_6$Y pattern as **3** at 68.2 ppm with $^1J_{PRh}$ = 194.3 Hz, $^2J_{PP}$ = 44.5 Hz, $^2J_{PF}$ = 76.7 Hz, $^4J_{PF}$ = –0.3 Hz (Figure 1c).

7.4 Conclusion

In summary the first examples of ruthenium, cobalt and rhodium complexes with the (perfluoroalkyl)phosphine ligand dfmpf were synthesized. [HRu(dfmpf)Cp] (**1**) and [HCo(dfmpf)(CO)$_2$] (**2**) as analogues of [HRu(CO)$_2$Cp] or [HCo(CO)$_{3-n}$L$_n$] containing a π-accepting phosphine were synthesized. Furthermore [Rh(dfmpf)(μ-Cl)]$_2$ (**1**) and [Rh(dfmpf)(NCMe)$_2$][BF$_4$] (**4**) were synthesized. **1** and **2** were studied by DFT methods regarding the potential reactivity of their M-H bonds. Structure optimization of **1** and **2** showed good agreement with experimental data. Both compounds were characterized by cyclic voltammetry and the HOMO energies were determined. The HOMO of **2** was found to be at lower energy than in **1**. Concomitantly the Co-H bond in **2** was calculated to be weaker and more acidic than the Ru-H bond in **1**. Reactivity studies of **1** and **2** are under way and will be reported in due course.

Table 1. Summary of crystallographic data.

	1	2	3
Formula	$C_{19}H_{14}F_{12}FeP_2Ru$	$C_{16}H_9CoF_{12}FeO_2P_2$	$C_{28}H_{16}Cl_2F_{24}Fe_2P_4Rh_2$
M_r	689.16	637.95	1320.71
Crystal system	orthorhombic	monoclinic	monoclinic
Space group	$Pna2_1$	$P2_1/n$	$P2_1/c$
a[Å]	12.1707(4)	7.3094(3)	18.0846(6)
b[Å]	11.1079(3)	14.4373(6)	12.2502(4)
c[Å]	15.8362(5)	19.5794(9)	17.8366(6)
α[°]	90.00	90.00	90.00
β[°]	90.00	91.326(4)	98.985(3)
γ[°]	90.00	90.00	90.00
V[Å^3]	2140.91(11)	2065.62(15)	3903.0(2)
Z	4	4	4
T[K]	133(2)	133(2)	133(2)
μ[mm^{-1}] (Mo-K_α)	1.643	1.780	2.001
Rflns collected	32942	31588	56992
Indep Reflections	4992	4661	8291
GoF	1.033	1.059	0.921
R_1 [I>2σ(I)]	0.0282	0.0681	0.0460
wR_2 (all data)	0.0716	0.1854	0.0939

7.5 Experimental Section

General Procedures. All manipulations were carried out under a dry and oxygen free argon atmosphere using Schlenk techniques or in a nitrogen filled glovebox (mBraun 120-G) with a high capacity recirculator (below 0.1 ppm O_2). THF, hexane and heptane were distilled from sodium benzophenone ketyl. Acetonitrile and CH_2Cl_2 were dried over CaH_2. Methanol was dried over magnesium. Deuterated solvents were obtained from Cambridge Laboratories and were degassed, dried and distilled prior to use. Ru_3CO_{12},[42] $[Rh(COD)(\mu\text{-}Cl)]_2$,[43] and dfmpf[19] were prepared according to published procedures. Co_2CO_8, $AgBF_4$ (Strem) and $[NBu_4][PF_6]$ (Aldrich) were used as received.

Instrumentation. ^{1}H, ^{11}B, ^{13}C, ^{19}F and ^{31}P NMR spectra were recorded on Varian Unity 300 MHz, Bruker AC 300 MHz and Bruker ARX 500 MHz spectrometers. Chemical shifts are given in ppm being positive in the downfield. Signals for ^{1}H and ^{13}C are referenced to the residual solvent resonance. ^{11}B chemical shifts are referenced to external $BF_3{\cdot}Et_2O$, taken as 0 ppm, ^{19}F chemical shifts are referenced to external, neat CF_3COOH taken as –76.55 ppm, and ^{31}P chemical shifts are referenced to external, aqueous H_3PO_4 (85%), taken as 0 ppm. Higher order NMR spectra were calculated using the program gNMR.[25] IR spectra were recorded with a JASCO FT/IR-6100 FTIR spectrometer. Samples were prepared as Nujol mulls between NaCl plates. Elemental analyses were carried out using a Vario El III. X-ray crystal structure analyses were performed by using a STOE-IPDS II equipped with an Oxford Cryostream low-temperature unit. Structure solution and refinement was accomplished using SIR97,[44] SHELXL97[45] and WinGX.[46] Summary of crystallographic data is given in Table 1.

Synthesis of [HRu(dfmpf)Cp] (1). Ru_3CO_{12} (100 mg, 156 μmol) and freshly distilled CpH (0.42 mL, 4.84 mmol) were refluxed for 1 h in heptane (30 mL), after which time dfmpf (326 mg, 625 μmol) in heptane (5 mL) was added and refluxing continued. After 18 h the reaction mixture was concentrated and stored at –35 °C to give yellow crystals of **1**. Concentration of the mother liquor and storing at –35 °C gave a second crop of crystals (combined yield: 124 mg, 180 μmol, 38%). Single crystals of **1** suitable for X-ray analysis were grown from a concentrated methanol solution at –20 °C. ^{1}H NMR (300 MHz, C_6D_6, 298 K): δ = –11.82 (m, J_{PH} = 35.1 Hz, 1H, Ru*H*), 3.76 (m, 4H, C_5H_4), 4.53 (m, 4H, C_5H_4), 4.95 (s, 5H, C_5H_5) ppm. ^{13}C{^{1}H} NMR (125.8 MHz, C_6D_6, 296 K): δ = 72.7 (d, $^3J_{CP}$ = 6.6 Hz, C_5H_4), 73.0 (d, $^3J_{CP}$ = 7.7 Hz, C_5H_4), 73.5 (m, C_5H_4), 74.5 (d, $^2J_{CP}$ = 14 Hz, C_5H_4), 82.6 (s, C_5H_5), 125.2 (qd, $^1J_{CF}$ = 324 Hz, $^1J_{CP}$ = 16 Hz, CF_3), 125.6 (q, $^1J_{CF}$ = 324 Hz, CF_3) ppm. ^{19}F{^{1}H} NMR (282.4 MHz, C_6D_6, 290 K): δ = –63.2 (m, $^2J_{PF}$ = 71 Hz, 6F, C*F*$_3$), –62.2 (m, $^2J_{PF}$ = 71 Hz, 6F, C*F*$_3$) ppm. ^{31}P{^{1}H} NMR (202.5 MHz, C_6D_6, 298 K): δ = 91.1 (AA'X$_6$X'$_6$, $^2J_{PP}$ = 30 Hz, $^2J_{PF}$ = 71 Hz, $^4J_{PF}$ = 0.8 Hz, $P(CF_3)_2$) ppm. IR (Nujol): ν = 1970 (Ru-H) cm^{-1}. Anal. calcd. for $C_{19}H_{14}F_{12}FeP_2Ru$ (689.16): C, 33.11; H, 2.05. Found: C 33.19; H, 2.00.

Synthesis of [HCo(dfmpf)(CO)$_2$] (2). A solution of Co_2CO_8 (66 mg, 192 μmol) in hexane (2.5 mL) was treated with DMF (0.7 mL, 9.1 mmol) and stirred at ambient temperature. After 15 min a pink bottom layer had separated. Addition of HCl resulted in a color change to blue. After 1 h the top hexane layer was transferred to a solution of dfmpf (100 mg, 192 μmol) in hexane (10 mL) and stirred for 1 h. Evaporation of the solvent afforded [HCo(dfmpf)(CO)$_2$] (**2**) (113 mg, 177 μmol, 92%) as a yellow solid. Single crystals of **2** suitable for X-ray analysis were grown from a concentrated hexane solution at –20 °C. ^{1}H NMR (300 MHz, C_6D_6, 298 K): δ = –12.56 (t, $^2J_{PH}$ = 36.9 Hz, 1H, Co*H*), 3.72 (m, 4H, C_5H_4), 4.24 (m, 4H, C_5H_4) ppm. ^{13}C{^{1}H} NMR (125.8 MHz, C_6D_6, 296 K): δ = 73.6 (d, $^3J_{PC}$ = 6.7 Hz, C_5H_4), 74.2 (d, $^2J_{CP}$ = 10.6 Hz, C_5H_4), 75.2 (d, $^1J_{CP}$ = 17.8 Hz, C_5H_4), 125.5 (qd, $^1J_{CF}$ = 321 Hz, $^1J_{CP}$ = 48 Hz, CF_3), 202.7 (br s, *C*O) ppm. ^{19}F{^{1}H} NMR (282.4 MHz, C_6D_6, 290 K): δ = –61.4 (m, $^2J_{PF}$ = 80 Hz, 12F, C*F*$_3$) ppm. ^{31}P{^{1}H} NMR (202.5 MHz, C_6D_6, 298 K): δ = 71.2 (m, $P(CF_3)_2$) ppm. IR (Nujol): ν = 1955, 1993, 2010, 2051 cm^{-1}. Anal. calcd. for $C_{16}H_9CoF_{12}FeO_2P_2$ (637.95): C, 30.12; H, 1.42. Found: C, 30.57; H, 1.43.

Synthesis of [Rh(dfmpf)(μ-Cl)]$_2$ (3). [Rh(COD)(μ-Cl)]$_2$ (118 mg, 239 μmol) and dfmpf (250 mg, 479 μmol) were refluxed in THF (10 mL) overnight. All volatiles were removed in vacuo and the remainig orange residue was washed with hexane (5 mL) to give **3** as an orange solid (281 mg, 212 μmol, 89%). Recrystallization from hexane/THF gave **3** as orange X-ray quality needles. ^{1}H NMR (300 MHz, [D$_8$]THF, 298 K): δ = 4.77 (br s, 8H, C_5H_4), 4.88 (br s, 8H, C_5H_4) ppm. ^{13}C{^{1}H} NMR (125.8 MHz, [D$_8$]THF, 296 K): δ = 75.7 (d, $^2J_{CP}$ = 11 Hz, C_5H_4), 76.0 (d, $^3J_{PC}$ = 7.7 Hz, C_5H_4), 122.7 (qd, $^1J_{CF}$ = 325 Hz, $^1J_{CP}$ = 64 Hz, CF_3) ppm. ^{19}F{^{1}H} NMR (282.4 MHz, [D$_8$]THF, 290 K): δ = –53.3 (m, $^2J_{PF}$ = 73 Hz, 12F, C*F*$_3$) ppm. ^{31}P{^{1}H} NMR (202.5 MHz, [D$_8$]THF, 298 K): δ = 66.2 (AA'X$_6$X'$_6$Y, $^1J_{PRh}$ = 213.5 Hz, $^2J_{PP}$ = 39.5 Hz, $^2J_{PF}$ =

73.0 Hz, $P(CF_3)_2$) ppm. Anal. calcd. for $C_{28}H_{16}Cl_2F_{24}Fe_2P_4Rh_2$ (1320.69): C, 25.46; H, 1.22. Found: C, 25.59; H, 1.43.

Synthesis of [Rh(dfmpf)(NCMe)$_2$][BF$_4$] (4). $AgBF_4$ (162 mg, 833 μmol) was added to a solution of [Rh(dfmpf)(μ-Cl)]$_2$ (**3**) (550 mg, 416 μmol) in MeCN (10 mL) while stirring. Immediately a precipitate of AgCl was observed. The reaction mixture was stirred for 1 h to complete the reaction. AgCl was separated by filtration through a glass frit packed with filter flocks. After the residue was washed with MeCN (2 x 10 mL) all volatiles were removed in vacuo to give **4** as an ochre solid (650 mg, 818 μmol, 98%). ^{1}H NMR (500 MHz, CD_3CN, 298 K): δ = 1.96 (s, 6H CH_3CN), 4.87 (s, 4H, C_5H_4), 4.89 (s, 4H, C_5H_4) ppm. ^{11}B{^{1}H} NMR (160.5 MHz, CD_3CN, 298 K):δ = –1.1 (s, BF_4) ppm. ^{13}C{^{1}H} NMR (125.8 MHz, CD_3CN, 298 K): δ = 1.8 (s, CH_3CN), 76.3 (d, J_{CP} = 11.9 Hz, C_5H_4), 77.7 (d, J_{CP} = 8.4 Hz, C_5H_4), 122.6 (qd, $^1J_{CF}$ = 322 Hz, $^1J_{CP}$ = 63 Hz, CF_3) ppm. ^{19}F{^{1}H} NMR (282.4 MHz, CD_3CN, 290 K):δ = –54.1(m, $^2J_{PF}$ = 76.9 Hz, $^4J_{PF}$ = –0.8 Hz, 12F, CF_3), –149.5 (s, 4F, BF_4) ppm. ^{31}P{^{1}H} NMR (202.5 MHz, CD_3CN, 298 K): δ = 68.2 (AA'X$_6$X'$_6$Y, $^1J_{PRh}$ = 194.3 Hz, $^2J_{PP}$ = 44.5 Hz, $^2J_{PF}$ = 76.7 Hz, $^4J_{PF}$ = –0.3 Hz, $P(CF_3)_2$) ppm. Anal. calcd. for $C_{18}H_{14}BF_{16}Fe_2N_2P_2Rh$ (793.80): C, 27.24; H, 1.78; N, 3.53. Found: C, 27.01; H, 2.31; N, 3.35.

Electrochemistry. Cyclic voltammetry was performed using a standard three-electrode assembly connected to a EG&G Princeton Applied Research model 263A potentiostat. All scans were conducted under an atmosphere of nitrogen in CH_2Cl_2 (5.0 mL). The supporting electrolyte was 0.1 M [NBu_4][PF_6] and the analyte had a concentration of 2.0 mM. A AMETEK Advanced Measurement Technology model G0228 Pt-milli-electrode was used as working electrode. A platinum wire in supporting electrolyte solution separated from the analyte by a frit was used as the counter electrode. The reference electrode consisted of an Ag-wire in 0.1 M $AgNO_3$ in acetonitrile separated by a frit from the analyte solution. All scans were conducted at scan rates of 50 mV s^{-1}. At the end of each experiment ferrocene was added and the Fc/Fc$^+$ couple was used as internal standard. The energy levels were determined using the empirical relation E_{HOMO} = [–e($E_{1/2}$ (analyte/analyte$^+$ vs Ag/$AgNO_3$) – $E_{1/2}$ (Fc/Fc$^+$ vs Ag/$AgNO_3$))] –5.16 eV.[47]

Computational details. Density functional theory (DFT) calculations were performed with the TURBOMOLE[33] program package. The RI-DFT method[30–32] applying the B3-LYP functional[48–53] with the default grid size m3 was used for all calculations. The starting structure was obtained from the X-ray crystal structure of the corresponding complex. Initial optimization of the geometry was performed with the split-valence basis set def2-SV(P)[54] for all atoms. For the geometry optimization and orbital analysis of **1** and **2** the obtained geometry was optimized a second time applying the split-valence basis set def2-TZVP[54] for all non-metal atoms. The valence double zeta basis Hay-Wadt VDZ (n+1) ECP[55] and the effective core potential (ECP) HAY/WADT (N-1) ECP[55] were used for Fe, Ru and Co. Vibrational modes and resulting thermodynamic data

were computed from the optimized structure. The canonical molecular orbitals (MOs) were plotted as obtained from a single point calculation of the optimized structure with the basis sets of the previous geometry optimization. The VMD Molecular Graphics Viewer[56] was used for graphic representation of the MOs. The threshold of the isosurface was set to 0.05. Population analysis was performed with the program population analysis based on occupation numbers (PABOON) implemented in the TURBOMOLE package.[57]

Supporting Information. CIF files for compounds **1**, **2** and **3**. Further details of DFT calculations.

Corresponding Author *E-mail: kempe@uni-bayreuth.de

Acknowledgment Financial support by the Deutsche Forschungsgemeinschaft (DFG, KE 756/ 21-1) is gratefully acknowledged.

7.6 References

[1] For recent review articles, see: (a) D. Patel, S. T. Liddle, *Rev. Inorg. Chem.* **2012**, *32*, 1–22; (b) B. Oelkers, M. V. Butovskii, R. Kempe, *Chem. Eur. J.* **2012**, *18*, 13566–13579.

[2] (a) G. K.-I. Magomedov, A. Z. Voskoboynikov, E. B. Chuklanova, A. I. Gusev, I. P. Beletskaya, *Metalloorg. Khim.* **1990**, *3*, 706–707; (b) I. P. Beletskaya, A. Z. Voskoboynikov, E. B. Chuklanova, N. I. Kirillova, A. K. Shestakova, I. N. Parshina, A. I. Gusev, G. K.-I. Magomedov, *J. Am. Chem. Soc.* **1993**, *115*, 3156–3166.

[3] Polymeric structures that contain both isocarbonyl-linked and direct RE-TM interactions were reported shortly afterwards: (a) H. Deng, S. G. Shore, *J. Am. Chem. Soc.* **1991**, *113*, 8538–8540; (b) H. Deng, S.-H. Chun, P. Florian, P. J. Grandinetti, S. G. Shore, *Inorg. Chem.* **1996**, *35*, 3891–3896.

[4] M. V. Butovskii, O. L. Tok, F. R. Wagner, R. Kempe, *Angew. Chem. Int. Ed.* **2008**, *47*, 6469–6472.

[5] M. V. Butovskii, C. Döring, V. Bezugly, F. R. Wagner, Y. Grin, R. Kempe, *Nat. Chem.* **2010**, *2*, 741–744.

[6] C. Döring, A.-M. Dietel, M. V. Butovskii, V. Bezugly, F. R. Wagner, R. Kempe, *Chem. Eur. J.* **2010**, *16*, 10679–10683.

[7] M. V. Butovskii, O. L. Tok, V. Bezugly, F. R. Wagner, R. Kempe, *Angew. Chem. Int. Ed.* **2011**, *50*, 7695–7698.

[8] T. Bauer, F. R. Wagner, R. Kempe, *Chem. Eur. J.* **2013**, *19*, 8732–8735.

[9] M. V. Butovskii, B. Oelkers, T. Bauer, J. M. Bakker, V. Bezugly, F. R. Wagner, R. Kempe, *Chem. Eur. J.* **2014**, *20*, 2804–2811.

[10] (a) P. L. Arnold, J. McMaster, S. T. Liddle, *Chem. Commun.* **2009**, 818–820; (b) M. P. Blake, N. Kaltsoyannis, P. Mountford, *J. Am. Chem. Soc.* **2011**, *133*, 15358–15361; (c) M. P. Blake, N. Kaltsoyannis, P. Mountford, *Chem. Commun.* **2013**, *49*, 3315–3317.

[11] A. P. Humphries, S. A. R. Knox, *J. Chem. Soc. Dalt. Trans.* **1975**, 1710–1714.

[12] A. P. Sobaczynski, T. Bauer, R. Kempe, *Organometallics* **2013**, *32*, 1363–1369.

[13] J. Apel, J. Grobe, *Z. Anorg. Allg. Chem.* **1979**, *67*, 53–67.

[14] A. L. Fernandez, M. R. Wilson, A. Prock, W. P. Giering, *Organometallics* **2001**, *20*, 3429–3435.

[15] See, for example: (a) A. B. Burg, *Acc. Chem. Res.* **1969**, *2*, 353–360; (b) D. M. Roddick, R. C. Schnabel, *ACS Symp. Ser.* **1994**, *55*, 421–437; (c) M. Brookhart, W. A. Chandler, A. C. Pflister, C. C. Santini, P. S. White, *Organometallics* **1992**, *11*, 1263–1274; (d) L. D. Field, M. P. Wilkinson, *Organometallics* **1997**, *16*, 1841–1845; (e) B. Hoge, C. Thösen, T. Herrmann, P. Panne, I. Pantenburg, *J. Fluor. Chem.* **2004**, *125*, 831–851; (f) I. G. Phillips, R. G. Ball, R. G. Cavell, *Inorg. Chem.* **1988**, *27*, 4038–4045.

[16] See, for example: (a) M. F. Ernst, D. M. Roddick, *Inorg. Chem.* **1989**, *28*, 1624–1627; (b) J. J. Adams, A. Lau, N. Arulsamy, D. M. Roddick, *Inorg. Chem.* **2007**, *46*, 11328–11334.

[17] See, for example: M. S. Keady, J. D. Koola, A. C. Ontko, R. K. Merwin, D. M. Roddick, *Organometallics* **1992**, *11*, 3417–3421.

[18] M. B. Murphy-Jolly, L. C. Lewis, A. J. M. Caffyn, *Chem. Commun.* **2005**, 4479–4480.

[19] E. J. Velazco, A. J. M. Caffyn, X. F. L. Goff, L. Ricard, *Organometallics* **2008**, *27*, 2402–2404.

[20] See, for example: (a) J. D. Gilbert, G. Wilkinson, *J. Chem. Soc. A* **1969**, 1749–1753; (b) M. I. Bruce, N. J. Windsor, *Aust. J. Chem.* **1977**, *30*, 1601–1604.

[21] See, for example: (a) G. S. Ashby, M. I. Bruce, I. B. Tomkins, R. C. Wallis, *Aust. J. Chem.* **1979**, *32*, 1003–1016; (b) P. M. Treichel, D. A. Komar, P. J. Vincenti, *Synth. React. Inorg. Met.-Org. Chem.* **1984**, *14*, 383–400.

[22] M. I. Bruce, M. G. Humphrey, A. G. Swincer, R. C. Wallis, *Aust. J. Chem.* **1984**, *37*, 1747–1755.

[23] M. S. Chinn, D. M. Heinekey, *J. Am. Chem. Soc.* **1990**, *112*, 5166–5175.

[24] M. S. Chinn, D. M. Heinekey, *J. Am. Chem. Soc.* **1987**, *109*, 5865–5867.

[25] P. H. M. Budzelaar, gNMR, version 5.0.6, **2006**.

[26] A. C. Ontko, J. F. Houlis, R. C. Schnabel, D. M. Roddick, T. P. Fong, A. J. Lough, R. H. Morris, *Organometallics* **1998**, *17*, 5467–5476.

[27] For the calculation of the mean value, 43 $CpRuP_2H$ fragments were considered [WebCSD (Cambridge Structural Database) v. 1.1.1].

[28] For the calculation of the mean value, 52 $CpRuP_2$ fragments were considered [WebCSD (Cambridge Structural Database) v. 1.1.1].

[29] For details on coordination modes of bis(phosphino)ferrocenyl ligands, see: K.-S. Gan, T. S. A. Hor in *Ferrocenes*, (Eds.: A. Togni, T. Hayashi), VCH, Weinheim, **1995**, pp. 18–34.

[30] K. Eichkorn, O. Treutler, H. Öhm, M. Häser, R. Ahlrichs, *Chem. Phys. Lett.* **1995**, *240*, 652–660.

[31] K. Eichkorn, F. Weigend, O. Treutler, R. Ahlrichs, *Theor. Chem. Acc.* **1997**, *97*, 119–124.

[32] M. Sierka, A. Hogekamp, R. Ahlrichs, *J. Chem. Phys.* **2003**, *118*, 9136–9148.

[33] TURBOMOLE V6.5 2013, a development of University of Karlsruhe and Forschungszentrum Karlsruhe GmbH, 1989-2007, TURBOMOLE GmbH, since 2007; available from `http://www.turbomole.com`.

[34] D. Patel, F. Moro, J. McMaster, W. Lewis, A. J. Blake, S. T. Liddle, *Angew. Chem. Int. Ed.* **2011**, *50*, 10388–10392.

[35] A. L. Ward, W. W. Lukens, C. C. Lu, J. Arnold, *J. Am. Chem. Soc.* **2014**, *136*, 3647–3654.

[36] L. Kirch, M. Orchin, *J. Am. Chem. Soc.* **1958**, *80*, 4428–4429.

[37] M. J. Krafft, M. Bubrin, A. Paretzki, F. Lissner, J. Fiedler, S. Záliš, W. Kaim, *Angew. Chem. Int. Ed.* **2013**, *52*, 6781–6784.

[38] See, for example: (a) R. C. Schnabel, D. M. Roddick, *Inorg. Chem.* **1993**, *32*, 1513–1518; (b) A. J. Price, R. Ciancanelli, B. C. Noll, C. J. Curtis, D. L. DuBois, M. R. DuBois, *Organometallics* **2002**, *21*, 4833–4839.

[39] For details on $[(R_3P)_nRhCl]_x$ systems, see: F. H. Jardine, P. S. Sheridan in *Compr. Coord. Chem.* (Eds.: G. Wilkinson, F. G. A. Stone, E. W. Abel), Pergamon, Oxford, England, Vol. 4, **1987**, pp. 906–928.

[40] L. F. Dahl, C. Martell, D. L. Wampler, *J. Am. Chem. Soc.* **1961**, *83*, 1761–1762.

[41] See, for example: C. White, A. Yates, P. M. Maitlis, D. M. Heinekey, *Inorg. Synth.* **1992**, *29*, 228–234.

[42] M. Fauré, C. Saccavini, G. Lavigne, *Chem. Commun.* **2003**, 1578–1579.

[43] J. L. Herde, J. C. Lambert, C. V. Senoff, *Inorg. Synth.* **1974**, *15*, 18–20.

[44] A. Altomare, M. C. Burla, M. Camalli, G. L. Cascarano, C. Giacovazzo, A. Guagliardi, A. G. G. Moliterni, G. Polidori, R. Spagna, *J. Appl. Crystallogr.* **1999**, *32*, 115–119.

[45] G. M. Sheldrick, *Acta Crystallogr. A.* **2008**, *A64*, 112–122.

[46] L. J. Farrugia, *J. Appl. Crystallogr.* **1999**, *32*, 837–838.

[47] K. Gräf, M. A. Rahim, S. Das, M. Thelakkat, *Dyes Pigm.* **2013**, *99*, 1101–1106.

[48] P. A. M. Dirac, *Proc. R. Soc. A* **1929**, *123*, 714–733.

[49] J. C. Slater, *Phys. Rev.* **1951**, *81*, 385–390.

[50] S. H. Vosko, L. Wilk, M. Nusair, *Can. J. Phys.* **1980**, *58*, 1200–1211.

[51] A. D. Becke, *Phys. Rev. A* **1988**, *38*, 3098–3100.

[52] C. Lee, W. Yang, R. G. Parr, *Phys. Rev. B* **1988**, *37*, 785–789.

[53] A. D. Becke, *J. Chem. Phys.* **1993**, *98*, 5648–5652.

[54] F. Weigend, R. Ahlrichs, *Phys. Chem. Chem. Phys.* **2005**, *7*, 3297–3305.

[55] P. J. Hay, W. R. Wadt, *J. Chem. Phys.* **1985**, *82*, 299–310.

[56] W. Humphrey, A. Dalke, K. Schulten, *J. Mol. Graph.* **1996**, *14*, 33–38.

[57] C. Ehrhardt, R. Ahlrichs, *Theor. Chim. Acta* **1985**, *68*, 231–245.

7.7 Supporting Information

Table S1. Comparison of DFT-calculated and experimental structure parameters of **1**.

	calc.	X-ray	rel. Error	abs. Error
Bond	[Å]	[Å]	[%]	[Å]
Ru1–C17	2.276	2.214	2.80	0.062
Ru1–P1	2.238	2.189	2.21	0.048
Ru1–P2	2.245	2.199	2.11	0.046
Ru1–Fe1	4.382	4.326	1.29	0.056
Ru1–H1Ru	1.603	1.429	12.19	0.174
Angle	[°]	[°]	[%]	[°]
P1–Ru1–P2	97.3	96.0	1.34	1.28
Cp–Cp (torsion)	23.1	26.4	12.50	3.3

Table S2. Comparison of DFT-calculated and experimental structure parameters of **2**.

	calc.	X-ray	rel. Error	abs. Error
Bond	[Å]	[Å]	[%]	[Å]
Co1–C1	1.772	1.748	1.37	0.024
Co1–C2	1.780	1.752	1.56	0.027
Co1–P1	2.162	2.111	2.39	0.051
Co1–P2	2.146	2.107	1.87	0.039
Co1–Fe1	4.147	4.045	2.53	0.102
Co1–H1Co	1.488	1.791	–16.92	–0.303
Angle	[°]	[°]	[%]	[°]
P1–Co1–P2	109.59	109.47	0.10	0.11
C1–Co1–C2	97.4	100.1	–2.72	–2.72
H1Co–Co-C1	81.2	77.3	5.07	3.92
H1Co–Co1–C2	177.3	175.8	0.9	1.5
Cp–Cp (torsion)	27.9	39.6	–29.5	–11.7

Table S3. Energy of frontier orbitals and HOMO-LUMO-gap for compounds **1** and **2**.

compound	E_{HOMO-1} [eV]	E_{HOMO-0} [eV]	E_{LUMO+0} [eV]	E_{LUMO+1} [eV]	$\Delta E_{LUMO-HOMO}$ [eV]
1	–6.31	–5.82	–1.41	–1.01	4.41
2	–6.50	–6.45	–1.50	–1.31	4.95

Table S4. Energy of deprotonation calculated with the def2-TZVP basis set for non-metal atoms and atomic charges acoording to the PABOON method[a].

compound	energy of deprotonation [eV]	metal/charge	H/charge
1	14.97	Ru 0.107	–0.063
2	13.71	Co –0.884	0.111

[a] C. Ehrhardt, R. Ahlrichs, *Theor. Chim. Acta* **1985**, *68*, 231–245.

8

List of Publications

The following publications have been published or are to be submitted during the work on this thesis.

1. A. P. Sobaczynski, J. Obenauf, R. Kempe, *Eur. J. Inorg. Chem.* **2014**, 1211–1217.
   "Alkane Elimination Reactions between Rare Earth Alkyls and Tungsten Hydrides"

2. A. P. Sobaczynski, T. Bauer, R. Kempe, *Organometallics* **2013**, *32*, 1363–1369.
   "Heterometallic Hydride Complexes of Rare-Earth Metals and Ruthenium through C-H Bond Activation"

3. A. P. Sobaczynski, S. Schwarz, J. Obenauf, R. Kempe; *to be submitted.*
   "Phenoxy Ligated Heteromultimetallic Hydride Complexes of Ruthenium and Rare-Earth Metals"

4. A. P. Sobaczynski, S. Schwarz, J. Obenauf, R. Kempe; *to be submitted.*
   "Transition Metal Hydride Complexes of dfmpf"

9

Acknowledgments

First of all I would like to thank my academic supervisor

Prof. Dr. Rhett Kempe

for admission in his research group and for giving me the opportunity to work on this very interesting topic. Furthermore, I am grateful for the constant interest on the progress of this work and the liberties granted to me.

I thank Prof. Dr. Lothar Weber and Prof. Dr. Norbert W. Mitzel for their support and the excellent education during my diploma studies.

My thanks to all the ones who provided me a trouble-free everyday laboratory life: the employees of the central materials and consumables distribution for the supply with all necessary consumables, the electronics workshop for repairs and construction of electrical devices, the metal workshop for craftsmanship, and in particular the employees of the glassblowing workshop for rapid repairs and manufacturing of glassware of all kinds. I thank Anna Dietel and Heidi Meisel for providing dried solvents and other lab equipment.

I thank very much my interns Daniel Forberg, Sabrina Sachau and Dominic Tilgner for their commitment and their help during their advanced lab courses.

I wish to thank Johannes Obenauf, Dr. Tobias Bauer, Dr. Awal Noor and Dr. Benjamin Oelkers for X-ray crystal structure analyses and their efforts in structure solutions.

A heartfelt thanks goes out to my lab mates Martin Friedrich, Dr. Muhammad Hafeez, Dr. Justus Hermannsdörfer, Walter Kremnitz, Johannes Obenauf and Simone Ott for the great atmosphere and the time spent together.

In addition, I thank Walter Kremnitz for his commitment to make everyones daily lab routine as enjoyable as possible.

My special thanks goes to Marlies Schilling for her help in all administrative and organizational matters.

I especially thank my colleagues Dr. Tobias Bauer, Martin Friedrich, Dr. Isabelle Haas, Dr. Justus Hermannsdörfer, Walter Kremnitz, Johannes Obenauf, Dr. Benjamin Oelkers, Susanne Ruch, Sina Rösler, Sabrina Sachau, Stefan Schwarz and Theresa Winkler for having a good time outside of the lab.

I thank the other members of the Kempe group, Dr. Christine Denner, Daniel Forberg, Dr. Awal Noor, Dr. Sadaf Qayum, Dr. Saravana Pillai, Dr. Emmanuel Sobgwi Tamne and Dr. Muhammad Zaheer for their helpfulness in many respects.

I am very grateful to Dr. Elena Klimkina and Dr. Oleg Tok for their help in recording numerous NMR spectra and their interpretation. Furthermore, I thank them for numerous scientific discussions and suggestions.

I thank Dr. Torsten Irrgang, Dr. Justus Hermannsdörfer and especially Dr. Benjamin Oelkers for proofreading of publications and this thesis.

I thank Dr. Jochen Bammert, Mark Burgis, Dr. Elena Klimkina, Dr. Ruth Lohwasser, Wolfgang Mühlbauer, Dr. Martti Pärs, Ulli Pöller and Dr. Oleg Tok for countless weekends in the Franconian Jura and the great time spent together.

Finally, I would like to thank Julia with all my heart for her endless love and her confidence, her encouraging words and her never-ending patience.

Danksagung

Zuallererst möchte ich meinem akademischen Lehrer

Prof. Dr. Rhett Kempe

für die Aufnahme in den Arbeitskreis und die Möglichkeit, dieses äußerst interessante Thema bearbeiten zu dürfen danken. Weiterhin bedanke ich mich für das stete Interesse am Fortgang der Arbeit sowie die mir gewährten Freiheiten.

Prof. Dr. Lothar Weber und Prof. Dr. Norbert W. Mitzel danke ich recht herzlich für die Unterstützung und exzellente Ausbildung im Diplomstudiengang.

Mein Dank gilt allen denen, die mir einen reibunglosen Laboralltag ermöglicht haben: Den Mitarbeitern der Materialausgabe für die Bereitstellung aller benötigten Verbrauchsmaterialien, der Elektronikwerkstatt für Reparaturen and Neuanfertigungen elektrischer Geräte, der Metallwerkstatt für handwerkliche Unterstützung sowie insbesondere den Mitarbeitern der Glasbläserwerkstatt für zügige Reparaturen und Neuanfertigungen von Glasgeräten aller Art. Anna Dietel und Heidi Meisel danke ich für die Bereitstellung von getrockneten Lösungsmitteln und sonstigen Gerätschaften.

Meinen Forschungspraktikanten Daniel Forberg, Sabrina Sachau und Dominic Tilgner danke ich sehr für ihr Engagement und ihre Hilfe im Labor.

Johannes Obenauf, Dr. Tobias Bauer, Dr. Awal Noor sowie Dr. Benjamin Oelkers danke ich vielmals für die Durchführung von Einkristall-Röntgenstrukturanalysen und ihren unermüdlichen Einsatz bei Strukturlösungen.

Ein herzlicher Dank geht an meine Laborkollegen Martin Friedrich, Dr. Muhammad Hafeez, Dr. Justus Hermannsdörfer, Walter Kremnitz, Johannes Obenauf und Simone Ott für die tolle Stimmung und die zusammen verbrachte Zeit.

Darüber hinaus danke ich Walter Kremnitz für seine Hilfe und seinen unermüdlichen Einsatz, um den Laboralltag so angenehm wie möglich zu gestalten.

Marlies Schilling gilt mein besonderer Dank für ihre Hilfe in allen administrativen und organisatorischen Angelegenheiten.

Meinen Arbeitskollegen Dr. Tobias Bauer, Martin Friedrich, Dr. Isabelle Haas, Dr. Justus Hermannsdörfer, Walter Kremnitz, Johannes Obenauf, Dr. Benjamin Oelkers, Susanne Ruch, Sina Rösler, Sabrina Sachau, Stefan Schwarz und Theresa Winkler danke ich ganz besonders für eine schöne Zeit außerhalb des Labors.

Den restlichen Mitgliedern des Arbeitskreises Kempe, Dr. Christine Denner, Daniel Forberg, Dr. Awal Noor, Dr. Sadaf Qayum, Dr. Saravana Pillai, Dr. Emmanuel Sobgwi Tamne und Dr. Muhammad Zaheer danke ich für ihre Hilfsbereitschaft in vielen Belangen.

Dr. Elena Klimkina und Dr. Oleg Tok danke ich sehr für ihre Hilfe bei der Anfertigung zahlreicher NMR-Spektren sowie deren Auswertung. Weiterhin danke ich ihnen für zahlreiche fachliche Diskussionen und Anregungen.

Für das Korrekturlesen von Publikationen und dieser Arbeit danke ich Dr. Torsten Irrgang, Dr. Justus Hermannsdörfer sowie ganz besonders Dr. Benjamin Oelkers.

Dr. Jochen Bammert, Markus Burgis, Dr. Elena Klimkina, Dr. Ruth Lohwasser, Wolfgang Mühlbauer, Dr. Martti Pärs, Ulli Pöller und Dr. Oleg Tok, danke ich für zahllose Wochenenden in der Fränkischen und die tolle gemeinsam verbrachte Zeit.

Zuletzt bedanke ich mich von ganzem Herzen bei Julia für ihre grenzenlose Liebe und ihr Vertrauen, ihre aufmunternden Worte und ihre nicht enden wollende Geduld.

10

Declaration

(Eidesstattliche) Versicherungen und Erklärungen

(§5 Nr. 4 PromO) Hiermit erkläre ich, dass keine Tatsachen vorliegen, die mich nach den gesetzlichen Bestimmungen über die Führung akademischer Grade zur Führung eines Doktorgrades unwürdig erscheinen lassen.

(§8 S. 2 Nr. 5 PromO) Hiermit erkläre ich mich damit einverstanden, dass die elektronische Fassung meiner Dissertation unter Wahrung meiner Urheberrechte und des Datenschutzes einer gesonderten Überprüfung hinsichtlich der eigenständigen Anfertigung der Dissertation unterzogen werden kann.

(§8 S. 2 Nr. 7 PromO) Hiermit erkläre ich eidesstattlich, dass ich die Dissertation selbständig verfasst und keine anderen als die von mir angegebenen Quellen und Hilfsmittel benutzt habe.

(§8 S. 2 Nr. 8 PromO) Ich habe die Dissertation nicht bereits zur Erlangung eines akademischen Grades anderweitig eingereicht und habe auch nicht bereits diese oder eine gleichartige Doktorprüfung endgültig nicht bestanden.

(§8 S. 2 Nr. 9 PromO) Hiermit erkläre ich, dass ich keine Hilfe von gewerbliche Promotionsberatern bzw. -vermittlern in Anspruch genommen habe und auch künftig nicht nehmen werde.

Bayreuth, den 18.08.2014 Adam Sobaczynski